UNIVERSITÀ
DEGLI STUDI
DI TRIESTE

UNIVERSITÀ DEGLI STUDI DI TRIESTE

XXXVI CICLO DEL DOTTORATO DI RICERCA IN

Dottorato in Nanotecnologie

Borsa MUR/Ateneo cofinanziata dal Dipartimento di Fisica su fondi CERIC-ERIC progetto INTEGRA

Mechanisms of extracellular vesicles (EVs) internalization by cells: role of cell membrane biophysical properties

Settore scientifico-disciplinare: **FIS/03**

DOTTORANDO / A
CAROLINA PABA

COORDINATORE
PROF. ALBERTO MORGANTE

SUPERVISORE DI TESI
PROF. LOREDANA CASALIS

CO-SUPERVISORE DI TESI
DR. PIETRO PARISSE

ANNO ACCADEMICO 2022/2023

UNIVERSITÀ DEGLI STUDI DI TRIESTE

XXXVI CICLO DEL DOTTORATO DI RICERCA IN

Dottorato in Nanotecnologie

Borsa MUR/Ateneo cofinanziata dal Dipartimento di Fisica su fondi CERIC-ERIC progetto INTEGRA

Mechanisms of extracellular vesicles (EVs) internalization by cells: role of cell membrane biophysical properties

Settore scientifico-disciplinare: **FIS/03**

DOTTORANDO / A
CAROLINA PABA

COORDINATORE
PROF. ALBERTO MORGANTE

SUPERVISORE DI TESI
PROF. LOREDANA CASALIS

CO-SUPERVISORE DI TESI
DR. PIETRO PARISSE

ANNO ACCADEMICO 2022/2023

Acknowledgements

I would like to express my sincere gratitude to the numerous people and institutions whose support and contributions made this PhD thesis project possible.

First, I extend my profound appreciation to my supervisor, Prof. Loredana Casalis, for her invaluable guidance, patience, and commitment to my academic growth throughout this journey. Your wisdom, mentorship, and continuous encouragement have been instrumental in shaping the direction of this research.

Secondly, I would like to thank my co-supervisor, Dr. Pietro Parisse, for his support with the experimental work. Your knowledge provided valuable guidance throughout these years.

I would like to express my gratitude to Prof. Kislon Voitchovsky. Working with you has been a source of motivation and inspiration. Your knowledge and experience provided insightful advice for my research activity. Finally, I wish to thank you and your group for including and considering me equal since the first day of my stay.

A warm thanks go to Nicolò Tormena and Clodomiro Cafolla, you contributed to making my stay at Durham pleasant and a stimulating research environment, with your interesting discussions, helpful advice, and great laugh together!

I wish to thank Prof. Valeria Rondelli, for helping me with the DSC measurements. The useful discussions with you have been a valuable guidance over the three years. I wish to thank you and Sally Helmy for helping during the analysis and interpretation of the results.

I gratefully acknowledge the Structural Biology Laboratory at Elettra-Sincrotrone Trieste S.C.p.A. for the instrumentation and constant support during the cell culture experiments.

I wish to thank Dr. Mario Gimona for providing the small EVs samples over the three years.

I would like to thank the members of the SISSI-Bio beamline, especially Hendrik Vondracek, for helping me in IR-measurements.

I am very grateful to CERIC-ERIC for financial funding within the framework of the INTEGRA and INTEGRA's PhD project.

To my friends and colleagues, in particular Caterina, Elena, Behnaz, Ana, Ahmed, Federica, and Virginia, who have provided moral support, understanding, and occasional comic relief during moments of stress and doubt, I am profoundly grateful. Your presence in my life has been a constant source of inspiration. A special thanks go to Beatrice and Hendrik, who have guided and helped me embark on this journey from the very first day.

Last but certainly not least, this thesis is dedicated to my family and Pierluigi. Your unwavering belief in me, consistent willingness, and endless support and encouragement have been the bedrock of my journey.

List of Figures

Abstract

Plasma membranes represent the crucial structural component of eukaryotic cells, serving as a selectively permeable barrier that separates the internal environment of the cell from the external surroundings. Over the last two decades, the vision of a homogenous fluid mosaic model gave the space to a more complex model of description, which sees the compartmentalization of lipids and proteins in functional and specialized subdomains, also called lipid rafts. They are described as dynamic regions, whose composition and lateral organization constantly change in response to cellular stimuli. In particular, they are believed to play central functions in cellular signaling, protein mobilization, and membrane trafficking. Moreover, diverse endocytosis mechanisms have been discovered, and some of these are thought to be regulated by lipid rafts, including the internalization of membrane pathogens such as viruses, cargo molecules targeting and delivery, as well as extracellular vesicles uptake. Focusing on extracellular vesicles, they have been described as nanometer-sized vesicles ($\sim 30 - 2000\ nm$), and recently proposed as important mediators of intercellular communication between all cells of our body. A particular sub-class of extracellular vesicles, also known as small extracellular vesicles (sEVs) ($\sim 30 - 150$), have attracted interest as a suitable drug delivery systems, displaying a composition that reflects their cells of origin, and a small size that makes them able to cross biological barriers through the body. These two features, combined with their high biocompatibility and specific targeting, make them primarily involved in the regulation of pathophysiological processes, such as cancer progression, metastasis formation, and cell proliferation. However, a clear knowledge of the sEVs functioning and their roles in biological systems, as well as the mechanisms that regulate their selective interaction with recipient cells, is still missing and fundamental for therapeutic usage. However, given the complexity of cell membranes, and the small size of sEVs, along with the development of new tools for investigating plasma membrane dynamics and sEVs interaction processes, the exploration and formulation of biomimetic cell membrane systems have been gaining great interest for investigating various cellular processes (e.g. biomolecules interaction, lipids redistribution).

Based on these considerations, a biophysical approach that focuses on the development of a model system mimicking lipid rafts subdomains is here proposed, followed by its application for analysis of small extracellular vesicles uptake mechanisms. The

protocol showed the possibility of using atomic force microscopy (AFM) to study the dynamics of sEVs fusion mechanisms, providing spatial and time-resolved information about lipid rafts morphological changes upon vesicles fusion, thus overcoming the limited detection ranges of the currently available techniques. A comparison with differential scanning calorimetry analysis (DSC), a commonly used technique for lipid bilayer characterization, allowed to explore the vesicles interaction with model systems without the influence of a rigid substrate.
More in detail, the system has been applied to sEVs from a cellular model of a metastatic cell line, the triple-negative breast cancer cells, interacting with a range of synthetic planar lipid bilayers displaying lipid phase separation with different cholesterol amount and degree of fluidity, designed to mimic the formation of 'raft'-like nanodomains in cell membranes. Using time-resolved AFM under temperature control, it has been possible to show the strong dependence of sEVs uptake, and the associated local membrane composition and membrane fluidity. The strongest interaction and sEVs mixing with the lipid bilayer has been observed over the less fluid regions, with sEVs even able to disrupt ordered domains at sufficiently high cholesterol concentration.
The obtained results highlighted the possibility of using the developed model system to investigate, from a biophysical perspective, the mechanisms regulating sEVs uptake, suggesting that tuning the plasma membrane characteristics might be instrumental to regulating sEVs uptake for EVs-based drug delivery applications.

Contents

Chapter 1

Introduction

1.1 The need of model membrane systems

Over the past decades, considerable efforts have been directed towards innovative methods for studying cell membrane organization and cellular process regulation [1]. These two aspects are in fact difficult to be disentangled, being governed by a complex and wide plethora of variables (e.g. membrane architecture, composition, spatial resolution, time evolution) [2, 3].
To successfully fulfill these objectives, biomimetic cell membrane systems of increasing complexity have been widely adopted, as they are as simple as powerful tools for studying problems ranging from phase behavior, molecules trafficking, to membrane fusion events [4, 5]. In particular, an ideal model should be able to retain the basic structure of cell membranes, composed of two opposing lipidic leaflets, such that the lipids assembly in domains and their packing with membrane proteins would be preserved. This approach would support the investigation of single lipid/protein components and their dynamics with high spatio-temporal resolution, in a more simple and cost-effective way.
An example of a representative model of cell membrane architecture, comprehensive of composition complexity, and degrees of freedom in terms of system environment, components mobility, and curvature degree to be explored, is the supported lipid bilayer system (SLB). This system is defined as a two-dimensional planar lipid-bilayer physisorbed on solid support (e.g. mica, glass, silica), with a typical thickness of a few nanometers [6, 7].
SLB have been widely adopted over the last decades for studying a broad number of biological phenomena ranging from the function of cholesterol in the regulation of amyloid-β (Aβ) generation and aggregation [8], iron-mediated interaction of alpha-synuclein (αS) [9], antimicrobial peptide diffusion and membrane poration [10], kinetics of protein sorting and protein binding affinity with membrane subdomains [11, 12]. In this regard, model membrane systems turn out to be innovative technologies for study-

ing recently discovered nanoscale membrane vesicles actively released by cells. They were defined by the International Society for Extracellular Vesicles (ISEV) community in 2018 as small-extracellular vesicles (sEVs) with a size in the range of $\sim 30-300\ nm$. However, despite their recognized role in diverse biological processes, ranging from cell homeostasis to cancer progression, which led them to be in the spotlight of the scientific community for the past two decades, many challenges have yet to be addressed [13]. In particular, the extracellular vesicles journey in terms of EVs docking on the cellular port and the EVs internalization by cells remains far from comprehensive. There is evidence that EVs targeting is not only dependent on the cellular origin and molecular cargo, but also on the specific properties of the recipient cells. It has indeed been demonstrated that EVs isolated from the same cell line, displayed a different internalization pathway and much diverse ability in modulating the fate of the recipient cells between different cell types [14]. Over the years, many approaches have been developed to track the EV-cells communication routes, ranging from extracellular vesicles labeling with fluorescent probes, inhibition/activation of membrane receptors, and characterization of the changes in cell morphology and migration using fluorescence microscopy. However, even if many technological improvements have been made in terms of temporal and spatial resolution that can be achieved with optical microscopes, the main drawbacks rely on the high complexity of sample preparation, the ability to discern between single molecular components, and in the limited time-frame, consequently giving a restricted number of information about the dynamics of the process [15].
Considering these critical aspects, it is clear that identifying and classifying the chemical and physical cellular components involved in the EVs uptake, with a simple and representative model of the cell membrane, would be beneficial for significantly contributing to a better understanding of the EVs intracellular route. In the following chapters, the molecular mechanisms that govern the extracellular vesicle journey during the interaction with cell membranes will be discussed. In particular, the uptake process will be investigated by comparing the behavior of EVs isolated from two different cell lines and testing different cell model membrane properties.

1.2 Objective of the thesis

The thesis focuses on the development of a model membrane system for the characterization of cholesterol role in regulating lipid-lipid phase separation and morphology changes, as well as the detection of small extracellular vesicles interaction mechanisms with the proposed model. The aim is to provide new insights into the chemical and physical parameters of the cell membrane that might be crucial in the regulation of sEVs uptake and in their ability to fuse with the recipient cell membrane as a consequence. The proposed study aims to i) overcome some of the detection challenges associated with the spatio-temporal resolution required in EVs studies; ii) increase the

fundamental understanding of the driving forces regulating sEVs interaction mechanisms; and iii) show the prospects of using model membranes as versatile tool for both EVs analysis and integral protein localization within a biomimetic model membrane.
To fulfill these objectives, two approaches are considered and analyzed: atomic force microscopy (AFM) on supported lipid bilayer, and differential scanning calorimetry (DSC) on liposomes. The application of pore-spanning membranes, still under optimization, will be briefly introduced in future plans. In particular, a protocol for lipid bilayer formation over a rigid and flat substrate as mica is optimized. Variables such as pH, temperature, buffer, and lipid components were selected in order to work under 'physiological conditions'.
The vesicles used throughout the thesis belong to the category of small EVs ($30 - 300\ nm$), isolated with the optimized isolation method of ultracentrifugation [16] from a triple-negative breast cancer cell line (MDA-MB-231). A comparative analysis has been performed for sEVs isolated from umbilical cord mesenchymal stem cell line (UC-MSC) from GMP production provided by Mario Gimona's lab at the Paracelsus Medical University Salzburg. In parallel, small EVs collected from SARS-CoV-2 spike expressing human embryonic kidney (HEK-293T) cells, provided by Benedetta Bussolati's lab at the University of Turin, have been used as a tool for studying with a simplified model, the possible mechanisms governing the different interaction routes of EVs expressing the spike protein (s-EV) and the control (c-EV) with the host cell membrane.

1.3 Thesis outline

This thesis is structured as follows.

Chapter 2 gives an introduction to cell membrane biology, highlighting their architecture, composition, and role of lipid-lipid interaction and phase separation into subdomains. It further describes the role played by cholesterol in regulating fundamental features of a specific class of subdomains known as lipid rafts.

Chapter 3 describes the currently available model membrane systems for mimicking the cell membrane structure and dynamics. Various fabrication and characterization methods will be discussed. Furthermore, it includes the applications in cell biology and the motivation of the selected model for the study of the EV uptake mechanism.

Chapter 4 gives an overview of EVs, highlighting their classification and most common isolation methods. The role in cell-cell communication, with particular attention to EVs isolated from cancer cells, will be discussed. Furthermore, the challenges related to the EV detection limits will be pointed out, underlying the importance of high spatial and temporal resolution.

Chapter 5 describes the materials and methods used to perform the thesis, with technical details about the protocols that have been followed.

Chapter 6 presents the development of the cell model membrane system. Experi-

mental details of the parameters that have been taken into account to obtain a stable system will be illustrated. The preliminary tests of EVs interaction with the lipidic system, performed during the optimization, are reported as well.

Chapter 7 summarizes the main findings reported in the published paper 'Lipid bilayer fluidity and degree of order regulates small EVs adsorption on model cell membrane' on JCIS, 2023.

Chapter 8 concludes this work and gives a brief future outlook to the new technology, still under optimization, for the formation of suspended lipid bilayer over a pore-spanning membrane.

Chapter 2

Biology of cell membrane

2.1 Cell membrane organization and composition

Cell membrane, studied since the 19^{th} century, represents the essential barrier for the cells survival and biological functioning [17]. It separates the extracellular environment from the intracellular space, and is actively involved in the regulation of a variety of cellular processes such as the transport of molecules through a selective permeability, cell signaling with the regulation of cellular response to extracellular physical or chemical signals, and ion conductivity with the regulation of various electrochemical processes [18].

Over the years, the concept of the mosaic model describing the cell membrane as a uniform fluid and flexible lipid bilayer made up of phospholipids and proteins able to laterally diffuse in the membrane, has given way to a more complex vision of the cell membrane structure and activity [19], as schematically illustrated in Figure 2.1. Cell membranes are now seen as more 'dynamic' objects, with a nonrandom distribution of the principal membrane elements, but instead with compartmentalization at the submicrometric level of lipids, proteins, and sterols [20]. This has a significant impact on the cellular processes, now actively regulated by the dynamic redistribution of proteins and lipids in clusters and subdomains, typically characterized by a lower degree of lateral mobility within the lipid bilayer. More in detail, the term 'lipid rafts' was coined to define those areas of the cell membrane featuring a different lipid composition than the surroundings, and as a consequence different biological and mechanical properties [22]. They are identified as areas with a certain degree of asymmetry, with the outer leaflet mostly enriched with cholesterol and sphingolipids, and the inner leaflet mainly composed of cholesterol and saturated phospholipids [23]. The introduction of such domains as functional areas of the cell membrane has been fundamental for providing a better explanation of many cellular processes, including protein trafficking, cell polarity, and signal transduction [24], regulated by the selective recruitment and translocation

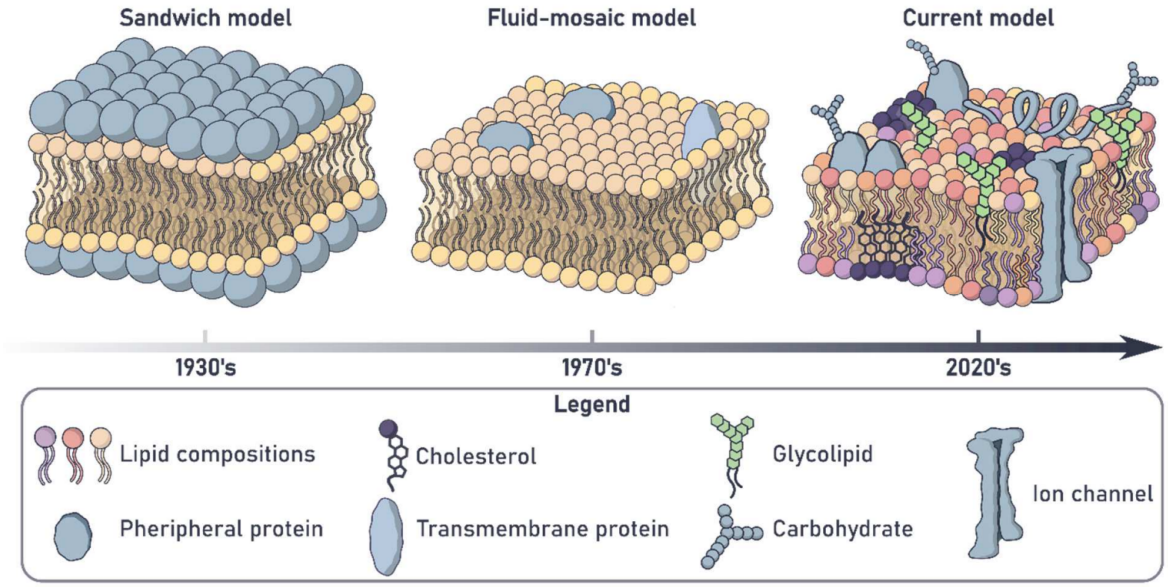

Figure 2.1: Overview of the cell membrane models evolution from 1930's to 2020's, which see the progressive increase of complexity and cell membrane components compartmentalization [21].

of proteins and lipids across the bilayer. In particular, it has been demonstrated that the movement of lipids across the membrane, can be either spontaneous, as in the case of the lipids that belong to the family of phosphatidylcholines (PC) and sphingolipids, or a protein-mediated process, as for the transport of the aminophospholipids family [25].

In this scenario, the main lipids in cell membranes can be divided into three families: glycerophospholipids, glycolipids, and sterols. They are defined as amphipathic molecules, characterized by a basic structure that consists of a glycerol backbone, two fatty acid tails (hydrophobic part), and a phosphate group (hydrophilic region). Because of that, to minimize the area exposed to the aqueous environment, the hydrophobic domains preferentially self-associate, forming an energetically stable molecular barrier with the polar domains in close interaction with water, and the hydrocarbon chains facing towards each other [26]. It is important to notice that, depending on parameters such as the chain length, saturation, or head group species, each lipid will be involved in multiple roles, influencing cellular processes [27, 28]. Moreover, the chain length and saturation of the fatty acid tails, also regulate the lateral packing of lipids against one another, thus influencing their mobility and the resulting fluidity of the cell membrane. In particular, the presence of *cis*-double bonds in the unsaturated lipids creates a kink in the lipid tail, reducing the ability of the lipids to pack together.

Moreover, for short chain lengths, the packing efficiency is even more compromised. In this context, sterol molecules have a fundamental role by orienting themselves close to the polar head groups they are interacting with, thus forming segregated regions in the lipid bilayer characterized by different lateral mobility and packing degrees.
The last parameter that can affect the lipid bilayer fluidity of the system is the temperature. Indeed, lipids are characterized by a phase transition temperature (T_m) that defines their existence in two distinct states, identified as follows: the liquid state above this value features a low packing degree and high lateral mobility; the two-dimensional rigid crystalline state, also known as gel phase, below T_m, characterized instead by high packing degree and low lateral mobility [29].

The main features and functions of the three families will be briefly discussed hereafter and a schematic representation of the three types of membrane lipids is reported in Figure 2.2.

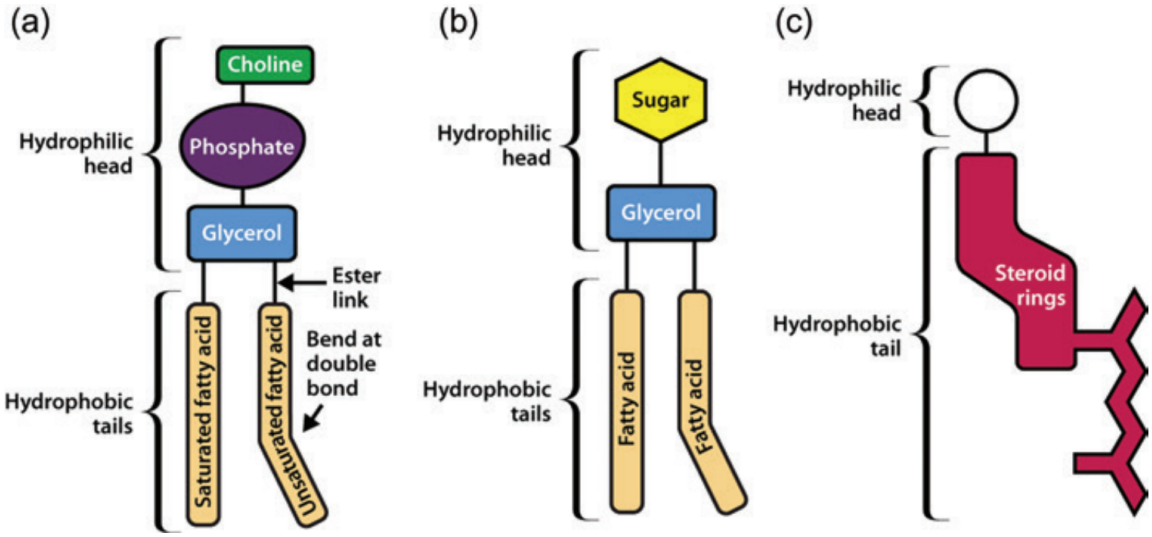

Figure 2.2: Schematic representation of the three main families of membrane lipids constituting the eukaryotic cell membranes. Adapted from [30].

Glycerophospholipids are usually referred to as phospholipids, with phosphatidylcholine (PC), phosphatidylserine (PS), and phosphatidylethanolamine (PE) the most abundant species. They are characterized by a hydrophobic portion called diacylglycerol (DAG), and a glyceride consisting of two fatty acid chains esterified to a glycerol molecule. Since the molecular structure can be modified both in terms of the head group at the level of the sn-3 position of the glycerol backbone and in terms of length and degree of saturation at the level of the fatty acid chains, many diverse phospho-

lipids populate the molecular machinery of cell membranes [31]. PC constitutes the most abundant lipid, representing the 50% of the total cellular phospholipids. Predominantly localized at the outer leaflet of the plasma membrane, in addition to being a major structural component of cellular membranes, PC also takes part in many signaling events, being a key regulator of cell membrane homeostasis [32].

Glycosphingolipids (GSL) are a class of lipids that mostly enrich the outer leaflet of the bilayer, in minor abundance compared to the glycerophospholipids, but still fundamental for the structural integrity of cell membrane. They present a lipid backbone, the sphingosine, which is amide-bonded to a fatty acid forming the ceramide, the hydrophobic portion of the molecule. Depending then on the origin of the polar head, which can be either a glycan or phosphocholine group, thousands of combinations arise [31]. They are typically characterized by long acyl chains with a low degree of unsaturation, responsible for their high transition temperature [33]. Moreover, such lipids display marked hydrogen-bonding properties, with a peculiar affinity with cholesterol molecules, but more in general with lipids and proteins. The close association with these components and their spontaneous segregation in the lipid bilayer, is considered to be the major responsible for the biogenesis and correct functioning of cell membrane functional domains [34]. More in detail, GSL functions can be divided into two main categories: trans-recognition through the mediation of cell–cell interactions via binding to surrounding lipids and molecules, and the cis-regulation via the regulation of proteins activities. In this regard, many studies pointed out the function of GLS in the regulation of many diseases, including cancers, playing a crucial role in cellular processes such as cell proliferation, intracellular transport, and gene regulation [35, 36].

Sterol molecules are characterized by a complex four-ring structure, presenting a hydroxyl group (OH) on the first 6-C ring, responsible for the upright orientation in the bilayer and for the amphiphilic character as a consequence [37]. They are characterized by a much lower solubility compared to the surrounding lipids, with a maximum limit of around $50-60$ mol % depending on the local composition of the cell membrane [38]. In contrast to the wide heterogeneity of phospholipids and sphingolipids that can be counted in the cell membrane, cholesterol is the most abundant sterol in mammalian membranes, and the major regulator of cell membrane structure [38, 39]. Numerous studies have demonstrated its function in regulating peculiar structural membrane properties such as fluidity and permeability, as well as mobility and thickness. This is mainly related to its preferential interaction with phospholipids and sphingolipids [39]. As it will be explained more in detail afterward, cholesterol interaction with the other lipids alters their behavior by means of the physical state to which they would naturally belong. In particular, it is responsible for the formation of an intermediate lipid phase, also known as the liquid-ordered (L_o) phase, typically increasing the fluidity of those acyl chains with high T_m as for the sphingolipids, and decreasing the fluidity of

the acyl chains below the T_m, like in the case of most phospholipids. Besides the well known role in regulating the membrane physical properties, the ordering effect has also a secondary effect on the behavior and activation of those proteins that are sensitive to physical changes, as well as in the modulation of signaling events, being the building block of cell membrane domains [38, 40].
The important functions and mechanisms of cholesterol in regulating lipid rafts subdomains will be further discussed in detail in Section 2.3.

In addition to what has been shown so far, a mention should be given regarding the importance of membrane proteins in the cellular machinery as well. They are indeed responsible for carrying out most of the cellular membrane functions. They can be divided into two main classes: integral or transmembrane proteins and peripheral membrane proteins, which mainly differ in association with the surrounding lipids. In a simplified description, the former span the bilayer thickness, whereas the latter enriches the membrane surface [41]. Depending on the protein content and subcellular compartments, they will exert a different function. The proteins that are located at the plasma membrane can act as membrane receptors, as well as cell adhesion molecules, regulating either the membrane trafficking or the cell-cell interactions. On the other side, proteins embedded in the cell membrane might act as transduction receptors instead, transmitting the signals from the extracellular space to the recipient cells. To the former class of proteins, EGFR receptors have displayed critical functions in cancer, in particular promoting the tumor cell growth and survival of glioblastoma and breast cancer. The tumorigenesis is primarily driven by genetic mutations and autocrine stimulation, leading to increased activation of EGFR expression [42, 43]. Interestingly, it has been reported that EGFR receptors tend to migrate outside the region of the cell membrane where they are localized upon their activation [44]. However, the exact interplay of these receptors with the other proteins and lipids is still under debate and would be beneficial to elucidate the mechanisms regulating cancer cells' signaling and aggressiveness [45].
Lastly, proteins can also exert the function of membrane transporters, in the form of carriers and channels that undergo conformational changes, enabling the selective transport of molecules such as ions, sugars, and amino acids.

A more exhaustive discussion regarding a specific protein, called caveolin-1, will be given in the Future Plans section, underlying its importance in Her2 migration outside caveolae domains, where HER2 is an oncogene overexpressed in the majority of breast cancers and belongs to the family of EGFR [44].

2.2 Biological functions of cell membrane subdomains

Over the past decades, numerous studies highlighted the function of lipid domains in diverse cellular processes including cell adhesion and proliferation, cell survival, as well as cholesterol metabolism [46]. These processes, regulated by the dynamic interplay between lipids, proteins, and sterols, involve a diverse number of plasma membrane events that range from protein sorting, molecules trafficking, cholesterol recruitment, and signal transduction [47]. Among them, four main functions of our interest will be reviewed: cell signaling; lipid raft integrity; cholesterol recruitment; molecule trafficking.

At the basis of cell signaling events, there is the continuous regulation of protein-protein interactions and reshaping of lipid domains, in response to internal/external stimuli, thereby triggering signal transduction cascades, as well as the activation of specific membrane receptors. On these grounds, many signaling events have been reported, including those related to the immune system with the activation/inhibition of receptors such as T-receptors, or the one regulating cell adhesion and proliferation through the activation of EGF receptors [48]. In this regard, recent evidence has also reported that lipid domains by affecting the redistribution of integrins, may facilitate integrins' mediated cell adhesion and migration, contributing to cancer formation and tumor metastasis [49]. Thus, lipid domain composition changes, and the modulation of those membrane receptors populating these regions, might represent new strategies for early cancer detection, and for the development of new therapeutic strategies respectively [50]. In synergy with lipid rafts, another type of cell membrane sub-domains called caveolae, are involved in signal transduction within the cell, vesicular transport, as well as in cell migration. They are described as cell membrane invaginations enriched with gangliosides (e.g. GM1 and GM2), membrane receptors such as EGFR, and proteins clustering as for Her2 [51]. Interestingly, the ganglioside's interaction with Her2 protein is thought to modulate Her2 dimerization activity, thereby modulating its local density [52].

In a similar way, lipid subdomain integrity, usually dependent on cholesterol amount, represents a fundamental condition for cell survival and correct functioning. It indeed plays a primary function as a structural element of cell membrane architecture, and indirectly in the modulation of signaling events when its concentration is altered, being the key recruiter of signaling molecules. Even though the extent of the impact that lipid raft integrity loss has on cell behavior varies depending on the cell line and patho/-physiological status, common secondary events range from protein kinase activation or deactivation, alteration of intracellular calcium levels, to apoptotic membrane receptor

activation [53]. For the cell line of our interest, the MDA-MDA-231 triple negative breast cancer cell line, it has been observed that the lipid raft integrity loss can lead to a reduction of its invasiveness, adhesion, and to an inhibition of cell proliferation [54].

In addition to what has been reported so far, lipid domains also play a regulatory role in the molecules trafficking across the bilayer. In this regard, the possible routes for the intracellular trafficking can be distinguished into clathrin-dependent lipid raft-mediated endocytosis, or clathrin-independent caveolae-mediated endocytosis in the shape of coated pits [55], where caveolae and lipid rafts are identified as membrane microdomains enriched in sphingolipids and cholesterol molecules. These processes mediate the internalization of a heterogeneous population of molecules, ranging from GPI-anchored proteins, glycosphingolipids, and ligands, to external pathogens, as well as a recently discovered class of cellular vesicles known as extracellular vesicles [56, 57], whose potential in triggering diverse cellular events will be discussed in Chapter 4.
It is noteworthy that the diverse cellular trafficking events, are dependent or might be accompanied by membrane curvature changes, lipid acyl chains properties responsible for membrane fluidity, lipids and proteins partitioning over the membrane, as well their association and crosstalk [58]. A schematic representation of the cellular processes regulated by lipid raft domains is reported in Figure 2.3.

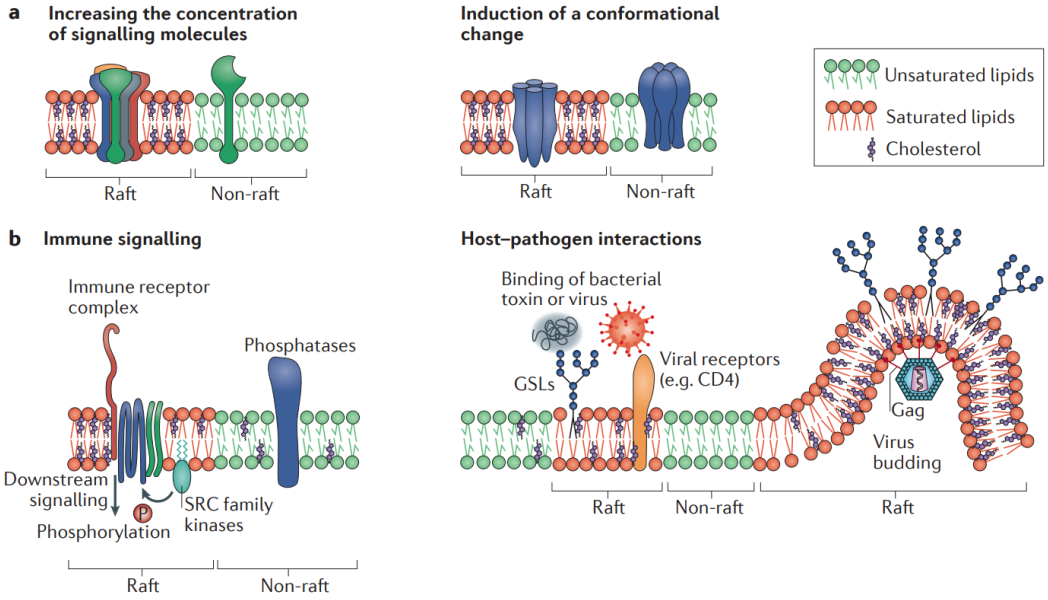

Figure 2.3: Mechanisms through which lipid rafts are able to regulate cellular functions [59].

For what concerns the class of extracellular vesicles, multiple mechanisms have been

proposed for the selective extracellular vesicle uptake and its delivery inside the target cell. Among them, the most accepted routes by the scientific community include clathrin-mediated endocytosis (CME), macropinocytosis, phagocytosis, and plasma or endosomal membrane fusion [60]. The roles of lipid rafts and specific protein-protein interactions have also been studied. The general picture of their intracellular journey is proposed to rely on three main stages: first the transport to the cell membrane, secondly the fusion with the membrane, and lastly the delivery. At this last stage, two possible fates can be met, either the formation of endosomes which will inherently mature into lysosomes, where the molecular content is degraded, or become multivesicular bodies (MVBs), thus transferring their molecular content into the extracellular space [61].
Even though a clear understanding of the EV uptake and delivery mechanisms is still missing, it is clear that it will be beneficial for the designing of novel drug delivery systems. With the proposed work we thus aim to explore, as reported in Chapters 6 and 7, the possible driving forces regulating the EV interaction with a biomimetic cell membrane.

2.3 Cholesterol role in lipid rafts

Cholesterol is one of the main regulators of cell membrane architecture, playing a central role in the modulation of membrane fluidity, segregation of lipids, and membrane trafficking by mediating many signaling events. Moreover, numerous studies proved its critical function as a precursor and signaling molecule of pathological conditions such as Alzheimer's disease and cancer, when its metabolisms are altered [62].
It represents the major building block of lipid rafts, functional areas of cell membranes, ranging from 10 to 200 nm in lateral size, where the selective recruitment and colocalization of membrane proteins and signaling molecules take place. Even though it is still not clear what are the main regulators of cholesterol lateral distribution and segregation within lipid bilayer compartments, it has been demonstrated that cholesterol interacts differently depending on the lipid acyl chains degree of saturation and headgroups, displaying a preferential affinity for phospholipids and glycosphingolipids with saturated acyl chains such as sphingomyelin (SM) [63, 64]. These findings were fundamental for the understanding of lipid raft formation principles. Indeed, the first consequence of this preferential interaction, is the lipid-lipid phase separation, explained as follows.

In the absence of cholesterol, depending on the geometry and nature of lipids, they can adopt different configurations, ranging from planar lipid bilayer or with positive/negative curvature (see Figure 2.4) [65], which depending on the temperature of the system, will be in the gel (or solid ordered, S_o) state and fluid (or liquid disordered, L_d) state. In most cases, the first condition (S_o phase) is verified when the lipids are below their

transition temperature (T_m), forming a bilayer with acyl chains tightly packed and fully extended. Whereas, when the lipids are analyzed above their transition temperature, they will typically be in the second configuration, characterized by a lower degree of order and the acyl chains now loosely packed. In other terms, the two states will be characterized by low and high fluidity respectively [66].

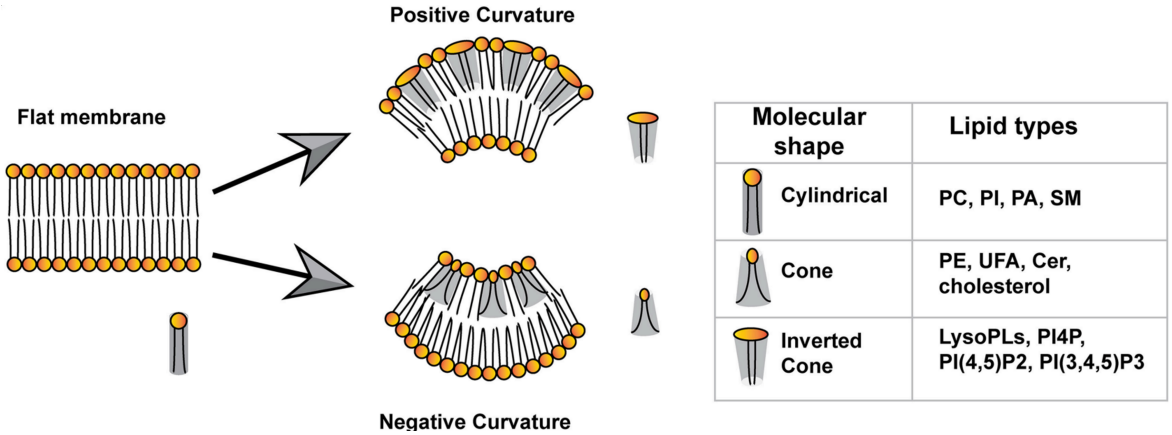

Figure 2.4: Models of lipid bilayer curvature depending on lipid molecular shape. The insertion of lipids with cylindrical shape generates a planar membrane, whereas for the case of a cone or inverted-con shape a negative or positive curvature arises. Adapted from [65].

Accordingly, when cholesterol molecule takes part in the membrane organization, it plays a mutual role depending on the characteristic T_m of the lipids is interacting with. For high-melting saturated lipids, cholesterol is known to have a fluidizing effect, shifting the tight packing of lipids to a more disordered state, the liquid-ordered phase. Contrarily, cholesterol association with phospholipids with low-melting T_m, has an ordering effect, also known as the condensing effect, leading again to the formation of a lipid bilayer with intermediate packing degree and fluidity [66, 67]. A schematic representation of the cholesterol ordering and packing effect is reported in Figure 2.5.

As a consequence, in a multicomponent lipid mixture, the phase behavior of each lipid will be determined by the relative association and distribution of cholesterol, leading to the coexistence of distinct phases. Based on that, the most accepted vision of cell membrane exhibits the presence of segregated liquid-ordered domains, surrounded by a sea of lipids in a more disordered and fluid state [69]. In Chapter 5 and Chapter 6, the lipid raft model will be illustrated, explaining the experimental details that have been considered for the formation of fluid-fluid phase separation and to achieve lipid bilayer stability in physiological conditions.

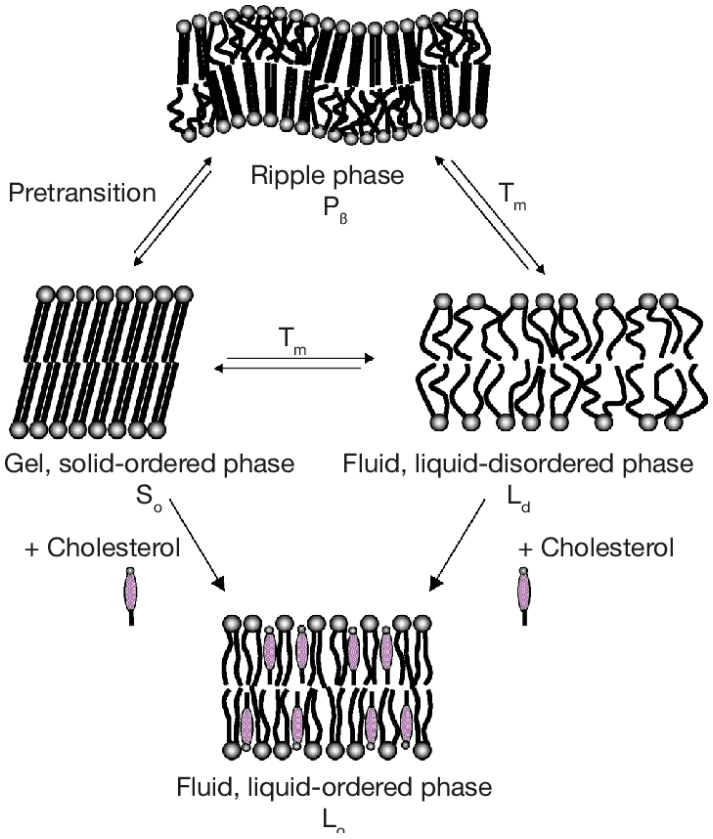

Figure 2.5: Lipids physical states depending on temperature and cholesterol molecule insertion within the acyl chains. Adapted from [68].

The nonuniform distribution of cholesterol within the lipid bilayer, and the dynamic turnover of lipids and proteins in lipid rafts, are believed to have pathological implications, ranging from neurological diseases, and inflammatory processes, as well as cancer formation. In particular, the modulation of membrane protein activity by cholesterol level alteration has been extensively studied. Surprisingly, it has been demonstrated that altered cholesterol concentrations can have a dual effect, both positive and negative, depending on the specific protein the cholesterol is interacting with [70]. In particular, it has been reported that cholesterol can modulate a large number of protein activities (e.g. membrane receptors, ion channels, transporters, and peptides), via both direct interactions with the protein, and indirectly by modulating the physicochemical properties of cell membrane such as with an increase in the lipid bilayer thickness, or by altering the hydrophobic mismatch between the lipid-phase separated domains and the surrounding lipid bilayer [71]. Numerous studies have demonstrated for example the high sensitivity of ion channels to cholesterol homeostasis, where in

most cases cholesterol leads to the suppression of ion channel activity. However, there are also some exceptions where cholesterol plays a fundamental role in the opening and conductance of ion channels such as for nicotinic acetylcholine receptor (nAChR), where it regulates the ligand-receptor channel activity [72, 71]. Cholesterol homeostasis has also been proposed to be critical in the regulation of cell membrane rigidity and lipid raft integrity, thus playing a central role in diseases such as Alzheimer's disease (AD) and cancer. In the first case, cholesterol was proposed as a regulator of the neuronal membrane structure, thus modulating the synaptic functions and neuronal cell plasticity. In particular, for AD patients, a reduction of cell membrane fluidity was observed. In this regard, a dual and controversial effect of cholesterol was observed, both preserving the membrane degree of order and fluidity of cell membrane from amyloid beta peptides ($A\beta$) disordering effect, while on the other side, a lowering of cholesterol level has been shown to be beneficial in AD therapies [73]. A possible explanation of this dual function has been provided and takes into consideration the cholesterol-$A\beta$ type of interaction and integration in the cell membrane. In the first case, cholesterol association with $A\beta$ prevents the entering of other peptides that would form fibrils. Conversely, in the second case, cholesterol would facilitate the tilting of $A\beta$ peptides, thus favoring the formation of open channels in the membrane [72]. In the context of cancer, the extent of the cholesterol impact has been shown to be dependent on the specific tumor-originating site and the cancer stage. Numerous studies have demonstrated that impairment of cholesterol level, in particular with cholesterol depletion from lipid rafts, is usually associated with a reduced rate of cell adhesion, proliferation, and invasiveness [54, 74]. Moreover, many oncogenic pathways have been associated with lipid rafts, including the impairment of apoptotic pathways where the up-regulation of AKt signaling promotes cancer cell survival and growth. This is also accentuated by the high colocalization and clustering of growth factor receptors such as HER2 and EGFR, within lipid rafts areas. In this line, upon lipid raft integrity loss or variations in plasma membrane cholesterol, the activity of integrins and glycoproteins like CD44 can be affected as well, leading to the progression of metastasis [75].
Given the remarkable importance of cholesterol in modulating cellular processes and lipid rafts associated integrity and functions, in Chapter 7 the role of cholesterol in mediating small-EVs adsorption processes will be discussed.

Chapter 3

Model membrane systems

3.1 Overview of lipidic platforms

Given the high complexity and dynamism of cell membrane architecture and composition, and the associated challenges (e.g. sample preparation, spatial and temporal resolution) in studying the factors involved in the regulation of its properties, many diverse model membrane systems have been developed over time. Despite differing in terms of size, composition, and geometry, they all should satisfy the main requirements of mimicking the lipid bilayer geometry and asymmetry when possible and also include the threesome of a phospholipid, sphingolipid, and cholesterol as the main chemical components.
The most diffused model systems include vesicles (e.g. liposomes, giant vesicles), planar bilayers (supported-, suspended-lipid bilayers), bilayer fragments from cell membrane, and hybrid systems. They have been widely used to investigate problems ranging from protein-lipid interaction, lipid phase separation, membrane fusion, and molecule trafficking. Recently, great effort has been also devoted to the development of increasingly sophisticated lipid bilayer atomistic models [76]. The great advantages of working with model systems are the versatility of tunable parameters and the number of techniques that can be applied to study, with a closer look, the roles of single components in the regulation of cell membrane's biological processes.

The three main model systems adopted in the thesis are discussed as follows [6].

Liposomes are defined as artificial and spherical vesicles, in the range of 30 nm to several micrometers, displaying a hydrophilic core and a hydrophobic lipid bilayer. Their structure is the result of the self-assembling of lipids when they are suspended in aqueous solution, forming an amphiphilic structure due to the hydrophobic effect [77]. Because of that, they are now widely adopted as nanocarrier systems, where the loading of both hydrophilic and hydrophobic molecules can be performed. Not only,

they are also suitable to study lipid phase separation, and membrane processes such as membrane pore formation or molecules uptake, this time without the influence of the rigid substrate [78].
They can be prepared following different methods, such as sonication, electroformation, sequential steps of lipidic solution extrusion through a porous membrane, or freeze and thaw cycles. They mainly differ in terms of size distribution that can be achieved (small size around $15-50\ nm$ for the first two methods, and larger diameter for the last ones, in the range of $50\ nm$ to $200\ nm$), sample integrity, and yield of drug loading and proteins insertion into the lipid bilayer. In particular, among the two most adopted methods, sonication and extrusion, the extrusion method is more suitable for good drug loading efficiency and lipid stability, also providing a higher integrity of liposome structure. The latter is indeed affected by the high-temperature generation during the sonication process. Lastly, the extrusion method ensures also a better size distribution and size reproducibility over the sonication method, by extruding the lipid solution through a polycarbonate membrane with a defined pores size [78, 77], as reported in Figure 3.1.

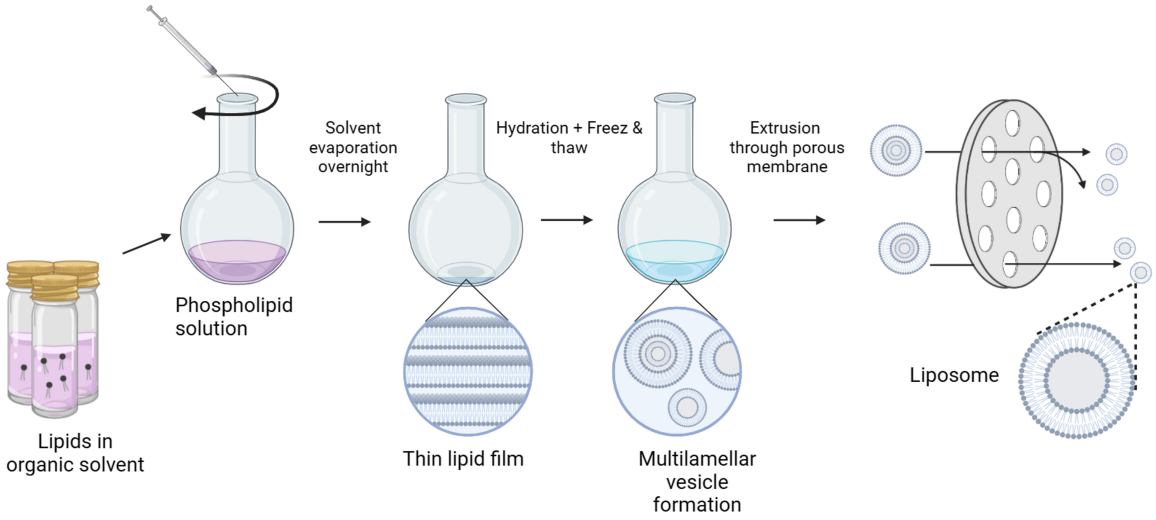

Figure 3.1: Schematic illustration of the liposome preparation method adopted in the thesis. The protocol consists in the two main steps of thin lipid film formation and lipid solution extrusion through a porous polycarbonate membrane of defined pore size.

On the other side, supported lipid bilayers were first proposed by Tamm and McConnell, in 1985, as a model for mimicking the lipid bilayer architecture of plasma membranes. They are described as planar lipid bilayers where lipids self-assemble when deposited over a rigid substrate. The main advantages of this platform are the following: easy preparation and low time-consuming; applicability to a wide number of detection techniques; versatility of applications depending on substrate properties;

stability under various environments and composition complexity. Even though the lipids are in close interaction with the substrate, it has been demonstrated that a thin layer of water (in the range of $1 - 2nm$) always forms, thus partially preserving the lateral and rotational mobility of the single lipids as well [79].
The most widely adopted deposition method relies on the direct vesicle fusion of unilamellar liposomes, obtained with the sonication or extrusion methods, as previously described, over rigid substrates. It consists of the drop-casting vesicle deposition, followed by their progressive adsorption and spontaneous rupture over the rigid substrate. Depending then on vesicles parameters, such as the lipid composition and concentration, buffer, and lamellarity, the supply of salt such as $CaCl_2$ is generally used to facilitate the vesicle rupture. A schematic representation is reported in Figure 3.2. Moreover, it has been demonstrated that the physical properties of the substrate itself

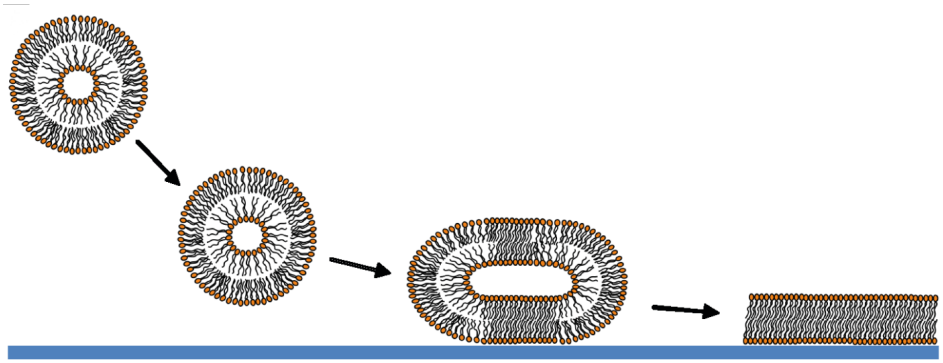

Figure 3.2: Direct vesicle fusion method for supported lipid bilayer formation [68].

can affect the successful lipid bilayer formation and lateral phase separation, including the roughness, chemistry, presence of impurities, morphology, and temperature [80, 81].

Despite the advantages proposed so far, some shortcomings of this approach are related to the difficulty in the reconstitution of transmembrane proteins within the two layers, often due to the strong protein-substrate interactions, and the lack of physical space depending on the structure and molecular weight of the protein of interest. To that end, tethered and suspended lipid bilayer were proposed to address the main problem of transmembrane protein integration within the lipid bilayer [76].
The first one consists of the interposition of a 'cushion' of long-chain molecules such as polymers, thiols, and silanes [79]. The second one instead, consists of the direct fusion of lipids over a porous membrane, in order to obtain free-standing lipid bilayers, with the proteins now localized within the suspended regions of the lipid bilayer [82, 83]. The two main advantages coming with these approaches are the increased space between the lipids and the substrate, but most importantly the preservation of protein activity, which otherwise would undergo denaturation. However, the analysis of these

platforms requires the use of non-invasive detection techniques, as the degree of the stability of lipids assembly is lower compared to the classic supported lipid bilayer.

For both the supported and free-standing lipidic systems, the most adopted substrates include atomically flat mica, gold, glass, and quartz, which mainly differ in terms of roughness, chemistry, and transparency. Apart from that, the main requirement to get a defect-free membrane and sufficient lipid mobility is substrate hydrophilicity. Moreover, the choice of the more suitable substrate should also take into account the possibility of chemical modification, and the compatibility with the techniques to be used for their characterization, combined with the specific application purpose.

Similarly to liposomes and supported lipid bilayers, giant unilamellar vesicles are used for the investigation of lateral lipid phase segregations, localization and activity of membrane proteins, mechanisms of structural membrane deformations upon interaction with chemical molecules, as well as for studying membrane proteins localization and activity when reconstituted within the lipid vesicle [84]. Being characterized by a much larger curvature and size over the other two systems, with a diameter in the range of $1 - 100\ \mu m$, they are able to better mimic the typical size of biological cells. This also extends their application to the light-microscopy investigation, which is otherwise critical for the previously discussed methods due to resolution limits. Lastly, because of their large size, they are often preferentially adopted in applications that involve the formation of a lipid bilayer over a pore-spanning membrane.
However, the main disadvantage of this platform is the critical preparation procedure, with limitations in terms of lipid composition (i.e. charged lipids) and solution (i.e. buffer with low ionic strength) [85]. The two most diffused methods are the electroformation and emulsion methods (w/o/w emulsion). The former displays the main limits of poor encapsulation efficiency of large water-soluble molecules, with constraints in terms of lipid ratio between charged lipids to get stable vesicles over time. The main drawbacks of the latter include the formation of lipid aggregates and the difficulty in the full removal of oil residues, causing sample contamination [84]. Preliminary tests with the water-oil emulsion method, not reported in the thesis, have been performed at the Nanoinnovation Lab, with the adopted protocol schematically illustrated in Figure 3.3.

3.2 Characterization methods

Numerous characterization techniques have been proposed for the study of lipid model systems and they can be divided mainly depending on the geometry of the model (spherical lipid vesicles and supported bilayers) and the final application purpose.

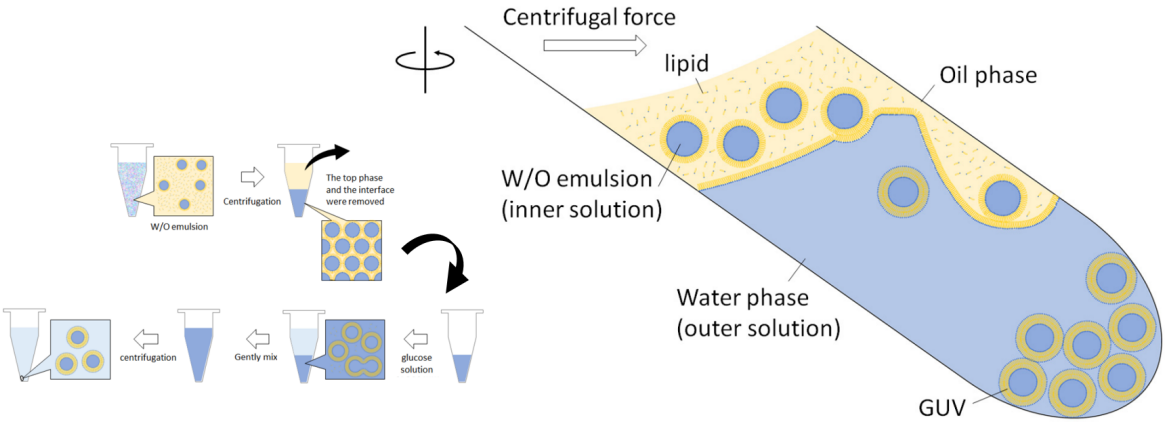

Figure 3.3: Schematic representation of the water-oil emulsion method for GUV synthesis. Adapted from [86].

For planar-supported bilayers, the main investigated features are the following: topography of lipid bilayer with analysis of lipid phase separation, usually performed with atomic force microscopy [87]; monitoring of lipid bilayer formation and quantification of mass deposition, with quartz crystal microbalance with dissipation monitoring (QCM-D) [88]; neutron reflectometry-based analysis to detect lipid bilayer thickness changes and asymmetry [89]; fluorescence recovery after photobleaching (FRAP) to monitor lipid lateral diffusion [90].

The working principles of QCM, neutron reflectivity-based method, and FRAP are briefly described as follows:

- QCM-D: the basic mechanism consists of the detection of the quartz crystal oscillation variations upon mass deposition. In particular, the crystal is positioned between two electrodes and an AC voltage is applied, causing the crystal to oscillate. The detected frequency change will thus be proportional to the quantity of mass deposited over the substrate. Based on these considerations, this tool is used to quantitatively measure the mass and energy-dissipation properties of thin films. These two parameters allow the monitoring of the lipid bilayer formation over time, providing insights into the kinetics of the lipid vesicle rupture over the substrate and the degree of coverage during the film formation process. This measurement capability makes this technique useful for providing quantitative information on lipid bilayer uniformity, and thickness, other than viscoelastic properties. Due to the high sensitivity to mass variation, the rate and dynamics of molecules interaction with the lipid bilayer can be characterized as well. Moreover, this platform has the advantage of being suitable to different types of

substrates (e.g. silicon, titanium oxide), thus widening the number of applications that can be tested, depending on the experimental needs [91, 92].

- Neutron reflectometry: the working principle consists of probing the intensity of neutrons that are reflected from the sample's surface, where the intensity of the reflection will change depending on the structure and composition of the sample. Displaying a sensitivity at the Å level, with neutron reflectometry is possible to investigate the structural composition of each leaflet forming lipid bilayer systems. In particular, a reflectivity curve is acquired by measuring the ratio between the incoming and reflected neutron intensities, and contains information about the composition and structure of the lipid bilayer. Depending then on the fitting model adopted, the single contributions of both the outer/inner heads/tails of the SLB can be characterized. [93]. As a consequence, this technique represents a valuable tool for investigating diverse phenomena, including lipids phase transition, packing density, chemical composition, and interaction with other biomolecules.

- FRAP: the working principle consists of the selective excitation and disruption of fluorescent molecules in a defined area of interest, via sample excitation with a high-intensity laser. The recovery of the excited fluorescent molecules is then monitored over time by exciting the sample with a low-intensity laser light. Based on this working principle, FRAP allows to investigate the dynamics of lipids and protein diffusion in biomimetic systems, where the parameter of the diffusion coefficient is determined by the recovery time of the fluorescent molecules. However, one drawback of this technique is that the diffusion coefficient is strongly dependent on the analyzed area, as well as on eventual transient trapping events that would limit the molecule diffusion. Moreover, the difficulty of accurately establishing the intrinsic photobleaching of the fluorescent probe, and estimating whether the molecule motion is Brownian or not, might in part limit the throughput of this technique [94, 95].

Among the above-mentioned techniques, the AFM has been chosen to be the master technique of the proposed thesis project. The working principle will be described, illustrating the advantages and limitations of this technique, as well as the possible applications.
AFM was first invented in 1986 by Gerd Binnig, Calvin Quate, and Christoph Gerber [96], and is now widely adopted in numerous research fields, ranging from material science, chemistry, physics, and biology. It is classified as a scanning probe technique, where a sharp tip, attached to a flexible cantilever is scanned over the sample. The tip is usually coated with a reflective material, over which a laser beam is first focused, and then reflected off the cantilever toward a four-quadrant position-sensitive photodetector (PSPD). During the scanning, the cantilever will deflect in response to the

interaction forces between the tip and the sample, causing a shift in the laser beam position. This electronic signal is then sent to two different paths: to a piezoelectric actuator through a feedback loop, causing the motion of the AFM probe (complex of cantilever and tip); to a converter unit and controller for the final image formation. A schematic of the AFM setup and working principle is reported in Figure 3.4.

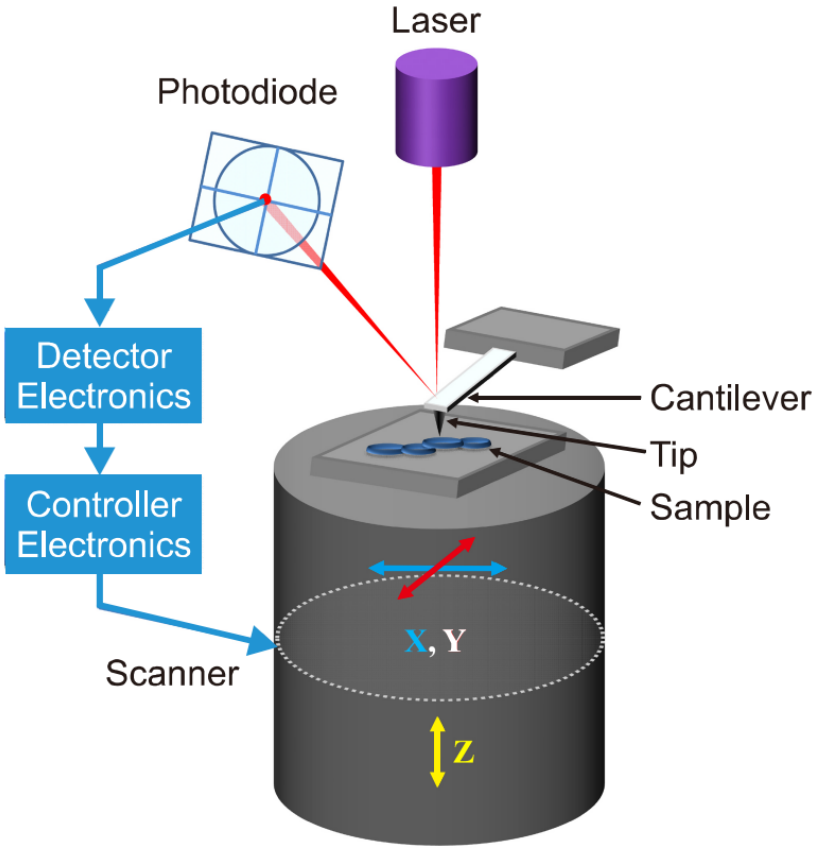

Figure 3.4: Schematic representation of an Atomic Force Microscopy setup and working principle. Adapted from [97].

AFM analysis is usually carried out to achieve high spatial resolution information of the sample under investigation. It is indeed able to provide a lateral resolution of around $\sim$ 30 nm in standard AFM imaging, and down to $\sim$ 3 nm in high-AFM modes, with a vertical resolution down to $\sim$ 0.2 nm [98, 99]. The lateral resolution is mainly limited by the tip, whose radius typically resides in the range of 10 nm to 40 nm. However, with the advent of new fabrication methods, cantilevers with progressively smaller sizes are now starting to be produced, thus allowing for improvement in the dimensional resolution limit. Moreover, with the introduction of the cantilever photothermal excitation, instead of the classic acoustic piezo actuation, more stable

and faster imaging can be performed. The AFM performance has then been recently further improved by converting the cantilever from a classic detector into a combined detector and actuator, leading to a significant increase in the scan speed (i.e. order of tens of seconds for a standard 256 $\times$ 256 pixel image) [100], and fine-tuning of the interaction forces between the cantilever tip and the sample. Using the cantilever as a direct actuator is now possible to perform quantitative mechanical measurements, with the application of unparalleled forces down to the pN [101]. The continuous launch and implementation of new AFM setups and imaging modes, is thus pushing further, year by year, the potential of AFM as a powerful and versatile technique.
The diverse imaging modes (i.e. contact, dynamic, electrical, and force spectroscopy), mainly differ in the type of interaction they can probe (i.e. physical, chemical, electrical), and on the sample properties that can be detected as a consequence (e.g. topography, composition, conductivity, deformability).
The basic working principles of the fundamental AFM modes are illustrated in Figure 3.5 and described as follows:

- Static Mode: the probe is kept in continuous contact with the surface while it scans the sample. This imaging mode is suitable for robust and rigid substrates, and usually performed in air environment. It can operate in two modes, constant force or constant height, but the former is the most diffused. It consists on the application of a constant force by using as a feedback signal the cantilever deflection.

- Dynamic Mode: the cantilever is oscillated close to its resonance frequency while the probe is scanned over the surface. This imaging mode is suitable for the analysis of soft samples, as there is a more gentle interaction and minimal torsional forces are applied, thus minimizing possible damages. It can operate in two modes, amplitude or frequency modulation, where amplitude is the most diffused. It uses as a feedback error the variation of oscillation amplitudes.

- Force Spectroscopy: the cantilever is approached to the sample, and a single force-distance curve is acquired for each point of the sample, or for a defined set of points. It is used to detect parameters such as adhesion forces, stiffness, and rupture forces, on both hard and soft samples.

They can be applied, in most cases, both in air and liquid environments, and in more advanced systems, with the control of environmental parameters such as temperature and CO_2 [102]. These advantages, combined with the possibility of fine force-control of applicable forces and the high sensitivity to an heterogeneous range of sample properties, made it an interesting technique in the field of life science [102].
Diverse applications include the morphological, topographical, and mechanical characterization of cell compartments; nucleic acids and proteins assembly; molecules binding affinity with chemically-modified tips; time-lapse analysis to observe dynamic processes.

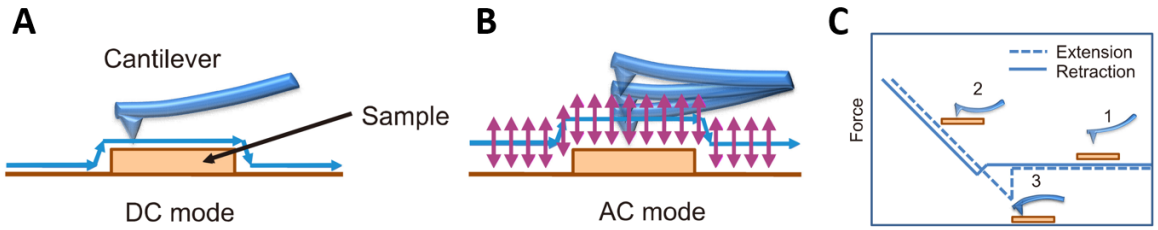

Figure 3.5: Principle of operation modes in AFM: (a) static mode (or contact, DC mode), (b) dynamic mode (or tapping, AC mode), (c) force spectroscopy. Adapted from [97].

For biological samples, the most used imaging method is the dynamic-mode (tapping or AC-mode depending on the company), which consists of scanning the tip while it is oscillating close to its resonance frequency. In this imaging mode, the variation of the amplitude of oscillation is the feedback error signal that is used to adjust the motion of the cantilever. The advantages of this imaging mode are mostly related to the intermittent contact between the probe and the sample, which allows to maintain the tip sharpness over long measurements, to preserve sample integrity, and finally to minimize the torsional forces. These are fundamental requirements when performing the imaging of soft samples, i.e. polymers, nanoparticles, cells. Moreover, the improvements that have been performed in terms of combined instrumentation of AFM with other optical and spectroscopical techniques, allowed to widen the number of applications and to assess a higher number of parameters and multiple sample's properties. Some examples relate to the combined systems of AFM-Fluorescence microscopy (AFM-FL), able to correlate for example cell biomechanical properties with their membrane potential, or AFM-Infrared (AFM-IR) microscopy to simultaneously obtain a topographical and chemical map of the sample of interest [103].

For liposome-based model systems, differential scanning calorimetry (DSC) studies are widely applied for the characterization of lipid phase transition. Scattering-based techniques, such as small-angle neutron scattering (SANS) and small-angle X-ray scattering (SAXS); cryogenic electron microscopy (cryo-EM) represent modern techniques for detecting both the structure of lipid vesicles, and the pathways governing the biomolecules uptake pathways with atomic resolution.

The DSC working principle will be here described, whereas the application related to the thesis project will be reported in Chapter 6.
DSC represents a thermodynamic technique that mainly studies the ability of a certain sample to return to its initial equilibrium state, upon thermal perturbation. More in detail, it detects the sample's temperature-dependent isobaric heat capacity, also known

as C_p (T) [104]. The main information that is extrapolated from a DSC analysis, is the first-order phase transition of the system, typically attributed to the maximum peak of the curve, with the identification of the respective characteristic transition temperature (T_m) of the system. This value defines the temperature at which the system transits from the solid to the liquid-crystal state. By then integrating the area under the peak, the enthalpy contributes (ΔH) is determined as well. The entropy contribution instead, can be estimated as a function of ΔH and T_m $(\Delta S = \frac{\Delta H}{T_m})$. A representative DSC setup is illustrated in Figure 3.6.

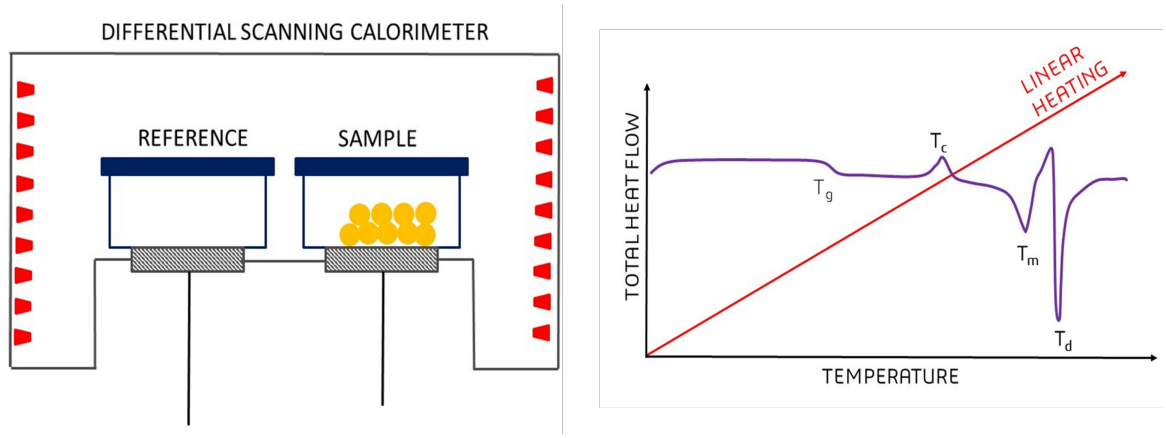

Figure 3.6: Schematic representation of a standard Differential Scanning Calorimeter setup. Adapted from [105].

Based on these considerations, and remembering that lipids have a characteristic phase transition temperature, above which they are found in the liquid-disordered (L_d) state, and below which they are in the solid state (S_o), DSC represents an interesting technique for studying the thermodynamics of lipid phase transition. Moreover, information about lipids cooperativity, degree of ion binding, or structural modification of the chain length can be extrapolated as well [106]. However, while for a system composed of one single lipid component, the identification of the main transition peak is relatively simple, for a more complex system this is not equally true. Indeed, for a multi-component system, the phase transition is not linear over the investigated temperature range, but it involves intermediate states, causing the formation of asymmetries in the DSC profile, with secondary peaks arising before or after the main transition peak. This is generally attributed to the nucleation of phase-separated domains along the investigated temperature range. For these systems, it is of particular interest the analysis of the degree of cooperativity between the lipids, described by the van't Hoff unit (ΔH_{vH}), which might differ between the heating and cooling ramp [107, 108]. In particular, a less cooperative phase transition generates wider peaks and describes the higher temperature dependence of the lipids during their transition. Despite the valuable information that

can be obtained with this technique, the two main drawbacks relate to the high sample concentration needed to have a good signal-to-noise ratio, and the non-straightforward post-processing of the acquired data and interpretation of results due to the low signal-to-noise ratio.
In conclusion, DSC is a thermal analysis technique, frequently used for studying and designing the lipid compositions of synthetic drug vehicles like liposomes. Indeed, by studying the cooperativity between the single lipids, and the thermodynamic behavior of the mix of lipids with drug molecules, it is possible to identify the optimal composition for maximizing both the molecule's incorporation and pharmacokinetics, but also the stability of the liposomal system in the biological environment after the molecules loading [109]. In this regard, the stability of the lipids system, evaluated through the contribution of enthalpy and T_m, depends on the van der Waals interactions between the lipid chains changes, leading to a different structural lipids conformation. As a consequence, depending on the physical properties of the lipid carrier (e.g. charge, fluidity, composition), and on the additive conformation and affinity for the investigated carrier, a different interaction can be detected by observing variations in the transition temperature of the system, i.e. shift of the T_m peak, increase of the T_m width, and in some cases the abolition of the pre-transition peak, or the formation of secondary peaks [107, 110]. In the same direction, recent studies have been carried out in the field of extracellular vesicles, to evaluate their uptake rate and kinetics, as well as possible structural conformation changes in the recipient lipid carrier. Moreover, by testing different functionalization strategies of the EVs surface, is also possible to evaluate in which physical and chemical conditions the uptake is maximized. In particular, it has been demonstrated that after EV interaction with the lipidic carrier in the shape of liposome, it was possible to observe two different effects between the inner and outer layer, with an overall increase of both T_m and ΔH, that have been motivated considering a global ordering effect given by the EVs mixing with the lipid bilayer [111].

Chapter 4

Extracellular vesicles

4.1 What are extracellular vesicles

The concept of extracellular vesicles was initially introduced in 1946 by Chargaff and West [112], and further explored by Wolf in 1967 [113], who referred to them as platelet dust. Subsequently, in 1980, the first insights into the mechanism of their secretion emerged [114]. This process was proposed to involve the formation of a multi-vesicular body (MVB) and its subsequent fusion with the plasma membrane (PM), ultimately resulting in the release of vesicles into the extracellular space. The increasing interest over the years led then to the formulation from the International Society for Extracellular Vesicles (ISEV) in 2018, of a new definition that describes them as "particles naturally released from the cell that are delimited by a lipid bilayer and cannot replicate, i.e. do not contain a functional nucleus" [57]. With this general definition, particles of heterogeneous size (30 nm to 1000 nm) and biogenesis mechanisms are included. Subsequently, the introduction of the MISEV 2018 guideline marked the initial effort to establish classification criteria based on their biogenesis, leading to their categorization into three primary families: exosomes that originate from the endolysosomal pathway, through the inward budding of the plasma membrane, with a size of $30 - 150$ nm in diameter; microvesicles (MVs) with a size of $50 - 1000$ nm and apoptotic bodies in the range of $500 - 2000$ nm, which both originate from the outward budding of the plasma membrane, from healthy and apoptotic cells, respectively. The corresponding biogenesis process and interaction with the recipient cell are illustrated in Figure 4.1. However, this classification only partially solves the issue of the clear distinction among different populations, as the study of the biogenesis mechanisms, as well as the identification of specific molecular markers, together with the great size overlap, still represents one of the major challenges in the EV field. For these reasons, a different nomenclature is now adopted, which refers for example to the physical parameter of the vesicle's size (i.e. small-EV for vesicles smaller than 200 nm, medium/large-EV for particles bigger than 200 nm).

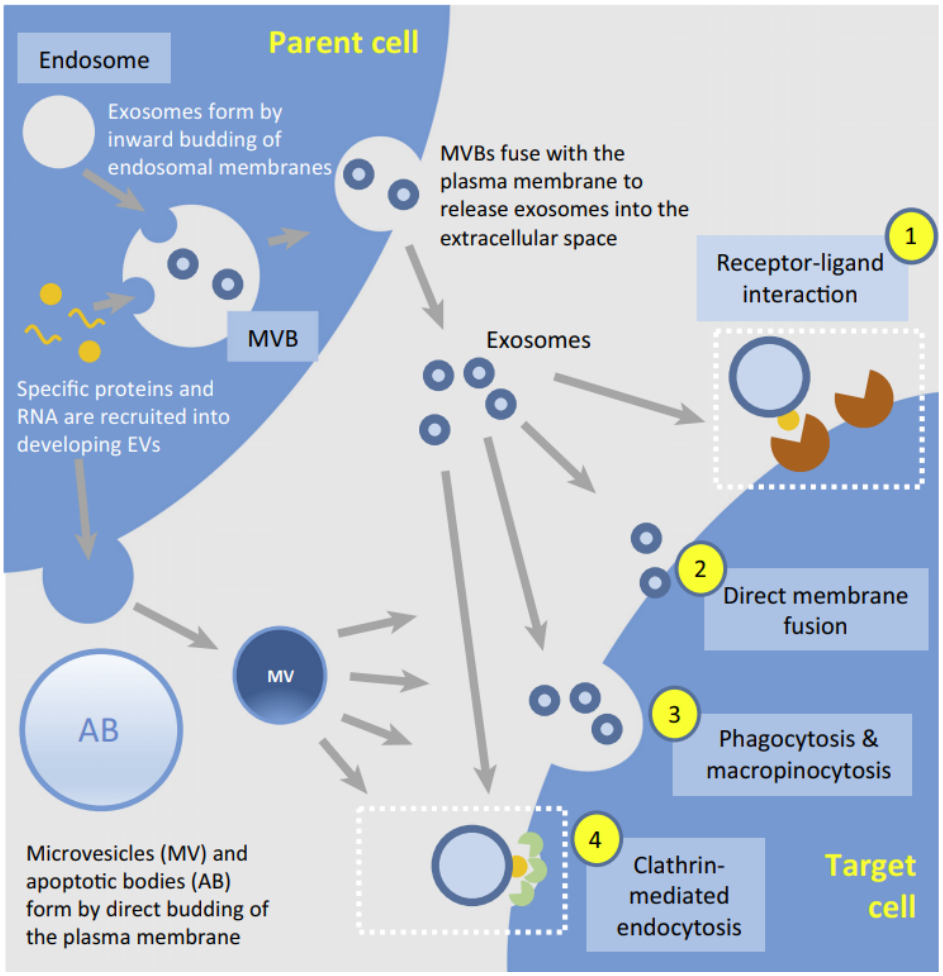

Figure 4.1: Schematic representation of EV biogenesis routes, and different pathways of small EVs interaction with recipient cell [115].

Focusing on small EVs, it has been demonstrated that they are released by all types of eukaryotic and prokaryotic cells, both in pathological and physiological conditions. The biogenesis process, as explained before, has its origin in the endosomal compartment, upon inward budding of the membrane with the formation of a multivesicular body (MVB). Extracellular vesicles are then the result of intraluminal vesicles formation within the endosomal MVB. Lastly, after late endosome maturation, the MVB can then release the vesicles, in the extracellular space upon fusion with the cell membrane. Subsequent studies have demonstrated that small EVs biogenesis is also directly correlated with the sorting of cargo molecules, through the Endosomal Sorting Complex Required for Transport (ESCRT) machinery. The process can be summarized in four steps as follows: the first recognition and binding to ubiquitinated proteins in the late

endosomal membrane, initiation of the inward budding of the endosomal membrane, and the final sorting of the proteins into the ILVs. Upon maturation of the late endosome, MVBs can either fuse with the plasma membrane, releasing the now-called exosomes (or small-EVs) in the extracellular space, or degrade their cargo upon fusing with lysosomes. However, it has to be underlined that MVB formation was observed even when the ESCRTs were inactivated.
Due to the suggested biogenesis process, extracellular vesicle composition is recognized for mirroring that of their parent cells. Consequently, they carry the biological information regarding the cell's condition at the time of production, encompassing a spectrum of lipids, cholesterol molecules, non-coding DNA or RNA, as well as membrane and cytoplasmic proteins. Furthermore, they exhibit an enrichment of a specific protein class known as tetraspanin proteins (such as CD9, CD63, and CD81), which have gained recognition as essential biomarkers for identifying and categorizing small EVs. Notably, the tetraspanin protein levels are found to be overexpressed in cancer cells.

Over the past decades, the vision of EVs as cell disposal systems for waste products has given way to a more complex picture that describes them as functional vesicles involved in the active regulation of numerous cellular processes including intercellular communication, tissue regeneration, immunostimulation, and cancer progression. Thanks to the small size and the great similarities with the cell of origin in terms of molecular composition, they can travel along the body fluids (i.e. blood, urine, saliva) and to cross the biological barriers, without inducing an adverse immune reaction.
Although a non-universal composition has been identified, many studies have demonstrated that EV functions are directly linked to specific cargo loading. In particular, depending on the cell line and biological context, it has been reported that DNA, found both on the surface or within the lumen, can be present both in single or double-stranded configurations, and depending on that it can affect the ability of EVs to interact with extracellular matrix molecules. On the counterpart, mRNA abundance can affect their ability to alter the recipient cell phenotype. Moreover, mRNA expression is highly dependent on variations in external genetic and environmental stimuli, hence represents an important biomarker for the early detection of pathological conditions. Lastly, protein content and spatial distribution over the EV membrane and lumen, are fundamental players in the regulation of EV biogenesis, cargo sorting, and tropism. Some examples report the functions of cytoskeleton proteins in the regulation of EV release and motility, whereas integrins being involved in the modulation of EV interaction and adhesion with recipient cells, play a central role in the EV's oncogenic activity [116].
In addition to their molecular cargo, recent studies have now discovered the presence of a second crucial mediator of EV activity, described as a thin layer of molecules that associate with the external layer of the EVs surface and are identified as 'protein corona'.

For decades, researchers have extensively worked on the protocol optimization for the production of 'contaminant-free' vesicles, purified from those proteins and lipoproteins normally present in bodily fluids, and now considered fundamental for the preservation of EV functions. The process of EV corona formation starts during their biogenesis and persists once they are released into the extracellular space. This corona is replete with membrane proteins, including apolipoproteins, immunoglobulins, albumin, and fibrinogen, which are shared with synthetic nanoparticles and viruses. Recently, there has been growing consensus regarding the pivotal functional role of the protein corona in modulating the functions of EVs. Many examples demonstrated that by removing the protein corona, the EV functional effects in angiogenesis or immunomodulation were lost, while by regenerating the protein corona with growth factors, these functions were restored [117].
Finally, vesicle size represents another critical parameter influencing the regulation of EVs' biological functions and their interactions with recipient cells. In this regard, numerous studies have been conducted to identify optimal methods for isolation and storage that preserve size and integrity. Interestingly, it was demonstrated that storing sEVs at $-80\ ^{\circ}C$ results in a time-dependent reduction in EV concentration, an increase in median size, and a concurrent rise in protein contaminants [118]. Therefore, it is generally recommended to assess vesicle size and integrity while samples are still fresh, as the isolation methods typically involve the application of gradients and rotational forces, which can inherently impact their integrity.[119, 120].

4.2 Extracellular vesicles in cell communication

Cell communication mediated by EVs is nowadays described as an alternative route through which cells can communicate with each other. The classic route of cell communication can involve the direct contact between neighboring cells, or the exchange of chemical signals between distant cells (i.e. autocrine-, paracrine-, endocrine-signaling). Is thus clear that an impairment in cell communication would have a drastic effect on the alteration of cellular processes, including adhesion and proliferation, survival, and differentiation, and as a consequence, tissue integrity and cellular environment would be altered [121]. In this context, EVs represent a new vehicle of cell communication, delivering biological information (e.g. lipids, proteins, mRNA, nucleic acids, growth factors) throughout the body, and initiating phenotypic changes in recipient cells [122]. Their innate ability to take part in intercellular communication is also linked to their low immunogenicity, and high biocompatibility, letting them travel around the body by escaping the immune surveillance.

They have been proposed to take part in both physiological and pathological processes. Some examples of the former include their role in tissue regeneration, angiogenesis, im-

munomodulation, and stem cell differentiation. On the counterpart, there is evidence of EV enrolment in the regulation of pathological processes such as cancer development, metastasis formation, and progression of neurodegenerative diseases [123].
In the context of cancer, numerous studies reported that EVs released from cancer cells carry this genetic information, which is then delivered to the recipient cell, initiating a cascade of impaired cellular processes, i.e. uncontrolled cellular growth, increased cell proliferation, inhibition of immune response, and induction of phenotypic changes by the selective delivery of RNA subsets, thus favoring tumor invasion [122]. Emerging evidence also recognized the contribution of EVs in the pre-metastatic niche formation and metastasis.
Nevertheless, on the other side, there is evidence that EVs carrying tumor suppressors, such as let-7a, can exert inhibitory effects on tumor cell growth and metastasis, inducing cell death and tumor regression. Moreover, chemical modification and gene engineering represent two approaches widely adopted to enhance the intrinsic inhibitory effect of EVs, and to increase the target specificity and therapeutic efficacy [124, 123, 125]. Finally, looking at EVs as nanocarriers of heterogenous cargo enriched in proteins, lipids, and nucleic acids, opens new paths for the use of EVs as diagnostic tools. Indeed, different studies identified the overexpression of those factors known to be involved in cancer formation, i.e. tumor specific RNA, proteins overexpressed in cancer cells like CD63, TSG101, and caveolin-1, addressing the use of EVs as biomarkers for early cancer diagnosis [126].
Not only, the function of EV in cell communication, can be positively exploited to develop personalized therapies. Different approaches can be followed depending on the desired application, ranging from the passive or active loading of therapeutic drug molecules, genetic engineering to let them overexpress functional molecules such as mRNA and miRNA, or modifying their surface with surface recognition molecules to improve the targeting of the site of interest. However, despite their worldwide accepted valuable role as innovative cell communication mediators, there is still a low understanding of the mechanisms regulating EV functions, as well as the lack of standardized production and purification protocols, and poor clear distinction of the features typical for each sEV subpopulation, limiting their applicability [123].

4.3 Extracellular vesicles isolation methods

Over the years, a wide array of isolation methods has been employed, encompassing size-, charge-, density-, and affinity-based techniques, all with the common objective of obtaining samples with substantial quantities and integrity. While purity has traditionally been a stringent requirement for the past two decades, it is no longer the sole focus. In fact, a less pure sample is now favored to better preserve EV functions. When considering isolation methods, it's essential to consider the specific application

of EVs. For instance, if the intention is diagnostic use, the method that yields the highest vesicle yield should be chosen. Conversely, when EVs are intended for use as delivery systems, the choice should shift to preserving their structural and compositional integrity.
The different methods can be divided as follows:

1. Density-based techniques: differential ultracentrifugation or most commonly UC, is one of the first methods that has been applied in the EV field and is still widely used. It consists of the application of serial centrifugation steps, separating the vesicles based on their density, and applying increasing centrifugation speeds at each cycle. Though is the most popular, it comes with many disadvantages: time demanding, large amount of material needed, high contaminant content, possible sample damaging, and aggregates formation. For these reasons, UC is usually combined with other complementary isolation techniques.[127].

2. Size-based techniques: size exclusion chromatography (SEC) is widely adopted as it is as fast as a simple method, which separates the vesicles based on their hydrodynamic volume or molecular size, by the elution of the sample through a porous stationary phase column. With this technique is only possible to isolate a heterogeneous population of EVs. To overcome this resolution limit, modern SEC platforms adopt two columns characterized by pores of different sizes. Compared to the differential centrifugation (DC) technique, which separates the EVs by applying different rotational speeds, the SEC method better preserves the vesicles integrity. On the counterpart, filtration methods are now taking the lead among the size-based methods, as they are becoming over the time faster, automated, and with higher resolution, even though high sample concentrations are needed. In particular, tangential flow filtration (TFF) is widely adopted and consists of delivering the vesicles under a tangential flow across a hollow fiber membrane. In this way, only the vesicles larger than the cut-off level will be retained in the membrane, to be then recirculated and concentrated [120].

3. Affinity-based techniques: they usually exploit the binding between proteins/receptors of the EV surface and antibodies covalently conjugated to a solid surface such as magnetic beads or polymer materials. A common extension of this technique includes the use of a microfluidic system that allows simultaneous isolation and characterization of EVs (i.e. size, charge) with minimal sample amount. It is generally used to identify subpopulations of EVs expressing specific markers, accurate sample preparation and great knowledge of the sEVs protein content to avoid non-specific interactions [128].

4.4 Challenges in EV analysis

The inherent diversity of extracellular vesicles, including variations in their physical and biological attributes, combined with the wide range of cellular sources from which they originate, renders the detection and characterization of these particles challenging. In addition, the presence of contaminants and the lack of universal isolation and purification methods, make this step even more challenging [129]. A large number of technologies and methods have been developed to characterize the numerous EVs properties. Due to the large variety of sEVs properties and applications, no defined guidelines have been provided in terms of mandatory analysis to be performed, nonetheless, the size and composition characterizations are generally recommended. Some of the most adopted techniques for sEVs characterization are reported in Figure 4.2.

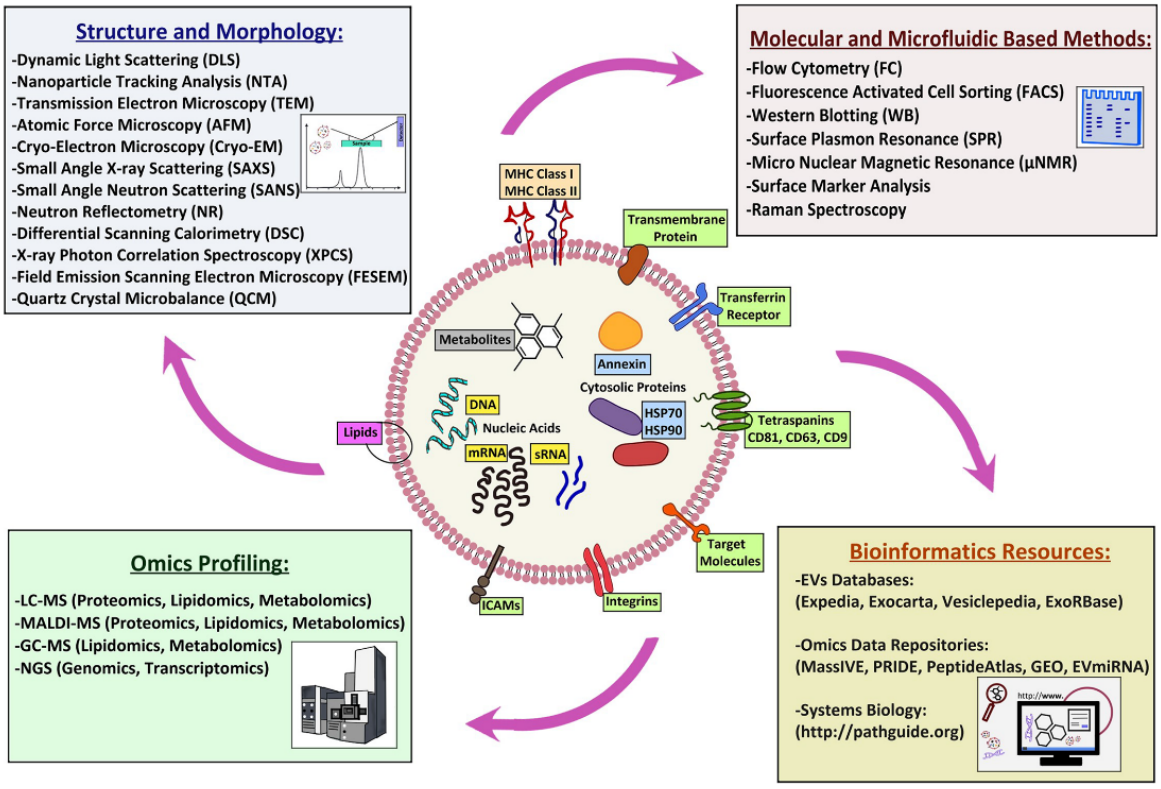

Figure 4.2: Examples of extracellular vesicles characterization techniques [130].

The common methods can be classified as follows: biophysical methods, molecular methods, and more recently microfluidic-based methods [131]. However, so far, each of these technologies comes with its own limitations (e.g. complicated sample preparation, time-demanding, detection limit, accuracy) and limited spectrum of EVs proper-

ties that can be analyzed (e.g. size distribution and concentration), a general approach is to combine the bulk methods, based on the analysis of the heterogeneous population of EVs, with single-particle methods. The main difference is that bulk methods are generally adopted to confirm the successful sEV isolation, and to verify their integrity and general properties as size distribution or protein expression, whereas single-particle analysis allows the characterization of individual vesicle properties, such as the expression of specific bio-markers, mechanical properties, size characterization, in a generally faster and more accurate way [132].

Among the physical technologies, nanoparticle tracking analysis (NTA) and dynamic light scattering (DLS) are widely applied for studying the size distribution. They are both optical-based techniques whose working principle consists of the detection of the light scattering generated by the Brownian motion of EVs in suspension. In the first case is recorded the scattering signal of the single EV Brownian motion is, while in the second case, the output is the percentage of the scattering intensity [133]. However, one of the main limits of these methods is the low detection sensitivity for those particles below 80 nm in diameter. Keeping in mind that EVs size range is $30 - 50$ nm, a great part of the information would be lost. Due to these reasons, ISEV recommends to combine these techniques, with high resolution imaging methods as AFM or scanning electron microscopy (SEM). They are both able to detect single particles with a resolution in the range of few nanometers, providing at the same time insights about the shape and purity of the sample [129]. Moreover, by performing AFM analysis, depending on the acquisition mode, information at the nanoscale related to mechanical properties or binding affinity can be acquired as well, providing a more extensive view of the sample's properties, including the identification of possible EV's subpopulations [133].

Regarding molecular techniques, colorimetric protein assays, such as Bradford, are employed to estimate the total protein content of EVs. Immunoblotting is a common method to confirm the presence of EV biomarkers (e.g., CD9, CD63, CD81, Tsg101) and the absence of contaminants (e.g., albumin, apolipoproteins). However, it is important to note that both of these methods are semi-quantitative and do not offer insights into the individual protein composition of each EV. Their operation involves lysing the EVs to extract the protein content they contain. In the first case, the binding between the Bradford reagent and the free proteins determines a color change that is recorded in the visible spectrum [134]. In the second case, a second step of protein spotting through the SDS-PAGE method is performed to separate the proteins, followed by the final detection of the interaction between labeled antibodies with the protein of interest. On the other hand, immunosorbent assays are used to detect diverse proteins on a larger scale, providing information on protein expression levels and potential EV subpopulations. If the standard methods exploit the EV binding to a functionalized

flat surface, modern approaches adopt the EV binding to the spherical surface (e.g. immuno-magnetic beads) or the integration into a microfluidic system (e.g. ExoChip), enabling a higher capture efficiency [129, 135].

4.5 Extracellular vesicles uptake

EVs have been shown to deliver their cargo through diverse routes, involving both clathrin-dependent pathways and clathrin-independent endocytosis (i.e. caveolin- and lipid rafts- mediated uptake, phagocytosis and macropinocytosis [60]. Despite the extensive effort that has been devoted to studying EVs and their biological potential, a clear understanding of the mechanisms regulating the interaction and fusion with recipient cells is still demanding. Moreover, it has been reported that EVs uptake is directly regulated by the EV molecular cargo and cell origin, with vesicles displaying multiple routes at the same time, but is also dependent on the specific properties of the cell they are interacting with [14]. Finally, the high spatial and temporal resolution required to follow EVs uptake, combined with the still critical steps of fluorescent labeling and isolation of single features, increase the degree of complexity, thus representing a limit to the degree of knowledge that can be reached.

Many different routes have been proposed for the EVs docking with the target cell and are reported in Figure 4.3, and summarized as follows:

1. Clathrin-dependent endocytosis: this process involves the first recruitment of proteins at the plasma membrane, followed by the induction of a negative membrane curvature upon the vesicle's binding to the external layer. The process then evolves with the formation of a clathrin-coated pit that will be released into the cell via membrane scission [136].

2. Membrane fusion: this process is described as a passive mechanism that requires as a first step the binding between proteins located at the EV surface and the specific receptors expressed at the level of the recipient cell membrane, followed by the lipid reorganization and protein depletion at the external layer, causing the final membrane dimpling and full fusion with the bilayer [137, 14].

3. Phagocytosis and macropinocytosis: phagocytosis is an active and highly regulated process that requires energy and an organized rearrangement of the cell's cytoskeleton, mainly involving actin filaments. It consists in the engulfment of the vesicles, with the formation of a large cup-shaped endosome, able to carry multiple vesicles in the intracellular route. Unlike phagocytosis, macropinocytosis is a less selective process that allows the cell to engulf vesicles from the

surrounding environment. This time the vesicles are enclosed by membrane ruffles facing outside the external layer in the shape of lamellipodia, followed by their folding and closing in on themselves, with final vesicles internalization [14].

4. Lipid raft and caveolae-mediated endocytosis: they are considered clathrin-independent endocytosis pathways, which differs from the clathrin-mediated one for the absence of clathrin coats. They are both described as functional areas of cell membranes, specialized in the selective recruitment and clustering of lipids and proteins. Caveolae are identified as flask-shaped invaginations, with a size in the range of $50 - 80nm$, enriched with the caveolin (Cav) protein family. In particular, there is evidence demonstrating a decrease in the EVs uptake with decreased activity or inhibition of Caveolin-1, suggesting its fundamental role in mediating their internalization [14, 138]. Lipid rafts are instead described as planar phase-segregated islands of the cell membrane, $10 - 200\ nm$ in size, where cholesterol represents the main structural and functional component, regulating molecule trafficking, including EVs endocytosis. Indeed, it has been demonstrated that the extent of lipid raft-mediated endocytosis is highly dependent on cholesterol levels, with evidence illustrating that cholesterol depletion might have an inhibitory effect on EVs endocytosis [139]. In this regard, it has also been demonstrated that the close interplay between caveolin-1 and cholesterol represents a critical regulator of EV uptake.

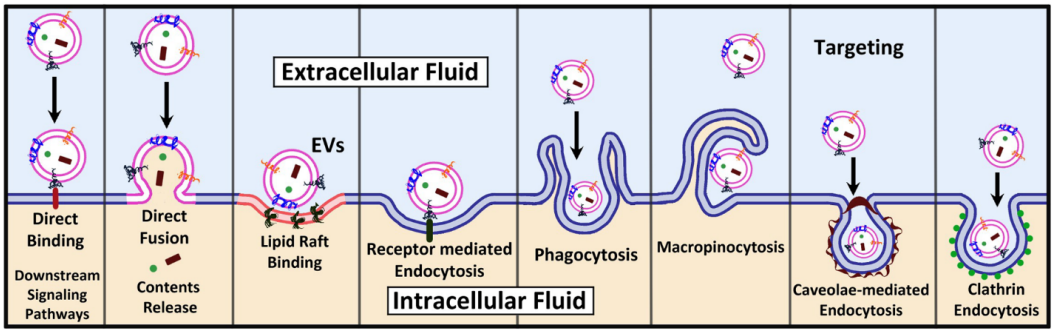

Figure 4.3: Routes of small EVs uptake by target cells. [130].

Based on what has been reported so far, regarding the mechanisms regulating EV uptake and the critical aspects of their detection, the following chapters will be proposed an innovative approach, to provide a solution as simple as effective for improving the knowledge regarding sEV uptake. In particular, a lipid raft model will be described in detail, combined with the investigation of the role exerted by cholesterol in sEV uptake regulation.

Chapter 5

Materials and Methods

5.1 sEV isolation and characterization

For sEV isolation, MDA-MB-231 cells ($2 \cdot 10^6$) were grown in a 175 cm^2 flask in DMEM (Sigma-Aldrich) with 20 % FBS (EuroClone) for 3 days. The cells were then washed two times with PBS and three times with DMEM without serum. The cells were further incubated at 37°C. After 24 h the medium was collected and centrifuged at 300 g and 4°C (Allegra X-22R, Beckman Coulter) for 10 min. With a 0.22 μm filter, the supernatant was filtered, poured into Amicon Filter Units (Ultracel-PLPLHK, 100 kDa cutoff, Merck Millipore, UFC9100) and centrifuged at $3900g$/4°C for 20 min (Allegra X-22R, Beckman Coulter). The samples collected were then transferred into the polypropylene (PP) ultracentrifuge tubes (Beckman Coulter, 361623), filled with PBS and centrifuged at 120000 g/4°C for 2 h in the ultracentrifuge (70.1 Ti rotor, k-factor 36, Beckman Coulter, Brea, CA, USA). After removing the supernatant, the pellet was then resuspended in 200 μL of PBS, aliquoted, and conserved at -20 °C until usage.

Bradford assay was then used to perform a semi-quantitative analysis of the total amount of proteins the EVs are enriched with. The working principle consists in the detection of the shift in the absorbance maximum of the Coomassie Brilliant Blue G-250 upon binding with the denaturated proteins of the sample under analysis. The main steps consist in the first lysis of the vesicles through the use of a RIPA 2X buffer, followed by 15 min of incubation at $-4\ ^\circ C$. Cold temperatures are needed to activate the RIPA buffer. Therefore, the mix of RIPA with EVs was centrifuged as $14,000\ xg$ for 10 min. The supernatant was then collected and equally spotted in triplicate in a 96-well plate. For each sample, three different volumes where tested (6 μL, 4 μL, and 2 μL) and mixed with 200 μL of Bradford solution. The blanck was performed, with the same dilution rate, by mixing the RIPA 2X buffer with the Bradford solution. After 10 min of incubation, the absorbance measurement was performed using the TECAN

infinite F200 PRO (Tecan Trading AG, Switzerland) spectrophotometer and exciting the sample at 595 nm. Lastly, the amount of proteins was quantified by comparing the results with a standard calibration curve made (Absorbance vs Concentration ($\mu g/ml$)) with defined concentrations of bovine serum albumin (BSA) (purchased from Sigma Aldrich).

AFM analysis was used to characterize the size and purity of the isolated sEVs. The measurements were performed on an MFP-3D Stand Alone AFM microscope (Asylum Research) with BL-AC40TS-C2 cantilever (from Olympus), in AC Mode and in liquid condition. The sample preparation consists in three steps: the incubation of a freshly cleaved mica disc (Nano-Tec V-1 grade, $0.15 - 0.21$ mm thickness, 10 mm diameter) with poly-L-ornithine (0.01 % solution, from Sigma-Aldrich) for 20 min at room temperature, in order to have a substrate positively charged; three washing cycles with milli-Q water followed by its complete removal; drop-casting vesicle deposition (30 μl of EVs diluted in $1X$ PBS) and incubation for 20 min at room temperature. An additional step of hydration was performed when needed. Depending on the starting sample concentration, the dilution rate was chosen in order to have a sufficient number of vesicles per scanned area. The images were acquired with 512×512 pixel, and with a scan rate of 0.75 Hz for a scanned area of 10 μm^2. The images were then processed with Gwyddion software, performing the standard steps of image correction, i.e. plane subtraction for data leveling, alignment of rows, removal of polynomial background when needed, application of a threshold mask to select only the particles with a height above 10 nm and to exclude the contributes coming from protein residuals or impurities.

Lastly, infrared (IR) measurements were carried out by the collaborator H. Vondracek from SISSI Bio Beamline (Elettra-Sincrotrone Trieste), to analyze the protein to lipid ratio of the isolated EVs. The setup was composed of an ATR crystal with an integrated GATR unit, with a hemispherical single-reflection Germanium crystal placed into the FTIR spectrometer (Vertex 70, Bruker). The measurements were performed by spotting 10 μl, followed by a sequence of 256 scans performed upon sample's dehydration, in the range from 530 to 5000 cm^{-1} at a resolution of 4 cm^{-1}. A baseline correction and atmospheric compensation for H_2O vapor and CO_2 was also performed. The last six spectra recorded were averaged and the spectral range was reduced to $700 - 5000$ cm^{-1}. After a baseline correction, the spectrum was dissected into various components and an additional baseline correction was performed (using a linear type for derivative spectra and a rubber-band type for the original spectra). The 2^{nd} derivative was calculated using a Savitzky-Golay filter with a window size of 29 and a third-degree polynomial. The peaks of the 2^{nd} derivative spectra were fitted using a series of Voigt profiles in order to determine the corresponding center frequencies. Subsequently, the original spectra were fitted using pseudo-Voigt profiles, fixing the central frequencies to the previously determined values.

5.2 Small unilamellar vesicles preparation

The lipids, 1,2-dioleoyl-sn-glycero-3-phosphoCholine ($18:1\ (\Delta 9-Cis)$ PC), 1,2-dipalmitoyl-sn-glycero-3-phosphoCholine (DPPC, 16:1), Sphingomyelin (brain, porcine, SM), and cholesterol (ovine wool, $> 98\%$), were purchased from Avanti Polar Lipids. The single lipids, suspended in chloroform, were mixed at the desired concentration and placed under vacuum overnight. The dry film was then hydrated with TRIS buffer (10 mM, $pH = 7.4$, equilibrated with HCl), to obtain a final concentration of 1 mg/mL. The lipidic mixture was sonicated for 40 min at 45 °C and vortexed. Lastly, the resulting solution was extruded 51 times at 40 °C (over the T_m of sphingomyelin) through a polycarbonate membrane with 100 nm pores (PC Membranes 0.1 μm, Avanti Polar Lipids).

5.3 Supported lipid bilayer preparation

Lipids were combined in three lipid mixtures: DOPC/SM (2 : 1 m/m) with Chol (5, 10, 17 mol%), DOPC/SM and DOPC/DPPC in a fixed molar ratio of 2 : 1, and lastly, DOPC and DPPC alone. The extruded solution of small unilamellar vesicles was then diluted in TRIS/$CaCl_2$ buffer to a final concentration of 0.4 mg/mL with 2 mM $CaCl_2$. For all compositions, the direct vesicle fusion method was adopted as a standard procedure for planar lipid bilayer preparation. The diluted sample was deposited on a freshly cleaved mica substrate (Nano-Tec V-1 grade, $0.15-0.21\ mm$ thickness, 10 mm diameter), and incubated at 50 °C for 30 min, followed by a cooling step to 27 °C at 0.02 °C/s. Lastly, the sample was extensively washed with TRIS buffer 10 mM to remove unfused vesicles and let stabilize for 10 min before starting the imaging.

5.4 Atomic Force Microscopy imaging

AFM measurements for SLB analysis were performed on a commercially available microscope (Cypher ES from Asylum Research), working at $27°C$ in high resolution AC mode. Sharp nitride levers ($SNL-10$ with A geometry from Bruker Corporation) were used to perform the imaging in liquid conditions. The choice of the cantilever was made considering as main requirement the need to perform the imaging in tapping mode in liquid environment. Moreover, the small size and the partial gold coating, make it suitable for adopting the photothermal excitation of the cantilever, thus having good stability in liquid conditions and over a long time of acquisition. Images were acquired at 512×512 pixel frames at 2.44 Hz. Lastly, for studying the sEVs interaction with the SLB, the AFM was moved out from the sample, and the vesicles were injected through

the holes of a perfusion holder. The imaging was then performed within $\sim 5\ min$ from the vesicle's injection. The collected images were then corrected using Gwyddion software, and a threshold mask was applied to select the phase-separated lipid domains (also known as lipid raft). These domains were analyzed in terms of number and area variation as a function of cholesterol concentration. The changes in these values were then observed before and after sEVs interaction with the lipidic system.

5.5 Differential scanning calorimetry analysis

The sample preparation for large unilamellar vesicle (LUV) preparation was followed as reported in the section number 5.2 of this chapter. However, the only difference was the hydration buffer adopted, $NaCl$ 100 mM instead of TRIS buffer. Calorimetry measurements were performed on LUV composed of DMPC, SM, CHOL with DMPC and SM in a molar ratio of 2 : 1 and 17 $mol\%$ of cholesterol. Because the investigated temperature range was 10 $°C < T < 52\ °C$, the transition of DOPC component used for the formation of supported lipid bilayer would not have been detectable in this window. For this reason, DOPC was replaced with DMPC, whose transition is visible and takes place around $24°C$. The measurements have been performed with the support and collaboration with V.Rondelli from Biometra Lab. (Università degli studi di Milano), with their non-commercial Double Differential Scanning Calorimeter (MASC), which is characterized by two identical cells placed in glass capillaries, that can be loaded respectively with the sample to be analyzed and with a reference sample that does not display any transition in the selected range. With this configuration is thus possible to analyze the difference between the power supplied to the two samples, and more in detail the specific heat with a sensitivity of $0.002°C$. It was decided to perform a total of 4 temperature cycles (comprehensive of both heating and cooling ramp) in order to have reliable results and to better track the sample thermodynamic. Once they were completed, the sEVs were added to the sample, and their amount was duplicated every 4 cycles for two times. DSC data analysis was performed using Origin and Python software, to evaluate the following information: T_m localization e modification before and after the EV interaction with LUV; possible asymmetries of $\Delta C_p(T)$ and the area under the main peak; presence of secondary peaks and corresponding thermodynamic contribute.

Chapter 6

Supported lipid bilayer characterization by AFM

The following chapter reports the key steps that have been followed to realize a cell membrane model system, featuring physiological conditions, i.e. representative lipid composition, salt buffer, and cholesterol concentration. The requirements of lipid bilayer stability and experiment reproducibility have been considered during the optimization. All the experiments reported have been performed at least in triplicate and with more than 10 images acquired per sample analysed. The outline of the model membrane development process can be summarized as follows: SLB has first been tested in aqueous solution with low cholesterol amount, starting from the work previously done by members of the NanoInnovationLab. As an extension of this work, the objective of the here proposed study was to work in a more physiological environment, testing the effect of the buffering agent adopted, in this case the sodium chloride ($NaCl$). Afterward, it was decided to use the model membrane system mimicking the lipid raft cell membrane subdomains, as a tool for investigating sEVs uptake mechanisms, analysing with high spatial and temporal resolution the site of interaction and the resulting impact of sEVs mixing with the model membrane. In order to have good control of the parameters to be considered when testing the sEVs interaction process with the proposed model, the study has been conducted with vesicles already investigated at the NanoInnovationLab in similar conditions, and produced from GMP production, thus ensuring high reproducibility. Based on the results obtained up to these steps, it was then decided to increase the molar ratio of cholesterol, to develop a model able to approach biological percentages ($15-50\ mol\%$). The buffering agent was also changed with TRIS at $pH\ = 7.4$, in order to work in neutral liquid environment. The system was then applied to the study of sEVs interaction mechanisms for vesicles isolated from breast cancer cells. Given the relevant role played by tumor-secreted sEVs, in regulating tumor progression and metastasis, and the lack of knowledge regarding the fusion mechanisms between sEVs and recipient cells. The ISEV community has in-

deed underlined the role of tumor-secreted extracellular vesicle (EVs) in the regulation of tumor progression and metastasis, and the intrinsic differences in the interaction process between sEVs coming from different cell lines and with diverse molecular cargo/composition. With this last step, we thus aim to provide insights via a biophysical approach, about the different fusion pathways and resulting effects on the model membrane architecture, for the two proposed sEVs samples.

6.1 Lipid model system optimization

The study here proposed is meant to develop a model system able to mimic the typical lateral phase separation of cell membranes into lipid rafts subdomains. To achieve this goal, a composition made of DOPC, SM, and cholesterol, was chosen to be the most representative for the outer leaflet of cell membrane. Indeed, DOPC mostly localizes in the outer leaflet, whereas SM and cholesterol are found in both leaflets but with a higher concentration in the outer layer [140]. A molar ratio of 2 : 1 was adopted for DOPC and SM respectively, with a starting 5 $mol\%$ cholesterol concentration, in order to have a stable lipid phase separation at room temperature, and a sufficient number of phase-separated subdomains per scanned area, according to the ternary phase diagram reported in Figure 6.1 for the selected components.
Given the importance, based on what has been discussed so far, of the lipid phase separation in the plasma membrane, and its implications in the regulation of cellular processes, many studies have investigated the possible parameters that would be involved in the modulation of lipid raft stability and morphology. In particular, it has been reported that these two variables can be affected by the interfacial tension between the two coexisting lipid phases, due to the hydrophobic effect, but also modulated by weaker interactions, such as Van der Waals and electrostatic interactions between the ions forming the hydration buffer and the headgroups of the lipids [142].
Following this line, we report a comparative study of lipid bilayer morphology changes as a function of the hydration aqueous buffer adopted. In particular, preliminary tests have been performed for a SLB composed of DOPC and SM in 2 : 1 molar ratio with 5 $mol\%$ of cholesterol, prepared in milli-Q and in $NaCl$, with $NaCl$ concentrations ranging from 100 mM to 150 mM. To that end, the direct vesicle fusion method was adopted for its good reproducibility, and control of lipid composition. The details of sample preparation are reported in the chapter Materials and Methods.

The typical lipid phase separation for the proposed composition analysed in milli-Q environment, is reported in Figure 6.2. The result here reported is in agreement with the typical lipid phase separation of ternary lipid mixtures, where a fluid-fluid lipid phase separation is observed. In particular, considering the phase diagram reported in Figure 6.1, the lipid bilayer features a L_d phase mostly enriched in DOPC and identified by

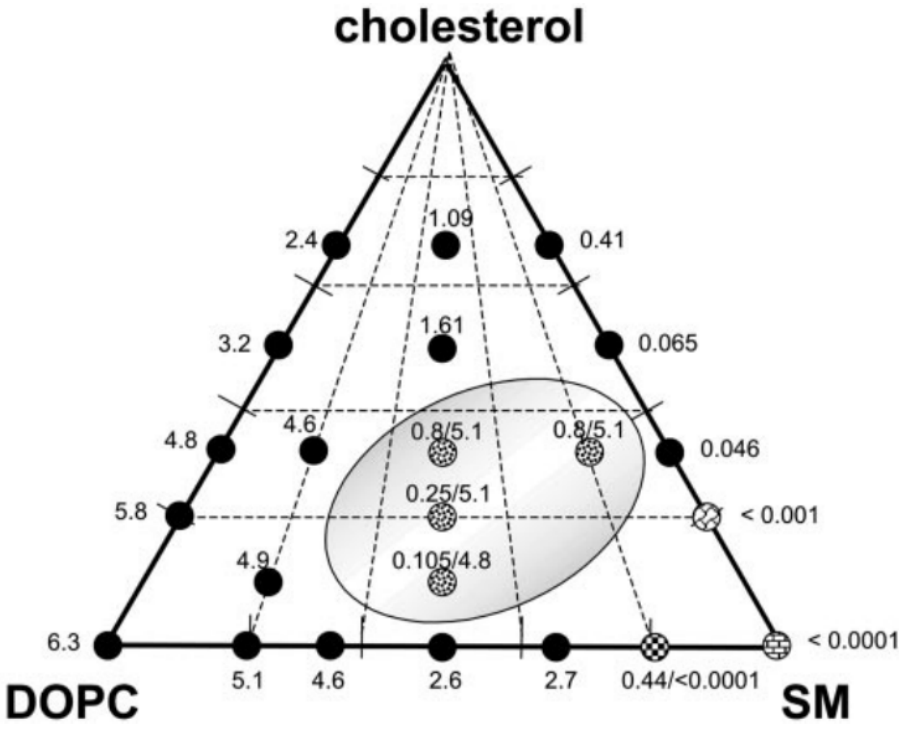

Figure 6.1: Ternary phase diagram for the SM/DOPC/cholesterol system at $25°C$, adapted from [141].

the dark orange area in the AFM height image, and a L_o phase mostly composed of SM and cholesterol molecules, in the form of bright light orange domains in the AFM height image. The coexistence of the two liquid-ordered and liquid-disordered phases occurs when the lipids adopted are characterized by a high-melting temperature and low-melting temperature respectively, when cholesterol is added to the system. The formation of the L_o phase is driven by the preferential interaction of cholesterol with saturated lipids [143], thus leading to a higher packing degree of the acyl chains. From the L_o height profile, it can be noted that the two lipid phases display a difference in height of $\sim 1\ nm$ which is in good agreement with previous studies reporting the lipid phase separation for similar mixtures [144, 145]. The difference in height between the two liquid phases has to be attributed to the perpendicular insertion of cholesterol molecules within the SM acyl chains, determining their arrangement in an extended and predominantly all-trans conformation similar to the gel phase that SM would form without cholesterol, but displaying a good lateral mobility within the lipid bilayer [146]. Compared to the typical averaged height difference of $1.25 - 1.7\ nm$ observed in bilayers of similar composition with coexisting L_d-S_o phases in the absence of cholesterol, the cholesterol partitioning in SM-rich domains is associated with the overall thinning

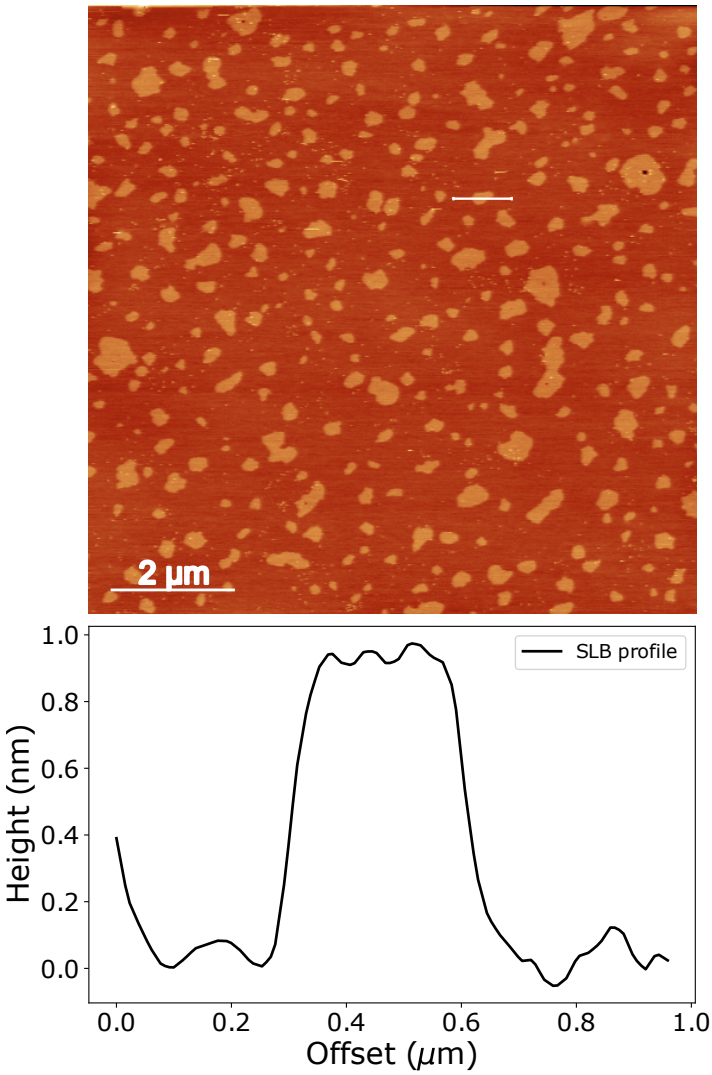

Figure 6.2: AFM topographic image of DOPC/SM 2 : 1 (m/m) SLB with 5 $mol\%$, in milli-Q environment, with corresponding height profile, here acquired at room temperature in AC-mode in liquid.

of the lipid bilayer due to steric hindrance, thus resulting in the difference in height reported in Figure 6.2. These results are in agreement with previous studies performed with X-ray diffraction methods, where a typical thickness of 6.35 nm was observed for SM, whereas for DOPC lipid bilayer a value of 4.57 nm was estimated [147, 148], thus confirming the intermediate ~ 1 nm thickness mismatch for the proposed composition. For what concerns the area occupied by L_o phase, it can be noted that the domains are characterized by an heterogeneous size distribution, with an average percentage

area of 20 %, slightly lower compared to the theoretical 33 % area they should occupy considering the initial molar ratio adopted. This result can be explained by considering two distinct aspects. The first one is that not the totality of the molecules takes part in the domain's nucleation event. In this direction, many studies have stressed the point that rising cholesterol amounts may lead to increased recruitment of dissolved saturated lipids such as SM in the surrounding fluid bilayer rich in DOPC, into the SM-rich ordered domains [149]. The second one is that lipid domains morphology and area occupied are highly dependent on the thermal history of the bilayer, thus leading to different kinetics of domains nucleation and growth depending on the temperature range investigated, and on the speed adopted for cooling the system [150, 151].

Thereafter, it has been decided to investigate SLB morphological variations and lipid bilayer stability in a more physiological environment, in order to be able to translate the membrane model system to possible biological applications (e.g. proteins reconstitution and migration, testing functionalization strategies and binding affinity, lipid-vesicle interaction events). To that end, in Figure 6.3 is reported a comparison between the system prepared in milli-Q (Figure 6.3a) and sodium chloride ($NaCl$) (Figure 6.2b,c) buffer at two different concentrations.

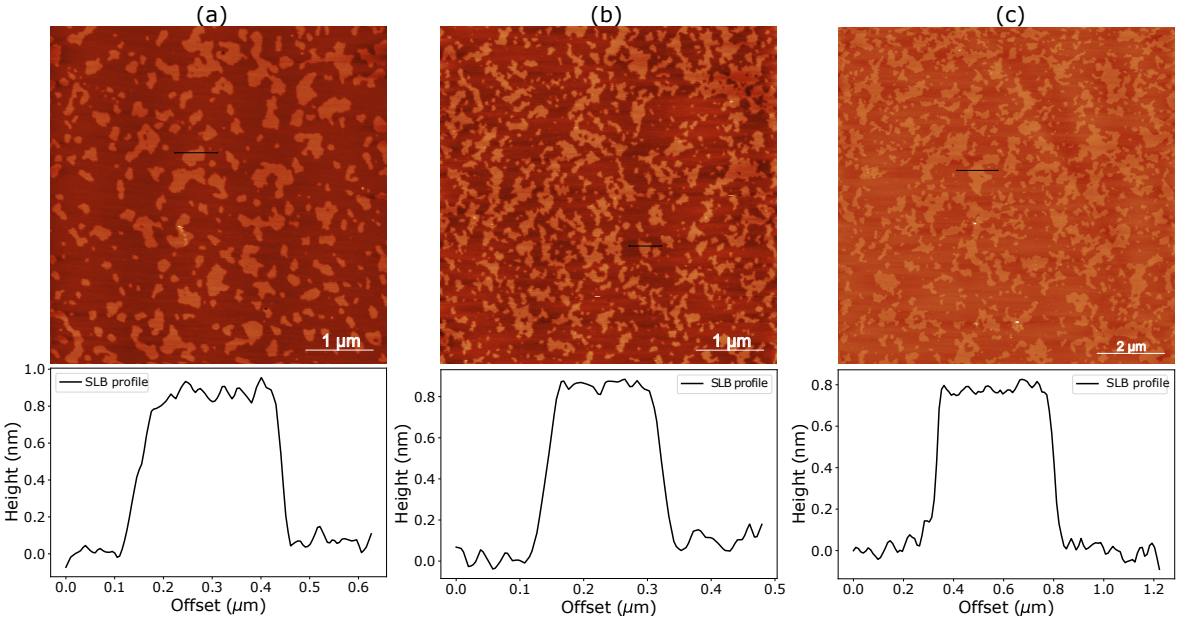

Figure 6.3: AFM topographic images of DOPC/SM 2 : 1 (m/m) SLB with 5 $mol\%$, in (a) milli-Q, (b) 100 mM $NaCl$, and (c) 150 mM $NaCl$. In each case a profile is shown to highlight the L_d (lower) and L_o (higher) domains, here acquired at room temperature in AC-mode in liquid.

Commonly used biological buffers are $NaCl$, phosphate buffer saline (PBS), Tris,

HEPES, which display different effects in altering the lipid bilayer structural properties and also their dimension. In particular, it has been demonstrated that the pathway of SLB formation is intrinsically different depending on the buffer adopted. Two mechanisms have been reported: one consists in the adsorption-rupture process that includes an intermediate step, through which a critical vesicle density on the surface has to be reached in order to get the SLB formation; the second one is based on the direct rupture of the vesicles once they are in contact with the surface. In particular, it has been demonstrated that HEPES and Tris buffers follow the second pathway, whereas $NaCl$ follows the first process, where the extent of the interaction between the vesicles and the surface is reported to be dependent on the salt concentration adopted due to electrostatic screening. The buffering agents also differ in terms of lipid solubility, which is higher for $NaCl$ and Tris, but also on the kinetics of the SLB formation, usually accelerated by the presence of $CaCl_2$ salts that favor the vesicles rupture, but still faster for $NaCl$ [152]. This difference is attributed to the strength of the interactions between the vesicles and the surface, with salt playing a central role in screening the electrostatic interactions. In the absence of salt, such as in the case of milli-Q liquid environment, the strong interactions between the vesicles and the surface, combined with the greater contact area over the mica surface, lead to a faster vesicle's destabilization and rupture. When testing the system with $NaCl$ at 100 mM and 150 mM concentration instead, as reported in Figure 6.3, a higher concentration of $CaCl_2$ it has been adopted, in order to favor the formation of a uniform SLB in the same incubation time that has been followed for the SLB prepared in milli-Q environment. This is in agreement with the known role played by Ca^{2+} in accelerating the vesicles fusion process over the substrate.

Interestingly, with the selected mix of lipids, a clear difference in the L_o domains shape can be noted. In particular, with increasing $NaCl$ concentration, a higher fragmentation rate of L_o is observed, with domains having a broader size distribution compared to what is obtained in milli-Q environment. The different domain patterns can be explained considering three parameters with high dependence on the aqueous environment: interaction of self-assembling molecules with the rigid substrate, the transition temperature of the system, d-spacing between molecules, which are both hindered by the buffer intercalation within the self-assembling molecules. This would affect not only the distance between the headgroups of the lipids (d-spacing parameter), with a greater d-spacing for the $NaCl$ case compared to the milli-Q environment, but also an electrostatic screening of the molecules interacting with the substrate [153]. Yet, the small molecule self-assembly over a rigid substrate rely on weak molecule-substrate interactions. Thus, when they last for a sufficiently long time, supramolecular ordered structures can form, as in the case of lipid bilayer formation in milli-Q environment. However, when using phosphate buffer saline (PBS) solution, or $NaCl$, the intermolecular interactions between the self-assembling molecules are affected, resulting in morphological changes of the ordered structures. Moreover, there are evidences

of a decreased lateral diffusion rate for self-assembling molecules in buffer conditions, which would explain the greater fractal and elongated shape of the L_o domains. According to these theories, by varying the molecular ratio of the lipids adopted, and the liquid environment ionic strength, both the morphology and the lipid bilayer stability can be modulated [154]. Lastly, depending on the liquid environment adopted and on the pH, some variation in the transition temperature of the system can be observed as well, thus impacting the dynamic of the nucleation process and the resulting domains morphology [155].

As next step, following the work previously performed at the NanoInnovationLab, it was decided to apply the membrane model system to the study of extracellular vesicles interaction mechanisms, performing an AFM-based analysis in liquid environment at room temperature. Over the years, diverse strategies and technologies have been proposed with the intent of providing insights about their uptake mechanisms, most of them involving labeling the EV's surface with fluorescent dyes to track their route. However, the main drawbacks of this approach are that sEVs behavior can be altered upon vesicle labeling, and the labeling itself can generate non-specific signals in the targeted cells. Moreover, sEVs are under the resolution limit of optical techniques such as fluorescence microscopy, thus limiting the detection of the uptake pathways [156]. The great advantages of performing AFM imaging are related to the fact that it is a label-free technique, and it provides information with spatial resolution at the nanometer scale, and temporal information in the order of seconds, at the nanoscale. Moreover, it is nowadays clear that sEVs uptake mechanisms are highly heterogeneous, regulated by the combination of a wide number of parameters that can be divided in EV-related properties (e.g. composition, origin, molecular cargo), and in cell-membrane associated features (e.g. composition, fluidity, temperature), thus requiring specialized setups, or the combination of multiple technologies to investigate such mechanisms, which is not cost effective approach. By implementing SLB for the study of sEVs uptake mechanisms, it would instead be possible to provide a simple and broadly accessible platform for screening, from a biophysical point of view, specific variables regulating the biological phenomena of interest, and in this study the regulators of sEV-uptake, which would otherwise be of difficult investigation in the cellular environment [156].

To that end, sEVs samples provided from the Paracelsus Medical University (PMU) of Salzburg, were used to validate the model system as a possible tool for studying EV-fusion kinetics. The tested samples were isolated from a umbilical cord mesenchymal stem cells (UC-MSC) line from GMP production, in standardized and optimized culturing conditions, thus ensuring a good rate of experiments reproducibility. The interaction with the model membrane described so far is first reported in Figure 6.4 for the SLB in milli-Q, and in Figure 6.5 for $NaCl$ liquid environment.

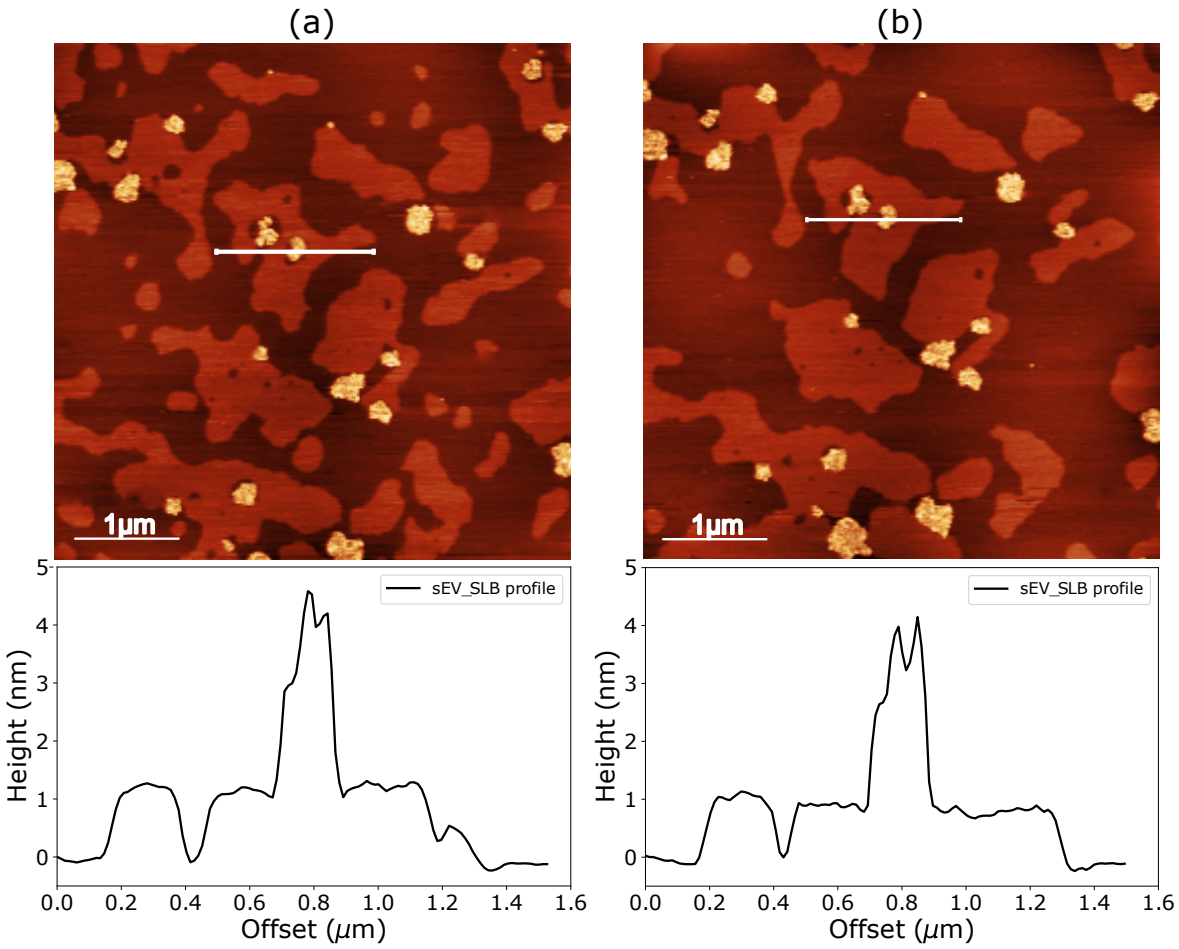

Figure 6.4: Time-resolved AFM topographic images of EVs (UC-MSC cell line) interacting with DOPC/SM 2 : 1 (m/m) SLB with 5 $mol\%$ Chol with corresponding height profiles, acquired at room temperature in milli-Q liquid environment in AC-mode, with a time-lapse of 1 h.

From the topographic images reported in Figure 6.4, acquired within few minutes upon vesicles addition to the system, it can be appreciated the formation of protrusions $4 - 5$ nm in height over the DOPC layer, localized at the interface of the two lipid phases. A similar interaction has been already reported in the literature, including lipid vesicles used as drug delivery system [157], pore-forming peptides [158], as well as gold nanoparticles [159]. The widely accepted explanation for this interaction mechanisms is that the packing defects of the SLB are expected to work as docking site for the interacting agent. Therefore, for SLB featuring a height mismatch between the two lipid phases, as observed in Figure 6.4, a preferential interaction along the edges of the domains will takes place. Upon vesicles interaction with the SLB, by

analysing the SLB evolution in a time range of 1 h, an overall lateral reorganization of the lipid domains forming the L_o phase is observed. Figures 6.4a,b refer to the same SLB investigated area even though a shift toward the upper direction can be observed, and explained as thermal drift during the image acquisition. In particular, the area occupied by sEVs protrusions rises from 2.6 % to a 3.29 %, with no considerable area variation for the L_o domains. Looking at the lipid domains morphology, the smaller domains not involved in the interaction progressively disappear, giving space to the formation of more domains with a more regular shape. This phenomenon would partially explain the possible lipid-EV mixing that is occurring, hence explaining the slight increase of the area occupied by the vesicles protrusions. The change in the lipid domain morphology, becoming less in number and larger in shape is also related to an overall reduction in the line tension [158]. These results are in agreement with the work previously published by the NanoInnovationLab [144], where a sEVs interaction at the edges of lipid domains was observed in similar conditions, with vesicles patches expanding in the L_d phase of the SLB. The hypothesis that has been postulated for this process is the following: sEVs interaction would consist of two phases, a fast diffusion of the lighter sEVs elements with preferential docking at the interface of the two lipid phases, followed by the diffusion of the other vesicles still present in solution.

Based on the preliminary results obtained in milli-Q liquid environment, the same SLB composition has been tested in $NaCl$ buffer, in order to investigate the possible influence of the buffering agent in altering the resulting interaction process. In Figure 6.5 is reported the sEV-UC-MSC interaction with SLB in 100 mM $NaCl$.
After vesicles addition to the SLB, in agreement with what has been observed in milli-Q environment, a preferential interaction along the edges of the SLB is observed, with vesicles forming protrusions with an averaged height of 5 nm over the DOPC layer. However, differently from the case reported in Figure 6.4, where lipid domains were homogeneous in shape and 'defect-free', the vesicles mixing with the SLB prepared in $NaCl$ buffer display the presence of small pores close to the interaction's site. This result can be explained taking into account two considerations. The first one is that the vesicles insertion into the SLB introduces both deformations and tension within the lipids. As consequence, for a sufficient number of vesicles interacting with the bilayer, the tendency of SLB poration is more likely to occur [158]. Moreover, being the SLB in the fluid state, it would be expected to see the pore close again, however the reduced line tension due to the sEVs mixing with the SLB, contributes to the change in the energetic balance of the system, favoring the stability of the pore within the bilayer architecture [158]. The mechanism of pore formation and stabilization is commonly investigated for pore-forming peptides, and proposed to be related to the specific insertion of the molecules within the packing defect at the edges of the interaction site [160]. However, in this context a clear understanding of the membrane poration process, either related to sEVs interaction or to the intrinsic lower mechanical integrity of

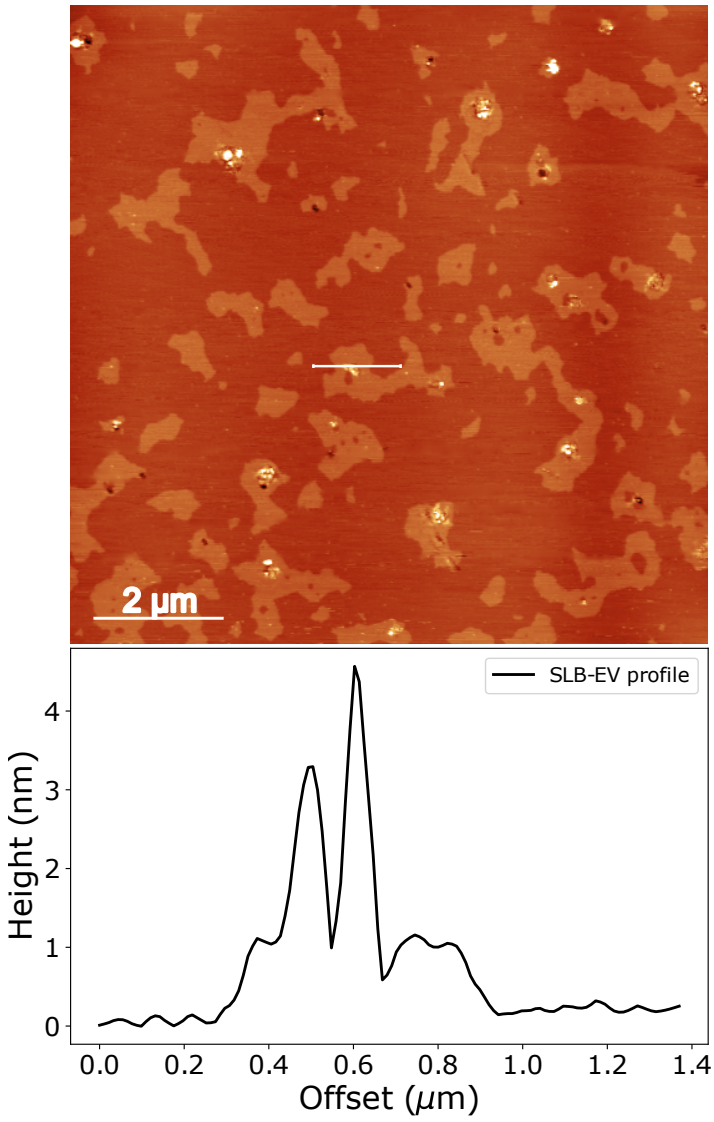

Figure 6.5: Time-resolved AFM topographic image of DOPC/SM 2 : 1 (m/m) with 5 $mol\%$ chol SLB with corresponding height profile, acquired at room temperature in AC-mode in $NaCl$ 100 mM liquid environment.

the model system in $NaCl$, requires further investigations. Lastly, the possibility of pre-existing pores can not be excluded as with the setup used for the AFM imaging, it was not possible to scan the same area before and after the sEVs interaction.
Concluding, cholesterol has been proposed to represent a possible mediator of the interaction between molecules and the targeted SLB. This role has been associated with its preferential localization between the lipids head group, which is reflected in the

increase lipid spacing between the lipids, and in the regulation of membrane flexibility by modulating the packing density of lipids. As a consequence, regulating these two parameters, the vesicles uptake might be facilitated for more fluid systems. The formation of protrusions at the edges of lipid domains would be then associated to lipid-EV coaggregates, causing a partitioning of cholesterol within the lipid bilayer, thereby leaving a modified membrane with local variations in lipid domains morphology and structure, resulting in the final structures reported in Figure 6.4 and Figure 6.5.

In the Appendix B is reported the control test, where 30 μl (equivalent volume used to inject the sEVs into the SLB) of PBS has been added to the SLB in order to evaluate possible effects related to the buffer interaction with the lipid bilayer.

6.2 SLB with increasing cholesterol

Given the intrinsic differences in the resulting EVs mixing and impact with the recipient SLB by varying the buffering conditions, it has been decided to work in a more neutral environment in order to disentangle the interaction process to the buffering agent adopted. To that purpose, the same SLB composition has been investigated in TRIS buffer with $pH = 7.4$. Moreover, considering the SLB morphological changes that have been observed upon vesicles mixing with the model system, it has been decided to validate the system with increasing cholesterol amount. This step was fundamental for creating a model with a representative cholesterol concentration, close to physiological values ($30 - 50$ mol %).

To that end, for SLB prepared in TRIS buffer, three different cholesterol concentrations were tested, varying from 5 mol% to 10 mol%, up to 17 mol%, keeping the molar ratio of DOPC/SM 2 : 1 constant. For the proposed mix of lipids, it was decided to not investigate higher values of cholesterol amount in order to work in a defined miscibility regime, where the L_o and L_d phases coexist [161, 162]. Moreover, working at $27°C$ with the chosen DOPC/SM molar ratio, it would not be possible to detect any liquid-liquid phase separation that features the nucleation of nanoscopic domains [141].
The AFM images for the three compositions are reported in Figure 6.6. What can be noted from the AFM imaging, is that with rising cholesterol, the phase separation between the L_o and L_d phase is confirmed, yet displaying a different average area and height mismatch. The quantitative data are reported in Figure 6.7 where a linear increase of the area occupied by the L_o domains is accompanied by a small decrease of the difference in height between the two liquid-liquid phases.
For a comparable number of domains between the three tested conditions, this result relies on the extensively investigated cholesterol 'condensing' effect. According to this theory, cholesterol's preferential interaction with SM lipid, would change the packing

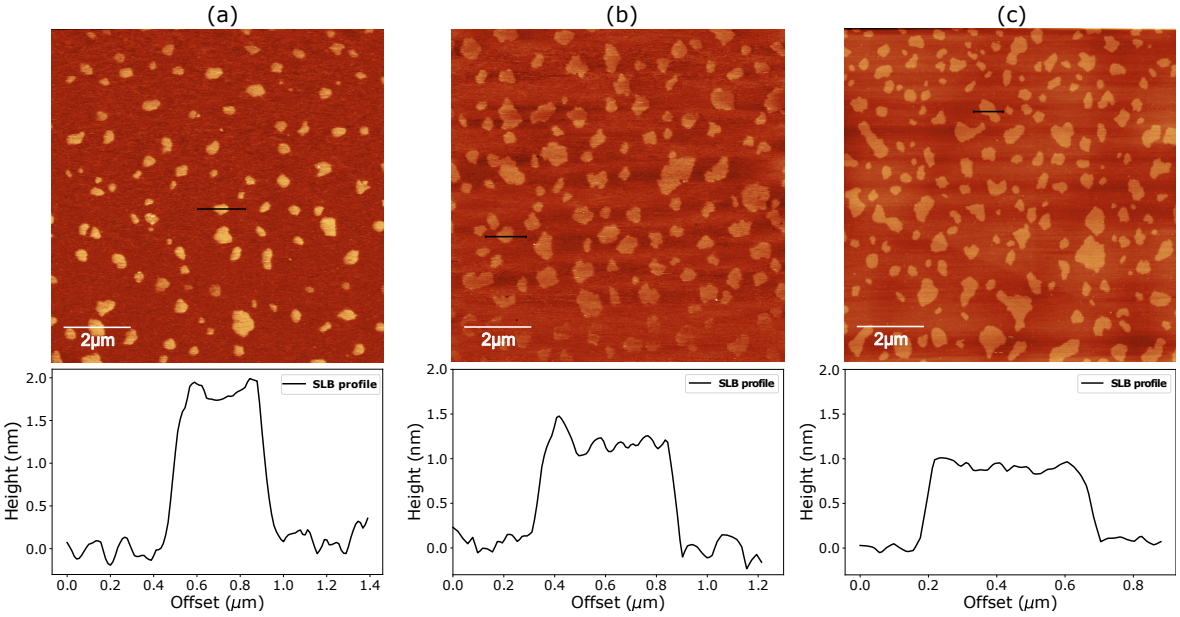

Figure 6.6: AFM topographic images of DOPC/SM 2 : 1 (m/m) SLB with (a) 5 *mol*%, (b) 10 *mol*% and (c) 17 *mol*% Chol. In each case a profile is shown to highlight the L_d (lower) and L_o (higher) domains, here acquired at room temperature, in AC-mode in liquid.

degree of the acyl chains, which can be reflected into two contributes: the change of the area occupied per lipid, and the total variation of the lipid packing density [66]. Respectively, considering no volume variation, with rising cholesterol amount, a decrease of the L_o packing density is observed, and is commonly associated with a decrease of the bilayer thickness in such areas, and by an overall increase of the area per lipid. The opposite trend is otherwise observed for the surrounding L_d phase.

However, by analyzing these soft supported lipid bilayer systems with AFM, caution should be given to the correct interpretation of results. Even though with AFM is possible to perform gentle imaging with the application of low forces, when analyzing the height mismatch of soft samples as for SLB, possible electrostatic interactions coming from the liquid environment should be counted, as well as it would be recommended to perform multiple acquisitions with different setpoints, in order to exclude height differences induced by the AFM acquisition parameters [163]. Lastly, it has been demonstrated that the transition temperature at which the L_o domains start nucleating is shifted to higher temperatures with increasing cholesterol amount. This is explained by the greater extent of the cholesterol screening that lipids have to actuate with increasing cholesterol moiety, resulting in the ordering of lipids acyl chains at higher temperatures [164]. Together with that, the close interaction of lipids with the

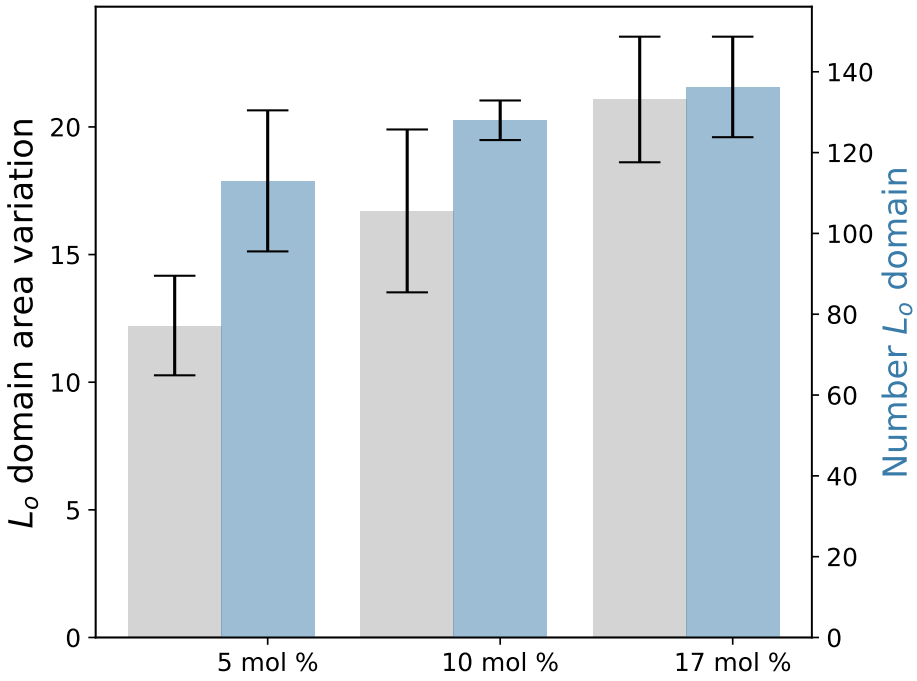

Figure 6.7: Comparative analysis of the area and number variations of L_o domains at increasing cholesterol percentage.

rigid substrate results in a shift of the main T_m of the system to higher temperatures as well, and in a broadening of the temperature range of the transition, due to a lower degree of cooperativity between the lipids. [165]. Thus, the L_o domain area and number variations reported in Figure 6.7 are the result of the combined cholesterol condensing effect and the boundary conditions just reported.
Lastly, moving from milli-Q and $NaCl$ to Tris buffer liquid environment, the incubation time required to get a uniform SLB has been modified, as well as the concentration of $CaCl_2$. In particular, the incubation time has been increased from 20 min at 38°C adopted for the first two conditions, to 20 min of incubation at 50°C followed by a cooling step to 27°C, for other 20 min. The longer incubation time it was fundamental to promote the process of lipid vesicles adhesion and rupture over the mica substrate, which is known to take place with a lower kinetic compared to the two hydration buffers previously described [152].

6.3 Investigating sEVs uptake mechanisms for EV from breast cancer cells

The following section aims to provide insights at the nanoscale level of the sEVs interaction with SLB composed of DOPC/SM (2 : 1) with 17 $mol\%$, by performing an AFM topographical and morphological analysis of the lipid bilayer evolution over time upon vesicle's uptake. The images were acquired under temperature control at $27°C$, with 512 $\times$ 512 pixel frames at 2.44 Hz.

To investigate the sEVs interaction mechanisms with the SLB model described in Section 6.2, a comparative analysis has been performed, with sEVs isolated from two different cell lines. The first one, reported in Figure 6.8, illustrated the interaction of sEVs isolated from a triple-negative breast cancer (TNBC) MDA-MB-231 cell line. The results were then compared with the interaction process followed by sEVs isolated from UC-MSC cell line, already investigated in the previous sections, and reported in Figure 6.9.

The molecular mechanisms that regulate the cell-to-cell interaction in the tumor microenvironment are known to be mediated by a family of molecules, including cytokines and growth factors, and now extended to the class of EVs, which are described nowadays as tumor mediators, being able to remodel the tumor microenvironment by interacting with the targeted cells and releasing functional molecules, thereby influencing cancer progression [166]. In the context of breast cancer, sEVs isolated from a high aggressive triple negative breast cancer cells (MDA-MB-231 cell line) have displayed the ability of transferring their oncogenic properties to the recipient cells, impacting their phenotype, morphology, but most importantly the mechanical properties. In particular, in a work recently published by the NanoInnovationLab, a biomechanical analysis has been performed on non-metastatic breast cancer cells from MCF-7 cell line [16]. Upon MCF-7 cells treatment with sEVs isolated from the MDA-MB-231 cell line, a decrease in the cell membrane stiffness was observed, with the cells assuming a phenotype more close to the metastatic cells. Based on these considerations, it has been decided to develop a model system able to exploit, in a simplified environment, the role played by different lipid bilayer compositions and degree of fluidity, in the regulation of the sEVs interaction process, and the eventual morphological changes detection upon vesicles uptake. To that end, a comparative analysis between sEVs isolated from the metastatic breast cancer cells (MDA-MB-231), with the non tumor-derived sEVs from UC-MSC cell line, has been performed with the aim of evaluating possible effects in the modulation of SLB structure and morphology, from a biophysical point of view.

Figure 6.8 reports the time-resolved interaction of sEVs from MDA-MB-231 with the

SLB.

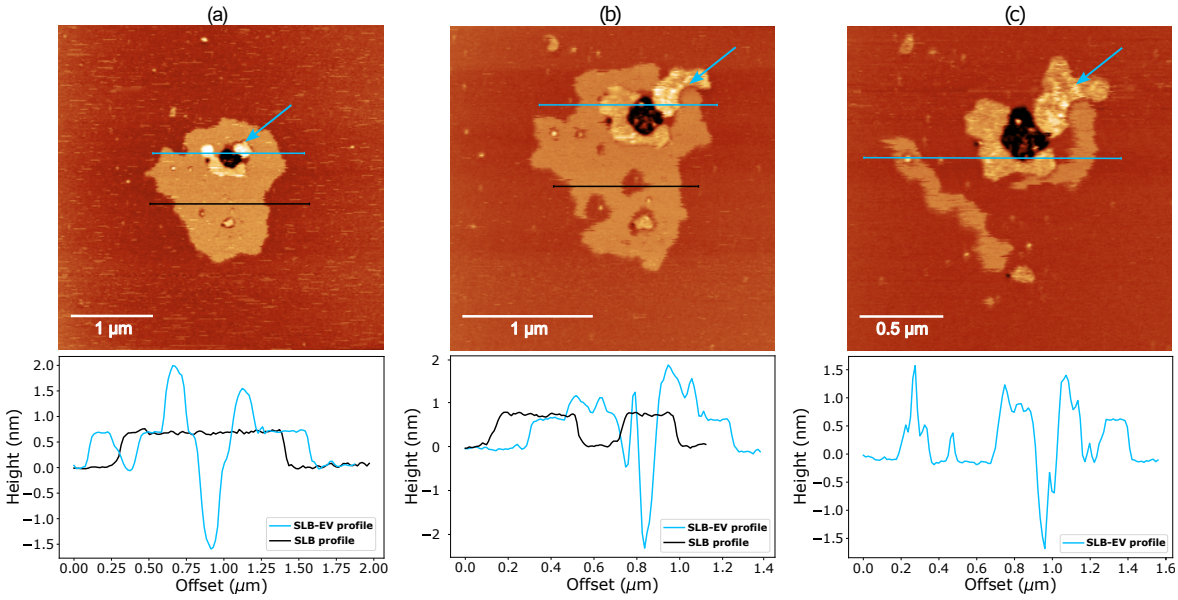

Figure 6.8: Time-resolved AFM topographic images of EVs (MDA-MB-231 cell line) interacting with DOPC/SM 2 : 1 (m/m) SLB with 17 $mol\%$ Chol with corresponding height profiles, acquired at 27 $°C$ in Tris buffer 10 mM, with a time-lapse of 10 minutes.

Due to the technical procedure, the first image was acquired within 10 min from the vesicles injection into the SLB. For this reason, it was not possible to follow the first part of the vesicles mixing with the SLB. The adsorption of sEVs on the membrane can be described by two features: the formation of small protrusions, ~ 1 nm in height over the L_o domain, highlighted with the blue arrow, and the presence of pores with a depth confined at the outer leaflet of the SLB. Moreover, the morphology of L_o domains before the sEVs addition, as reported in Figure 6.6, was defects free. Whereas, this degree of homogeneity is lost after the sEVs mixing, with the nucleation of small protrusions over time, to the detriment of L_o integrity.
This result can be explained considering a process that involves the first mixing of the vesicles with the SLB, accompanied either by their opening within the SLB and cargo release. The mixing would then be followed by the local destabilization of the SLB around the site of interaction, described by the formation of pores, and by the progressive decrease of the acyl chain packing, leading to the formation of a SLB characterised by a lower degree of order. The mixing of lipids with vesicles is also supported by the corresponding AFM phase channel reported in Appendix B, where a second distinct phase, in correspondence with the small protrusions, arises. This difference in height might be attributed to a redistribution of the SM and cholesterol molecules within the SLB. This theory is in part supported by previous work, where the EV fusion process with model system was investigated with neutron scattering technique [144]. The

main findings suggested that an overall increase of the SLB thickness was observed, with SLB becoming slightly asymmetric upon vesicles fusion. In line with this observation, given the average 15.43 nm height of EVs when spotted over a rigid substrate and measured with AFM (Appendix A), and the typical thickness of $\sim$ 5 nm of the SLB with 1 nm hydration layer at the substrate-SLB interface, higher protrusions in the range of $6 - 8$ nm instead of $\sim$ 1 nm would be expected, confirming again the insertion and opening of the EVs through the SLB thickness. Lastly, by performing the time-resolved analysis, an overall modification of the SLB profile is observed, with the L_o domains progressively disappearing, while the area occupied by the EV-SLB protrusions remained almost unchanged. The fragmentation of the L_o domains has been explained in the work recently published [167], as a 'fluidification effect' of the sEVs upon their interaction with the SLB. This result can be explained considering a redistribution of the lipids in the SLB, with an impairment of cholesterol molecule within the SLB. This hypothesis was confirmed by DSC study reported in Chapter 6.4, where for increasing amount of sEVs added to the system, the degree of order and cooperativity between the SLB components decreases.

In conclusion, these results have been fundamental to exploit the impact of sEVs isolated from MDA-MB-231 in altering the SLB morphology and degree of fluidity, with a massive effect on lipid raft integrity alteration. Thus, combining this information with the results previously published by our group [16] about the impact of sEVs isolated from MDA-MB-231 cells in regulating cell membrane mechanical properties and their oncogenic potency, the model system represents a valid tool to address the diverse contributes taking part in the interaction process, that would be not trivial to be identified in the complexity of the cellular environment. Lastly, given the fundamental role of lipid raft integrity in preserving cellular homeostasis, and the processes associated with it (e.g. molecules trafficking, cell signaling, cell adhesion) [54], these results would be instrumental for developing innovative strategies that consider, other than EV's surface properties, the cell membrane molecular structure and composition.

A comparative analysis was then performed to address possible differences in sEVs interaction mechanisms and the resulting impact on the recipient model system. by varying the vesicles cell origin. To that purpose, sEVs isolated from UC-MSC cell line were used, and their interaction, tested in the same conditions, is reported in Figure 6.9.
Contrary to what has been observed for sEVs isolated from MDA-MB-231 cell line, the interaction here mostly takes place at the interface of the L_o and L_d phases. In particular, the patches are characterized by small protrusions in the range of $2 - 3$ nm in height over the L_d level, conferring an irregular profile to the bilayer. Observing the images acquired over time, two distinct processes can be observed: the first one consists in the progressive melting of the L_o phase as previously observed for sEV-MDA-MB-

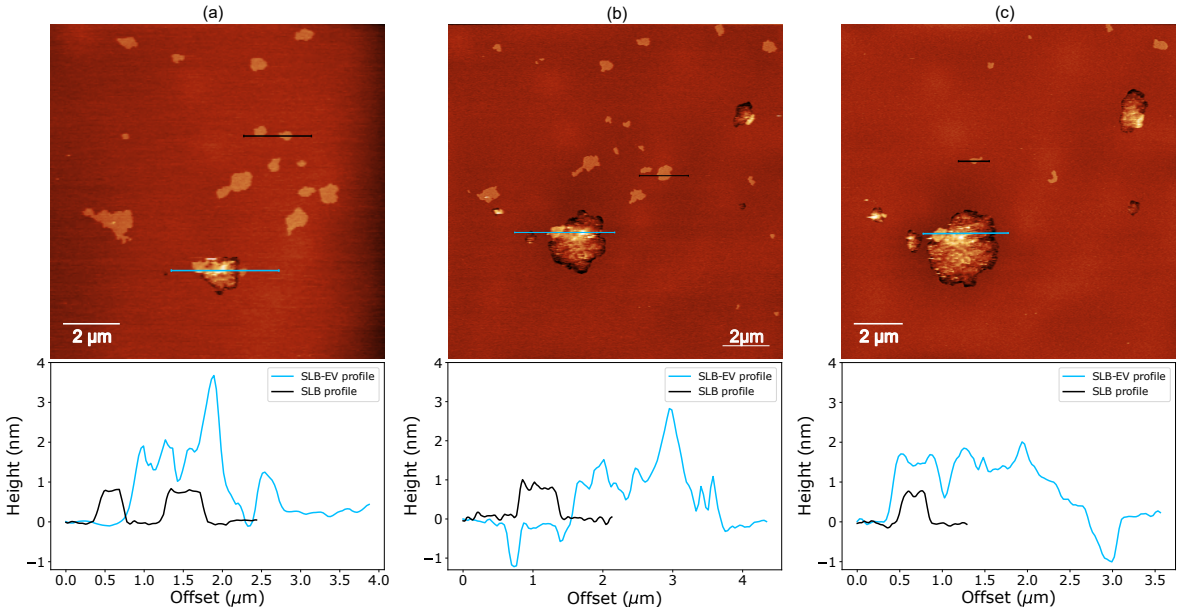

Figure 6.9: Time-resolved AFM topographic images of EVs (UC-MSC cell line) interacting with DOPC/SM 2 : 1 (m/m) SLB with 17 $mol\%$ Chol with corresponding height profiles, acquired at 27 $°C$ in Tris buffer 10 mM, with a time-lapse of 10 minutes.

231, leading to a final SLB in the fluid-state with the almost complete disappearance of domains. The second one instead consists in the progressive lateral diffusion of the sEVs patches from the edges of the L_o domains to the surrounding L_d phase.

These apparent differences in the docking site, and the different evolution of the process over the time, can be related to both intrinsic differences in the EV interaction mechanisms, but also on their molecular composition and isolation process that has been followed. In particular, sEV-UC-MSC were isolated with sequential steps of tangential flow filtration (TFF) and ultracentrifugation (UC) methods, while the sEV-MDA-MB-231 were isolated performing the standard ultracentrifugation. Moreover, a comparative spectroscopic characterization, based on Fourier transformed infrared spectroscopy (FTIR) analysis, was performed for both samples, and reported in Appendix B for sEVs-UC-MSC, and in literature for sEV-MDA-MB-231, from a previous study performed by the NanoInnovationLab [168]. The main findings report a higher protein to lipid ratio (P/L) for sEVs isolated from UC-MSC cell line compared to the sEVs isolated from the MDA-MB-231 cell line, more enriched in lipids. These two variables, based on recent studies that have been performed in the EV field, would motivate the difference in the resulting fusion process. Moreover, the difference in height between the two phases, and the greater concentration of packing defects at the interface of the two lipid phase, would provide a preferential energetically favor-

able route for lipid-protein association and vesicles insertion [169, 170], thus explaining the preferential insertion of sEVs-UC-MSC at the edges of lipid domains. This would contribute to the formation of patches, with high granularity, reducing the hydrophobic mismatch between the two lipid phases. Another more likely explanation, based on the results reported for sEV-MDA-MB-231 and the findings of previous work published by my group [144], would be the local redistribution of membrane components, accompanied by an overall thinning of the membrane upon vesicles mixing with the bilayer. This hypothesis would also better explain the progressive disappearance of L_o over time, a process previously described as the 'melting' of the L_o phase with the L_d phase, and attributed in literature to the overall thinning of the membrane, with reduced height difference between the two lipid phases [171], or to possible cholesterol depletion mechanisms upon vesicles fusion [149]. Further investigations are needed to confirm the prediction of cholesterol partitioning within the SLB, usually investigated in literature through high-resolution fluorescence microscopy [172].

6.4 Complementary analysis with DSC

DSC analysis, whose working principle is reported in Chapter 3, is here used to identify the dynamic of the lipids phase transition, and to provide insights about the interaction of sEVs for the system enriched with 17 $mol\%$ of cholesterol, this time without the contribution of the rigid substrate. Given the high concentration of lipids and the restricted amount of EV-sample to be used for these types of measurements, among the three compositions, only the 17 $mol\%$ has been studied with DSC, and chosen as the most representative of cholesterol physiological values. This approach allowed us to detect the main transition temperature of the system, and thus to identify the ideal temperature range to be investigated when performing high-resolution AFM imaging with the temperature-controlled AFM chamber (Cypher ES - from Asylum Research).

DSC measurements performed on the LUV composed of DMPC and SM in a $2:1$ m/m ratio in $NaCl$ are reported in Figure 6.10, including both the raw data in the range of $10-50°C$. The DOPC has been replaced with DMPC in order to be able to visualize the lipid phase transition in the investigated temperature range. The fitting has been performed in the temperature range of $10-40°C$, excluding the last part of the cooling ramp going from $40°C$ to $52°C$. For unilamellar vesicles composed of single phospholipid components analysed in comparable experimental conditions, the typical DSC curve of the lipid phase transition is characterised by a defined sharp peak that describes the gel-to-liquid phase transition occurring at the main T_m of the system. The other two peaks below the T_m, not always detectable, are usually localized below the T_m and describe the pre-transition of the system from the gel-to-ripple gel phase, before the complete transition to the liquid crystalline phase.

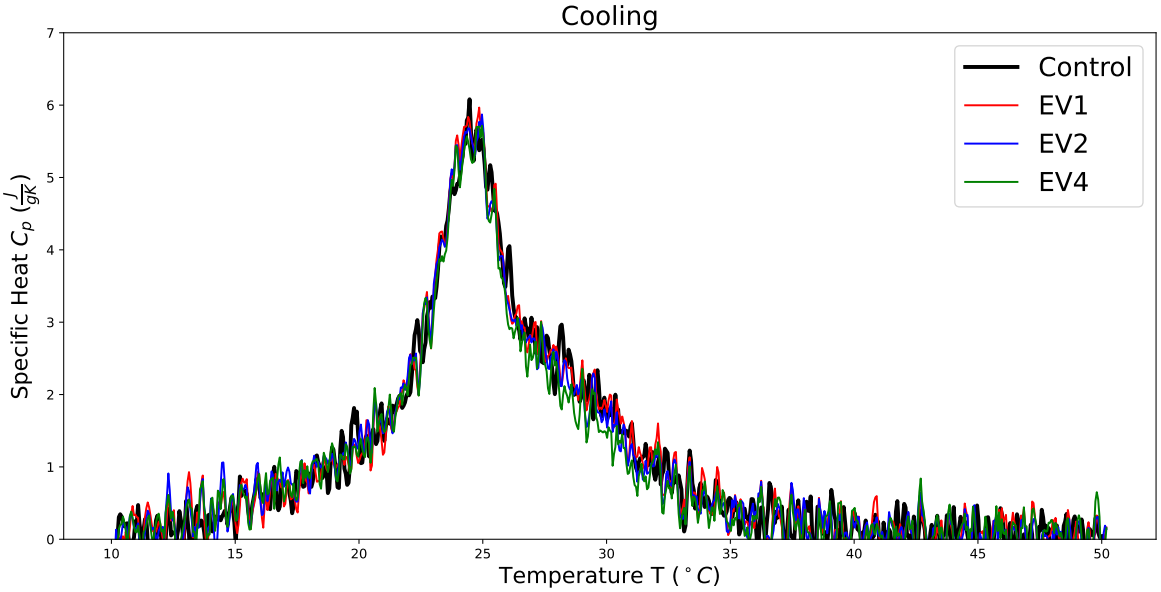

Figure 6.10: Trend of the specific heat C_p at varying temperatures, obtained by DSC measurements on DMPC/SM (2 : 1 m/m) with 17 $mol\%$ chol LUVs in $NaCl$ buffer, before (control) and after the interaction of incremental amount of sEVs. EV1 represents the first doses of EVs added to the system, whereas EV2 and EV4 are sequential doses with doubled amounts compared to the previous one. Scan rate $3°C/min$, cooling mode.

In a multicomponent system the peak identification is not trivial, and the signal-to-noise ratio is often lower compared to the single-component configuration. In Figure 6.10, and more clearly in Figure 6.11 and Figure 6.12, the fitting of the control before the EV addition, and the one for the highest amount of EV added are reported respectively. For the control sample before the EV addition, a broad transition can be observed, characterised by a sharp peak at $24.52°C$ and a wider one at $29.20°C$. The presence of two peak was already investigated in previous work [110], and explained considering an impairment of the lipid raft contribute within the lipid bilayer, with portions more enriched in SM and cholesterol forming the domains compared to others. In particular, since T_m provides information about the degree of cooperativity between the hydrocarbon chains during their melting process, the presence of the second peak in the thermogram would be associated with the portion of the lipid bilayer rich in lipid rafts [173, 110]. Afterward, the EVs were added to the LUV system, doubling the amount every four cycles of cooling and heating. With increasing concentrations of sEVs, a quasi-zero enthalpy variation can be observed for the first two doping amounts with respect to the control, while a small decrease in the enthalpy contribution in the thermogram region of the second peak around $28.96°C$ can be noted. Moreover, this

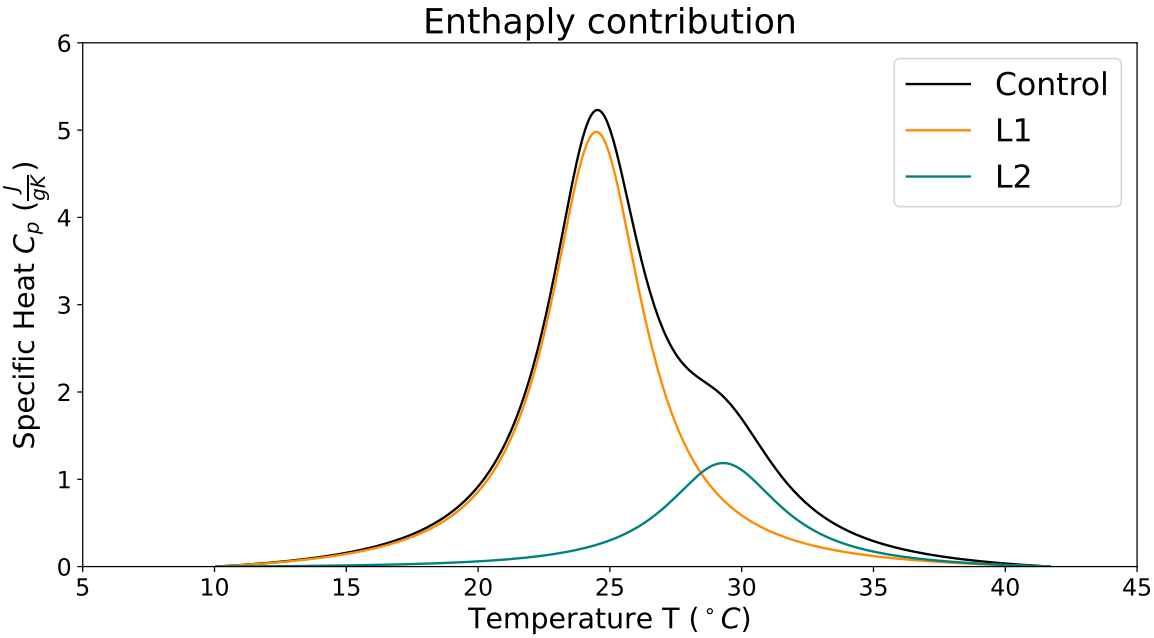

Figure 6.11: Fitting of the specific heat C_p at varying temperatures obtained by DSC measurements on the control sample composed of DMPC/SM (2 : 1 m/m) with 17 $mol\%$ chol LUVs in $NaCl$ buffer, with the first (L1) and second (L2) peaks of the lorentzian fitting highlighted. Scan rate $3°C/min$, cooling mode.

decrease is also accompanied by a small variation in the total entropy contribute of the system, calculated in the range of $12-42\ °C$, which decreases from 41.17 $\frac{J}{K}$ to 38.6 $\frac{J}{K}$, so a 7% of variation from the initial state without sEVs, to the last one where the highest amount of vesicles has been added. No relevant full width at half maximum (FWHM) have been observed for the peak describing the transition of the all system, with values of 4.23 and 4.82 for the control and the EV4 configurations respectively. Comparing this result with previous work performed in a similar system, and with the results obtained from the AFM study, a possible explanation of these values would be that EVs fusion with the LUV leads to a disordering of the lipid raft portion, accompanied by a consistent decrease of the cooperativity of the SM-Chol rich areas, whereas the peak describing the main transition temperature of the system, which is characteristic for the DOPC-rich region is not affected. This would be confirmed by the AFM imaging introduced in Chapter 6 and Chapter 7, where two main phenomena have been observed and discussed: the high affinity of the EVs for the L_o domains, and the fluidizing effect of the L_o domains upon vesicles fusion.

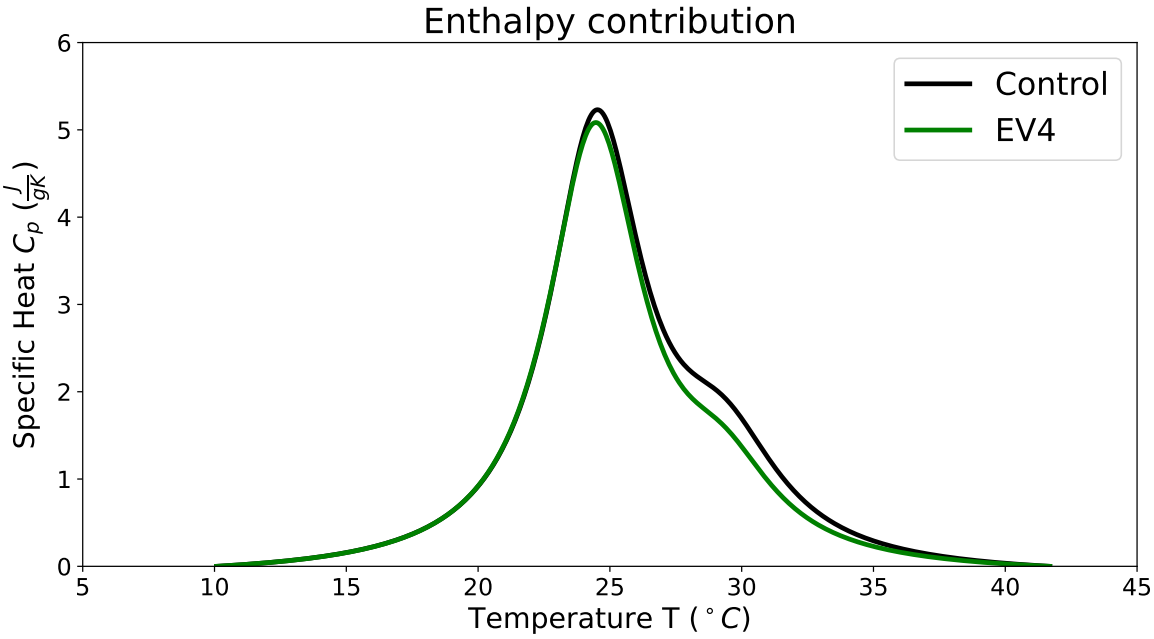

Figure 6.12: Comparison of the fitting of the specific heat C_p at varying temperatures obtained by DSC measurements for the control sample composed of DMPC/SM (2 : 1 m/m) with 17 $mol\%$ chol LUVs, and after the addition of the highest doping amount (EV4) of EVs, analyzed in $NaCl$ buffer. For both cases, the first (L1) and second (L2) peaks of the lorentzian fitting are highlighted. Scan rate $3°C/min$, cooling mode.

Chapter 7

Biophysical parameters involved in small EV interaction with model systems

7.1 SLB optimization with coexisting fluid-gel phases

The next step of the model system optimization focuses on the formation of a SLB without the cholesterol contribution. To that end, two different compositions have been tested, DOPC/SM and DOPC/DPPC, with a molar ratio of 2 : 1. The corresponding AFM images and height profiles are reported in Figure 7.1.
With this new configuration, the goal was to investigate possible differences in terms of sEVs uptake mechanisms, and to understand if they would be mediated or not by the different lipid bilayer fluidity. Many studies have indeed highlighted the important role of cholesterol in mediating molecular trafficking across the cell membrane as reported previously in Chapter 2, by modulating the packing degree of the lipids and their lateral mobility. Hence, it would be interesting to see how the process of sEVs uptake would be affected in this direction. Lastly, DPPC has been used as a counterpart of SM, to evaluate whether the sEVs interaction process would be mainly driven by chemical or physical forces.

The selected lipids, SM and DPPC, both display a similar phase transition, with a T_m around $\sim$ $37°C$ for SM, and of $\sim$ $41°C$ for DPPC. Therefore, at the selected imaging temperature of $27°C$ they are both in the solid-like gel state (S_o). The standard protocol for lipid deposition and SLB formation is reported in Chapter 5. However, for the SLB without cholesterol, and with the introduction of DPPC, it was decided to perform the first part of sample incubation at a temperature between $55 - 60°C$ for 40 min in order to let the self-assembling molecules stabilize at the solid-liquid interface at a temperature sufficiently far from their T_m. All the other parameters were

kept unchanged.

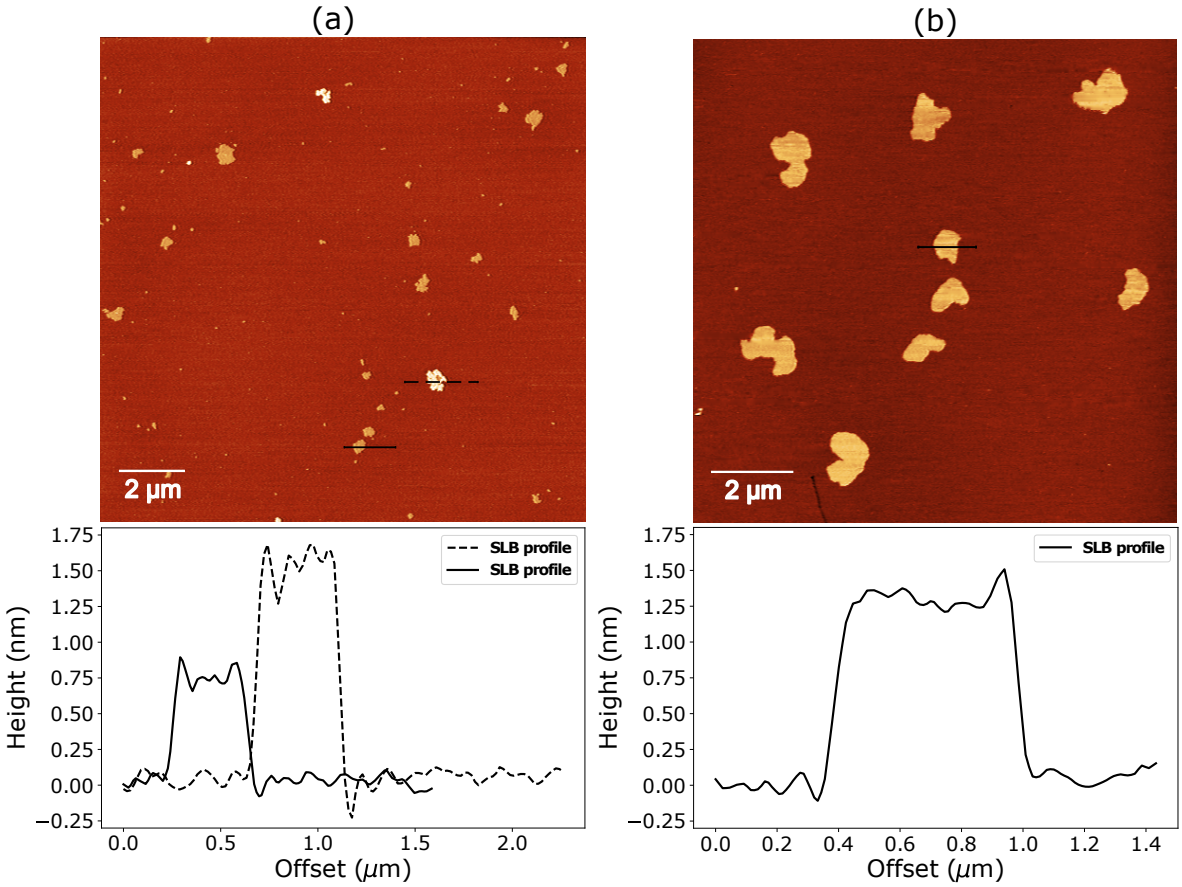

Figure 7.1: AFM topographic images of (a) DOPC/SM and (b) DOPC/DPPC 2 : 1 (m/m) SLB with corresponding height profiles, acquired at 27°C in Tris buffer 10 mM, in AC-mode in liquid.

From the AFM images reported in Figure 7.1 a clear difference in the S_o domain area and height profile can be appreciated. In both cases, the bilayer is expected to have domains in the S_o phase, with a greater difference in height compared to the system enriched in cholesterol. Respectively, SM domains cover an average percentage area of 1.17 % and protrude 1.75 nm over the surrounding L_d phase of DOPC layer, whereas DPPC domains are bigger in size, occupying an average area of 2.8 % with a relative height of 2 nm. Interestingly, the height profile of the two configurations differs as well. For the SLB with DPPC the domains are uniform in height and almost flat, while for SM a step profile is observed, with the lower height level around 0.75 nm, and the higher one around 1.50 nm. This result can be explained by referring to the DSC data of SM and DPPC phase transition. From the literature, it was reported that a mixture of DOPC/SM displays a broad peak in the range of $10 - 30°C$, which means that at

the investigated imaging temperature of $27°C$, SM does not undergo a full transition to S_o state. A fraction of the lipids, represented by the lower domains, might feature a leaflet-leaflet asymmetry, with one leaflet in the fluid state, and the other one in the solid state. Instead, those domains appearing 1.50 nm above the SLB would be in the solid state [174]. This asymmetry is not seen for the lipid mixture of DOPC/DPPC, with the domains uniformly protruding above the surrounding fluid phase of DOPC. This high homogeneity has been attributed to a high coupling between the two leaflets, undergoing phase transition along a less broad temperature range and with a higher degree of cooperativity compared to SM [175, 109].

7.2 Role of lipid bilayer fluidity in small EV adsorption on SLB

Given the relevance of cholesterol molecules in modulating SLB architecture, and in regulating the biomolecules trafficking across the membrane, it has been decided to investigate the sEVs interaction process with SLB of different fluidity, to understand whether cholesterol plays a role in driving the sEVs uptake and degree of mixing with the SLB.

To that end, in the following section a comparative analysis of the sEVs interaction with DOPC/SM SLB will be performed for sEVs isolated from both cell lines (see Figure 7.2 and Figure 7.3), whereas the interaction of sEVs-MDA-MB-231 will be also complemented with a SLB composed of DOPC/DPPC (reported in Figure 7.4), in order to investigate possible chemical affinities between the sEVs and the selected lipid component forming the SLB.

The first example of sEV-SLB interaction is reported in Figure 7.2, acquired within a few minutes after vesicles addition to the system. The area here reported is the same that has been analyzed and described in Figure 7.1a. A preferential interaction of sEV-MDA-MB-231 with SM domains is here observed. Upon vesicles fusion, height protrusions of $\sim 3-5$ nm are formed in correspondence with the highest second leaflet of SM domains. Interestingly, it would be expected to have a preferential insertion of the sEVs at the interface of the two SM asymmetric leaflets, or along the phase borders of the two lipid phases, as both would represent two energetically favorable sites for molecule interaction. However, the sEVs protrusions only localize over the symmetric part of the S_o domains. Moreover, by analyzing the same area in a time scale of $1; h$, an overall height increase of the protrusions can be noted, with no morphological variations in the area surrounding the site of interaction.
This result would give insight about the increasing amount of sEVs that are interacting over time. This can be explained by looking at the first portion of molecules,

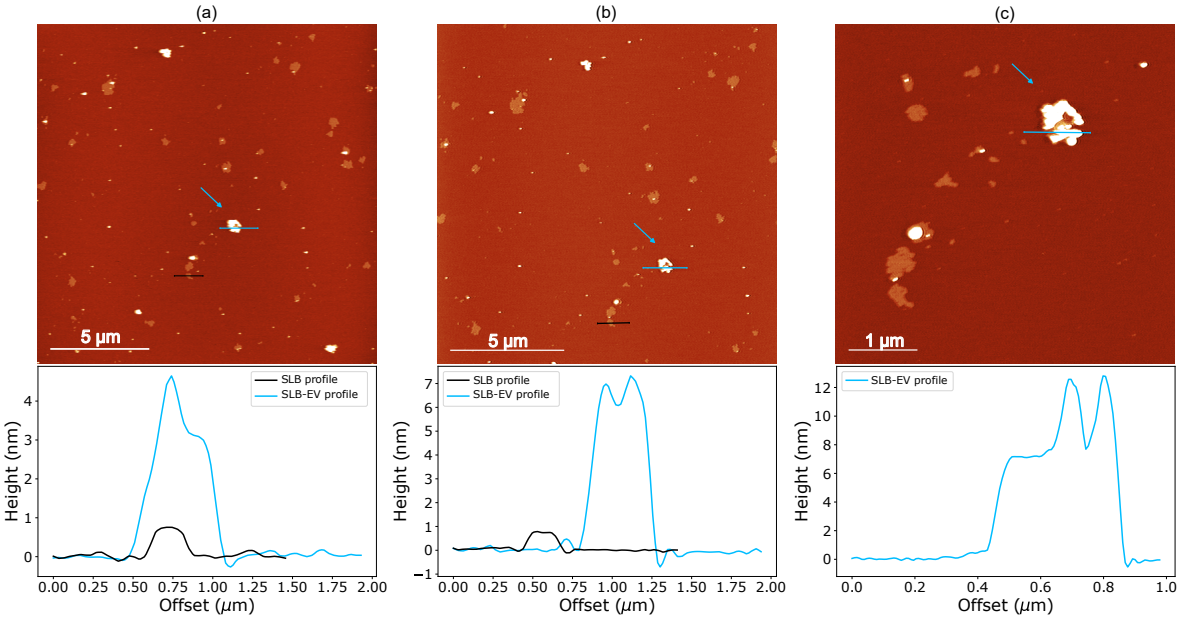

Figure 7.2: Time-resolved AFM topographic images of sEVs (MDA-MB-231 cell line) interacting with DOPC/SM 2 : 1 (m/m) SLB with corresponding height profiles, acquired at 27 $°C$ in Tris buffer 10 mM, with a time-lapse between (a) and (b) of 1 h. Figure 7.2c is a magnification of Figure 7.2b, acquired within few minutes.

already fused with the SLB, as a preferential docking site for the remaining part of sEVs still present in the solution. Lastly, taking into account the goal of using sEVs as a possible drug delivery system, it is fundamental to identify the optimal conditions through which sEVs would be able to fuse with the bilayer, and to permeate the interface they are interacting with. Thus, the selection of the parameters to be manipulated in order to maximize both EV-SLB interaction and mixing efficiency is of primary importance. For the case of DOPC/SM system, two information can be extrapolated by the AFM imaging of the vesicles uptake: the first one is that sEVs uptake is cholesterol-sensitive, being this process maximize with 0 $chol\%$ and localized in those areas with high ordering degree; the second one is that sEVs are no longer able to fully mix with the SLB as proposed in Figure 6.8, but remain semi-adsorbed over the lipid bilayer phase-separated domains, without altering the surrounding lipid bilayer architecture. A similar mechanism of nanometer size lipid vesicles interaction, with lipid bilayer membrane in the gel state, has been proposed in the field of drug-delivery based nanocarriers, with the goal of understanding the biophysical factors regulating the vesicles uptake. Among them, lipid bilayer ordering features a decreased permeability to external molecules compared to lipid bilayers in the fluid state [176]. This would explain the different impact of sEVs upon their fusion with the SLB, where the mixing and lipid redistribution are facilitated by the presence of cholesterol inferring

higher lateral mobility and permeability to the lipid bilayer, and instead being hindered by the more rigid and less permeable lipid bilayer barrier in the gel state.

The same system has then been tested in interaction with sEVs-UC-MSC (see Figure 7.3), in order to investigate possible differences in the vesicles uptake depending on the sEVs origin. Surprisingly, a similar interaction to the one previously reported

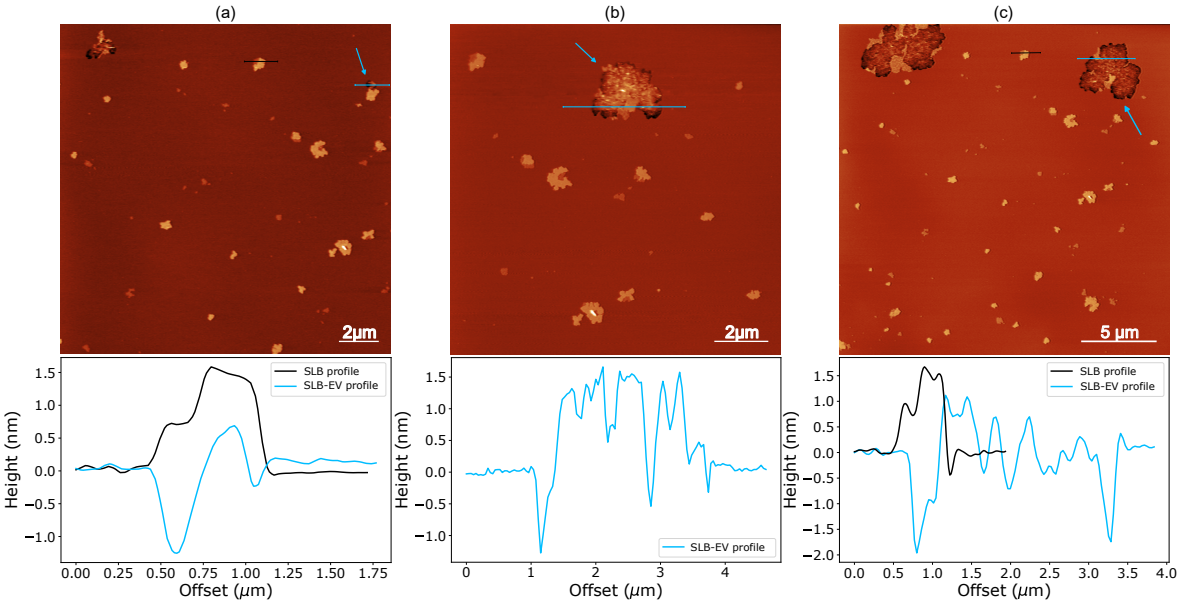

Figure 7.3: Time-resolved AFM topographic images of EVs (UC-MSC cell line) interacting with DOPC/SM 2 : 1 (m/m) SLB with corresponding height profiles, acquired at 27 $°C$ in Tris buffer 10 mM, with a time-lapse of 20 minutes. The blue arrow localize the same area in the three images.

for the system enriched in cholesterol (Figure 6.9) is observed. In particular, also in this configuration, sEVs-UC-MSC leads to the formation of patches within the level of SM domains, characterized by high granularity and gradually surrounding the S_o involved in the interaction. However, performing a time-resolved analysis, with a time interval of 20 min, it can be noted not that the area occupied by the lipids-EVs patches increases over time, and gradually surrounds the S_o domain involved in the interaction process. Moreover, from the first image (Figure 7.3a) to the last one of the time series (Figure 7.3c), it can be noted the lipid domains far from the interaction site do not undergo morphological variation, while the one involved in the sEVs uptake are progressively incorporated by the more irregular lipid patch at their edges, with an overall redistribution of lipids upon vesicles mixing. Differently from the sEV-MDA-MB-231, a higher degree of mixing is here observed, and confirmed by the formation of an intermediate likely lipid phase with a typical thickness of 1.5 nm, growing over the time

at the edges of the lipid patches. The intrinsic differences in the sEVs interaction with the same SLB configuration, might be related to a different sensitivity to cholesterol levels, with sEVs-UC-MSC displaying a preferential affinity for a more disordered SLB, in agreement with the results reported in the literature [144].

The next step of the proposed study, aimed to investigate whether the interaction between sEVs-MDA-MB-231 and SLB was driven by chemical or physical forces. To that end, in Figure 7.4 is reported the interaction of sEVs with a SLB now composed of DOPC/DPPC, where DPPC forms the S_o phase similarly to SM lipid.

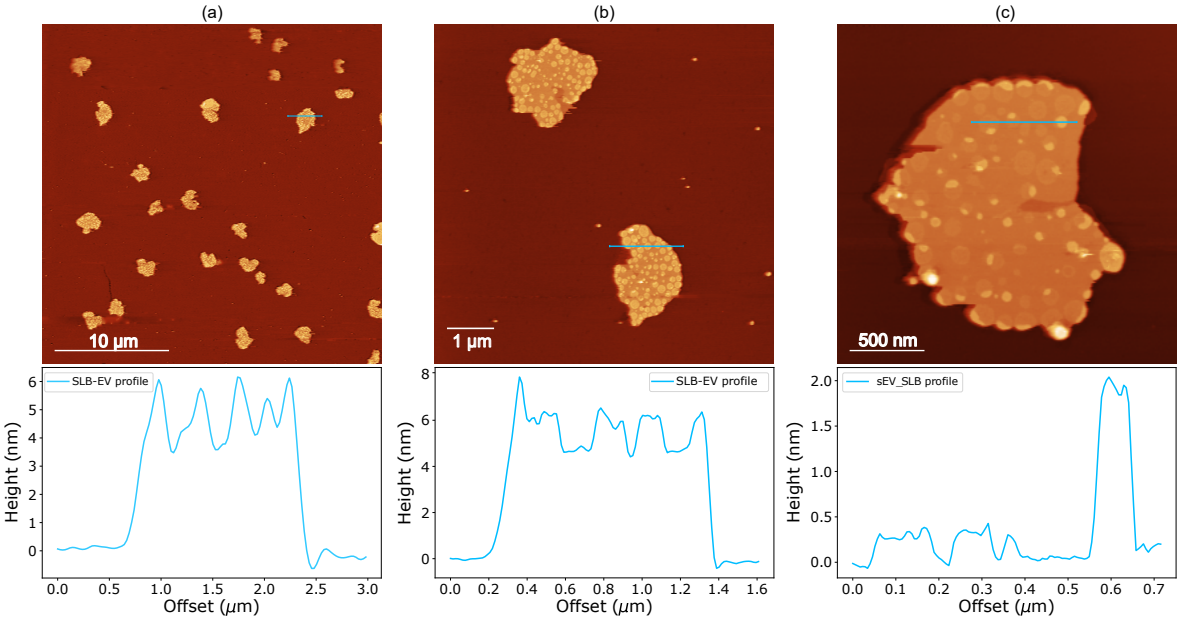

Figure 7.4: AFM topographic images of EVs (MDA-MB-231 cell line) interacting with DOPC/DPPC 2 : 1 (m/m) SLB with corresponding height profiles, acquired at 27 $°C$ in Tris buffer 10 mM, with a time-lapse of 15 minutes.

In line with what has been reported for sEV-MDA-MB-231 interacting with DOPC/SM SLB, also in this case a preferential interaction with the S_o domains is observed, with a full domain area coverage upon vesicles addition. However, differently from what has been reported so far, where protrusions in the range of $4 - 12$ nm were observed, now the overall SLB profile is changed. In particular, the initial difference in height of $1.5 - 2$ nm between the L_d and S_o phases reported in Figure 7.1b, gives space to a much higher step width of 8 nm. Moreover, the height profile of the domains is characterized by the presence of protrusions 0.5 nm in height, displaying a regular quasi-spherical shape, and following a profile that is typical of small lipid rafts as well. A possible explanation of this process would be the vesicles engulfment by the DPPC

domains, whose mechanism consists of the spreading of the molecules/vesicles onto the membrane, followed by their partial or complete engulfment within the membrane. This process would explain the presence of visible vesicular structure populating the S_o domains, and contributing to the massive increase of the overall thickness of the lipid bilayer [157]. Lastly, there is evidence that lipid vesicles diffusion, as well as membrane permeability, would be governed by diverse parameters, i.e. vesicles size and concentration, lipid packing, and the free surface area per lipid [176]. Thus, to be in the position of confirming this theory, and excluding other mechanisms such as selective cholesterol recruitment, or lipids flip-flop between the two layers, further investigations would be needed.

7.3 Investigating chemical vs physical sEVs affinity for SLB components

The last step of the model system optimization consists in the preparation of two lipid bilayer, one in the fluid state composed of DOPC, and one in the solid state composed of DPPC. The main reason was to evaluate and confirm the hypothesis of sEVs preferential affinity for a system characterised by a higher degree of order, and to have at the same time a simple system that allows to better evaluate the mechanism of vesicle fusion with the solid phase. The resulting AFM images of DOPC and DPPC are respectively illustrated in Figure 7.5.
DOPC is known to exist in the fluid state at room temperature, thus forming an L_d phase when analysed at $27°C$ with AFM. After being incubated for a sufficiently long time at $50°C$, upon cooling to the final imaging temperature, a complete and uniform SLB covering the mica substrate was obtained, with only small defects visible in the center of the AFM image. In order to reduce the number of visible defects in the lipid bilayer, a higher lipid concentration of 0.04 mg/mL was used, and the first step of incubation was performed at $50°C$ for 40 min. The opposite configuration is represented by DPPC SLB, forming the S_o phase at $27°C$. However, working under the same conditions used for DOPC, it was not possible to obtain a uniform SLB with good reproducibility. Several attempts have been made combining a longer sample incubation with higher temperature (up to $1h$ at $65°C$), with higher concentration up to a maximum of 0.08 mg/mL. At last, it was decided to hydrate the mica surface with 10 mM KCl before depositing the DPPC vesicles over the substrate. A final incubation temperature of $65°C$ for 30 min, followed by a cooling step to $27°C$ at $0.07°C/s$ was then chosen as the optimal parameter. The resulting SLB is illustrated in Figure 7.5b, displaying large patches partially covering the mica substrate. Small protrusions in the range of 4 nm in height above the SLB can be noted, and are usually identified, from previous studies, as adsorbed or partially fused vesicles [177, 178]. The introduction of KCl was useful for reducing the formation of molecular clusters over

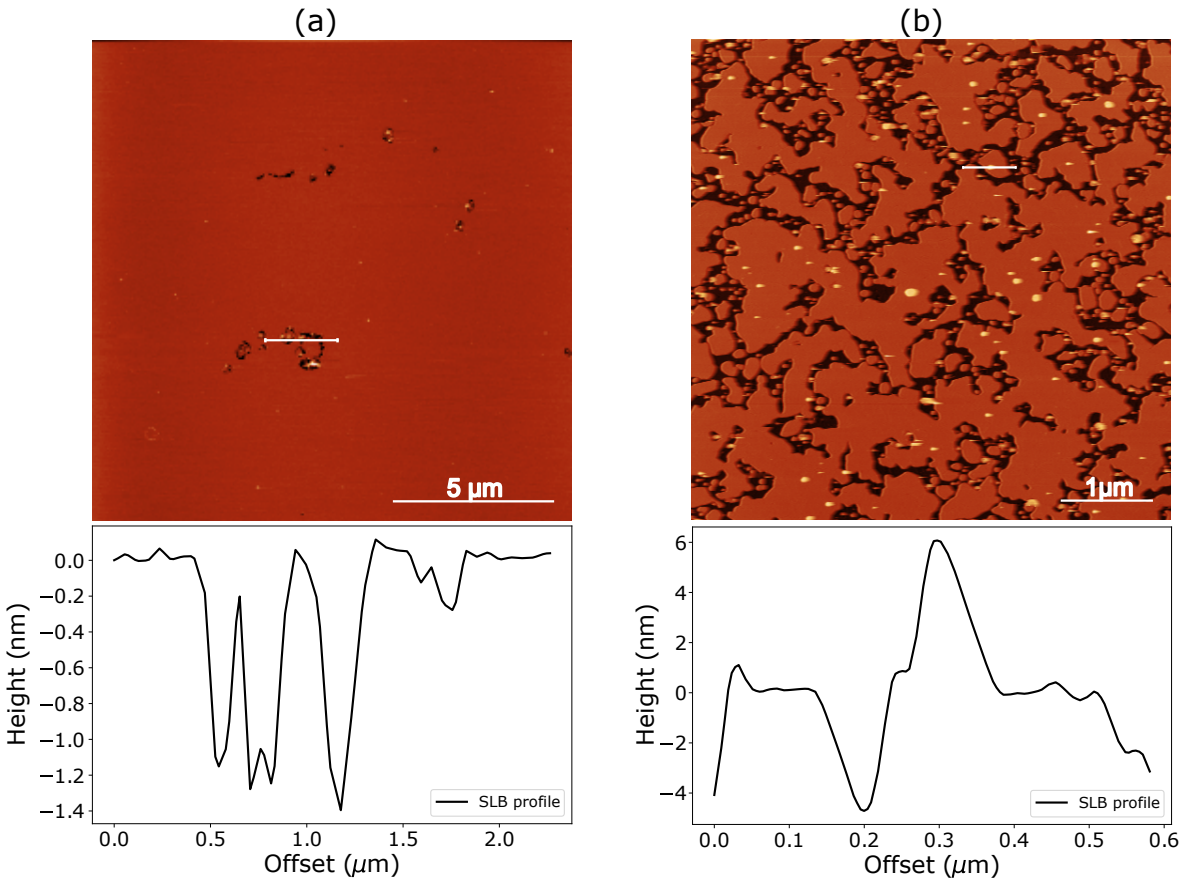

Figure 7.5: AFM topographic images of (a) DOPC and (b) DPPC SLB with corresponding height profiles, acquired at $27°C$ in Tris buffer 10 mM, in AC-mode in liquid.

the mica substrate where the DPPC molecules, quickly undergoing phase transition, would remain stacked. Moreover, since it has been demonstrated that the substrate contributes to the shifting of the phase transition to higher temperature values, the DPPC vesicles were incubated at $65°C$, far from their transition range. These two changes in the SLB protocol led to the successful SLB formation.

In order to confirm the hypothesis of the more physical instead of chemical interaction between sEVs and the SLB, two opposite control conditions have been tested and reported in Figure 7.6, with sEV-MDA-MB-231 interacting with SLB in the fluid state composed of DOPC (see Figure 7.6a), and with a DPPC SLB in the gel state in Figure 7.6b. In agreement with the results reported so far, for sEVs interacting with the DOPC SLB, only small protrusions can be detected within the bilayer defects, with no vesicles interacting with the L_d phase. Contrary, for the SLB composed of DPPC forming the S_o phase, the vesicles localize within the lipid bilayer patches, forming

regular protrusions with a 'raft-like' profile, as already observed in Figure 7.4 for the binary SLB made of DOPC/DPPC.

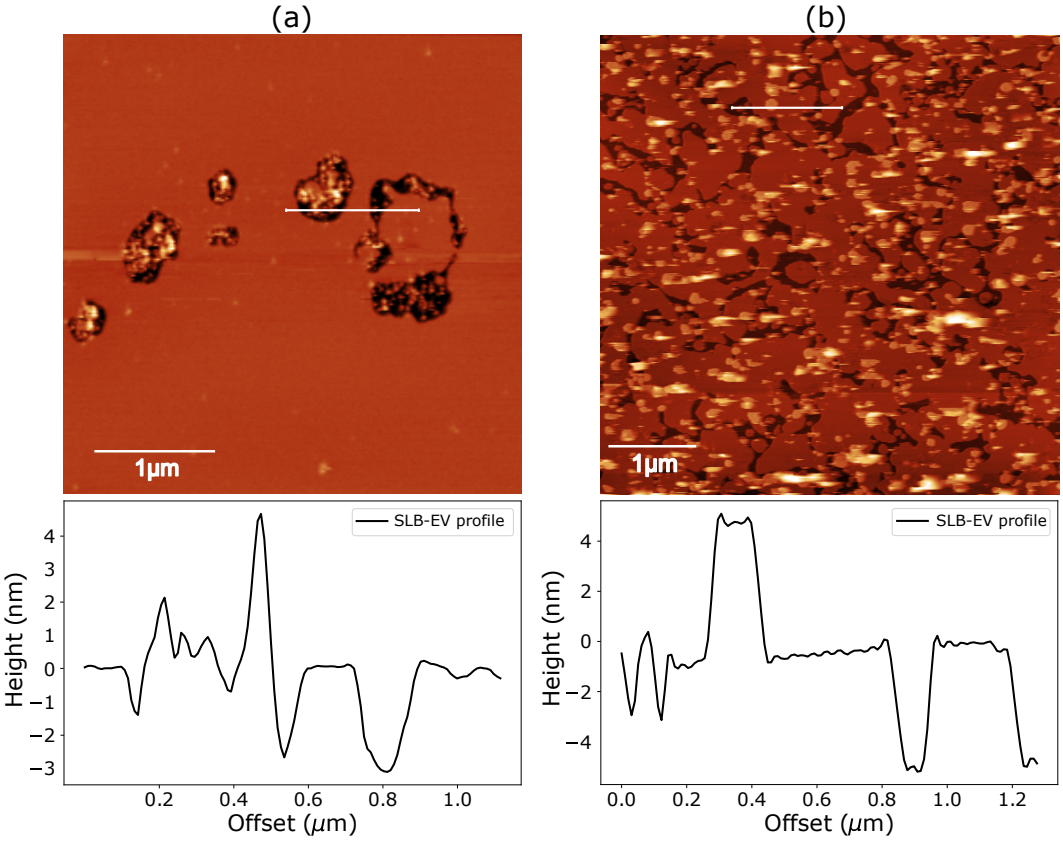

Figure 7.6: AFM topographic images of DOPC (a) and DPPC (b) SLB after sEVs (MDA-MB-231 cell line) interaction with corresponding height profiles, acquired at $27°C$ in Tris buffer 10 mM.

7.4 Application toward monitoring fusion kinetics of spike-EVs

Following the model system optimization, and its validation for the analysis of sEVs interacting with the SLB, the lipid bilayer platform was applied for the study of the interaction mechanisms of sEVs expressing the spike protein of SARS-CoV-2, provided by B. Bussolati from the University of Torino. For this study, the starting point was the already published work about the possibility of mimicking the interaction of SARS-CoV-2 with host cell, by means of sEVs expressing the spike protein of SARS-CoV-2 [179]. In particular, the possibility to specifically detect with high spatial resolution the

fusion process of sEVs with the SLB, and discriminate differences between the sEVs expressing or not the protein, were investigated. To simplify the description of the process, the vesicles representing the control not expressing the protein will be mentioned as C-EVs, whereas the vesicles expressing the spike protein will be nominated as S-EVs. In both cases, the samples provided by this collaboration were isolated from human embryonic kidney (HEK-293T) cells. They were transfected with a vector coding for the S1 and S2 subunits, in order to obtain spike engineered EVs. Their findings of the EVs interaction with primary human umbilical vein endothelial cells (HUVEC) via fluorescence measurements, reported a significantly higher S-EV uptake with respect to the C-EVs. This result was attributed to the presence of the spike protein and its preferential interaction with ACE2 receptor, which is known to have a high binding affinity for the SARS-CoV-2 virus, favoring the CoVs entry into the recipient cells [180].

Based on these considerations, a comparative AFM analysis has been performed to investigate possible differences between the C-EV and S-EV interaction with the SLB composed of DOPC/SM in $2:1$ m/m ratio, with 17 $mol\%$ of cholesterol.
The preliminary results of the C-EV and S-EV interaction with the SLB are reported in Figure 7.7 and 7.8 respectively. In both cases, a preferential interaction of the vesicles with the L_o domains was observed, with the clusters of vesicles and lipids forming protrusions characterized by high granularity and heterogeneous height distribution. However, the resulting impact on the SLB is quite different. For C-EV sample interacting with the SLB, after the initial mixing with the lipid bilayer, the EV clusters remain confined to the site of interaction with no detectable lipid bilayer structure modification after the uptake. Whereas, for the case of S-EV an overall rearrangement of the lipid domain distribution within the scanned area is observed, with no visible lipid domains around the site of interaction. This result is also accompanied by a higher area occupied by the EV clusters, meaning that after vesicles interaction with the SLB, a massive redistribution of the lipid elements takes place. These results would partially confirm the higher fusion rate of S-EV observed in the host cells, however, further studies have yet to be performed in order to shed light in this direction. As a next step, it would be interesting to investigate different binding affinity and fusion events between the EVs and the two spike protein subunits, the S-1 and S-2, by integrating them into the lipid bilayer system.

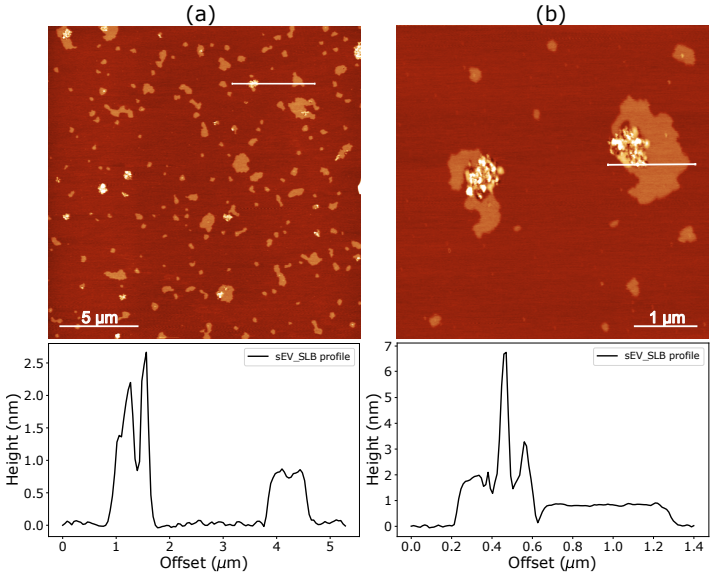

Figure 7.7: AFM topographic images of C-EVs interacting with DOPC/SM 2 : 1 (m/m) SLB with 10 $mol\%$ Chol with corresponding height profiles, acquired at room temperature in Tris buffer 10 mM.

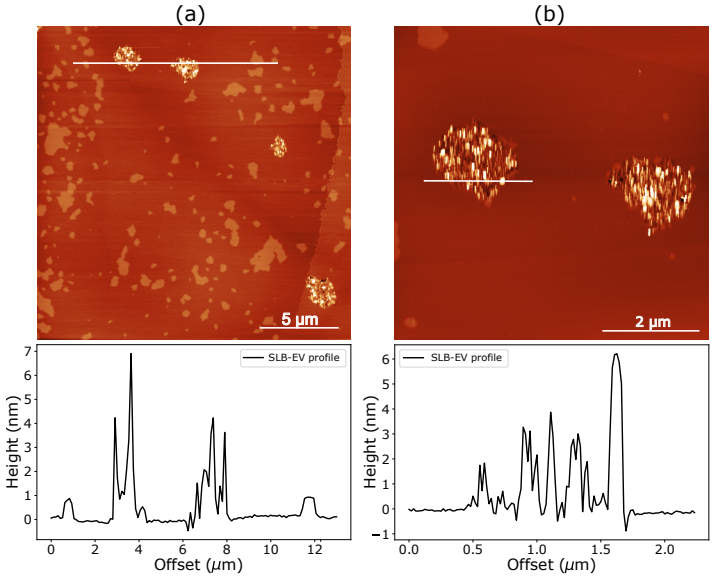

Figure 7.8: AFM topographic images of S-EVs interacting with DOPC/SM 2 : 1 (m/m) SLB with 10 $mol\%$ Chol with corresponding height profiles, acquired at room temperature in Tris buffer 10 mM.

Chapter 8

Conclusions and Future perspectives

In conclusion, this thesis presents the development and optimization of biomimetic model systems in the form of supported lipid bilayers. In particular, a protocol for atomic force microscopy imaging of a supported lipid bilayer in a liquid environment has been developed, with the ultimate goal of assessing a representative biological composition of cell membranes, able to mimic their typical lipid raft lateral compartmentalization. To this end, atomic force microscopy represents a powerful tool for studying the formation of lipid bilayer lateral organization, with the possibility of varying parameters, i.e. composition, buffer, and temperature. Moreover, it allows to perform the investigation of dynamic processes with high spatial and temporal details.
In the proposed study, morphological analysis has been conducted to elucidate lipid domain phase separation differences for a ternary lipid mixture of DOPC, SM, and cholesterol, depending on the buffering agent used to hydrate the sample. In particular, the reconstituted lipid bilayer has been investigated under three different liquid environments (milliQ, $NaCl$, Tris). In both cases, a lipid phase separation has been observed, with DOPC mostly forming a liquid disordered phase, and the SM and cholesterol, preferentially forming domains in a more ordered fluid state, also reported here with the name of lipid rafts. Among the three tested conditions, Tris buffer provided the best degree of reproducibility and lipid bilayer stability, working under controlled environmental conditions.
Given the high spatial and temporal resolution that can be obtained performing AFM imaging, as a next step the optimized model system has been applied to the study of small extracellular vesicles interaction with the reconstituted lipid bilayer. To that end, sEVs vesicles provided from a GMP facility and isolated from the UC-MSC cell line have been used to validate the model system, evidencing a preferential interaction at the lipid domain edges, and a progressive mixing with the fluid phase of the model system. Thereafter, the cholesterol concentration was raised to approach biological

percentages. Performing a morphological analysis of lipid raft domain variation as a function of cholesterol concentration, the cholesterol condensing effect widely investigated in literature has been highlighted.
Lastly, focusing on the ultimate goal of understanding biological relevant events taking part during the sEVs interaction with the cell membrane, sEVs isolated from a metastatic breast cancer cell line, the MDA-MB-231, have been isolated upon protocol optimization, following the guidelines provided by ISEV. Performing fast AFM imaging under temperature control, it has been possible to follow a different interaction pathway, compared to the previously investigated sEVs from the UC-MSC cell line. In particular, tumor-derived sEVs featured a preferential interaction with lipid rafts, highly impacting their structural integrity upon mixing. In this regard, the hypothesis of a combined fluidizing effect due to molecular cargo release upon mixing, and lipids redistribution within the lipid bilayer, has been postulated. On the other side, preliminary results of the sEVs from the HEK-293T cell line highlighted higher invasiveness and degree of interaction for the vesicles expressing the spike protein, in agreement with the results previously published by Bussolati's Lab [179]. Even though further investigations have yet to be performed, these results confirm the robustness of such a simple model system as a powerful tool for modeling much more complex cellular processes.
Finally, to investigate the possible influence of lipid bilayer fluidity in the regulation of sEVs uptake, it has been decided to play with the lipid bilayer composition, by testing the same system without cholesterol, the main regulator of this parameter. In this new configuration, a lipid phase separation between DOPC and SM has been observed, with SM now forming a solid-ordered phase characterized by low lateral mobility. The main results highlighted a high sEVs affinity for the lipid domains characterized by low lateral mobility, yet displaying a lower capability of mixing with the lipid components, with no detectable disrupting effects exerted by the sEVs interaction with the lipid bilayer. Moreover, replacing the SM with the DPPC lipid component, sEVs displayed an almost equal degree of affinity for the lipid domains, evidencing that the interaction process is more dependent on the lateral organization and mobility of the lipids they are interacting with, instead of their chemical composition.
Concluding, although the lipid composition is limited to a restricted choice of lipids and cholesterol range, with the proposed biophysical approach it has been possible to discern between the chemical and physical driving forces regulating the sEVs uptake. In particular, the lipid bilayer lateral organization and fluidity, are fundamental in the modulation of the sEVs rate of interaction and degree of mixing with the lipid raft domains. This result underlines the need to develop strategies in the future, which should combine the vesicles properties (e.g. molecular cargo, surface functionalization), with the chemical and physical properties of the target cell membrane. Moreover, in the perspective of using sEVs as possible drug delivery systems, the cell membrane fluidity and the eventual temporary loss of lipid raft integrity associated with the

tumor-derived sEVs might represent two key parameters to be investigated. Indeed, a balance between the two proposed events should be identified, in order to maximize the interaction process, while still ensuring the cell membrane homeostasis upon vesicle fusion. In this direction, further studies of possible lipids redistribution in the cell membrane after vesicles uptake would be helpful to rationalize the dynamics of the sEVs uptake. Along with this aspect, considering the loss of lipid domain integrity after sEVs interaction with the lipid bilayer, possible side effects on cell membrane integrity preservation would need further investigations, and would be meaningful for the improvement of the application of sEVs as drug delivery systems.
Furthermore, it is interesting to note that this versatile platform can be applied to study the impact of surface functionalization strategies (e.g. fusogenic proteins) on the vesicle uptake pathways, but it can also be easily integrated, besides cholesterol molecules, with other lipids and proteins.

Given the wide number of parameters that can be tested with a relatively simple and cost-effective approach, lipid model systems represent a powerful tool for investigating a plethora of different processes, ranging from protein insertion and migration within the lipid bilayer, molecules, and particle interaction dynamics (e.g. synthetic nanoparticles, liposomes, peptides), as well as binding affinity for functionalization strategies validation.

As future perspectives, the next step would consist of the development of a biomimetic system with increasing complexity. In particular, the possibility of reconstituting transmembrane proteins in the lipid bilayer is one of the topics under investigation at the NanoInnovation laboratory. More in detail, the platform would be applied to the study, in the context of breast cancer cells of Her2, a protein belonging to the family of EGF receptors and involved in cellular processes such as cell growth and differentiation. Altered levels of HER2, as for Her2-overexpressing breast cancer cells, are associated with a poor prognosis and high aggressiveness of these cells [181]. Moreover, numerous studies have also demonstrated Her2 clusterization with a specific class of cell membrane subdomains called caveolae, which are identified as membrane invaginations involved in the regulation of cellular processes such as vesicular transport, cell signaling, cell migration and proliferation [182]. However, controversial hypotheses have been postulated regarding the cellular site where the protein activation takes place. Given the relevant functions of caveolae domains, a better understanding of Her2 colocalization with or outside these domains, and their interplay with other membrane components involved in cancer formation and progression i.e. EGF receptors and gangliosides (e.g. GM1 and GM2), would be beneficial for improving the success rate of targeted therapies [44, 51, 182].
To exploit this topic, the first requirement is to develop a model membrane able to mimic the characteristic caveolae domains, which are found in the cell membrane as

nanometric membrane invaginations, with an average size of 60 nm [183]. In this direction, preliminary tests have been performed on silica-based porous substrates, found in literature as pore-spanning membrane, to reconstitute the caveolin-1 protein, primarily involved in the structural shaping of caveolae domains [184, 185]. However, further investigations are needed for the identification of the optimal substrate properties (e.g. cleaning procedure, functionalization, and hydrophilicity), as well as for the sample preparation and deposition protocols to get a uniform and stably suspended lipid bilayer over the porous substrate.

Appendix A

Characterization of small-EVs

A.1 AFM characterization

For AFM analysis of individual sEVs isolated from the MDA-MB-231 cell line, a freshly cleaved mica of 10 mm in diameter with $0.15-0.21$ mm thickness (from Micro to Nano) was first incubated with 30 μL of Poly-L-Ornithine (from Sigma-Aldrich) for 20 min; after an extensive washing with Milli-Q H_2O, 30 μL of sEVs were let to incubate for 20 min and then gently rinsed with 50 μL of 10 mM PBS before AFM imaging.
The AFM size characterization is reported in Figure A.1. From the size distribution in the scatter plot, we found a sEV's typical height was 15.43 ± 5.77 nm, with a mean diameter equal to 49.73 ± 18.24 nm, calculated on a number of 112 vesicles. These values reside in the typical range that can be found in the literature [186, 187].

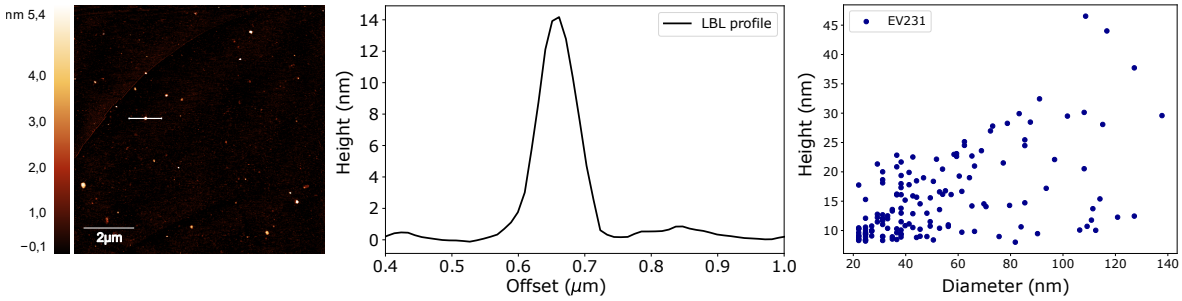

Figure A.1: AFM size characterisation of sEVs from MDA-MB-231 cell line, imaged in PBS 1X over MICA substrate.

A.2 ATR-FTIR spectroscopy for the evaluation of protein-lipid ratio in sEVs

ATR-FTIR spectroscopic measurement has been performed for UC-MSC-EVs, to evaluate their protein/lipid ratio in a semi-quantitative way. Indeed, by the analysis of the absorption bands of the .., looking at the position of the single peaks, is possible to extrapolate the chemical composition of the sample, which combined with the peak intensity and bandwidth, also provides semi-quantitative information of the relative concentration of the different components. Figure A.2 reports the absorbance spectrum, with highlighted in red the most representative regions, according to the literature [186].

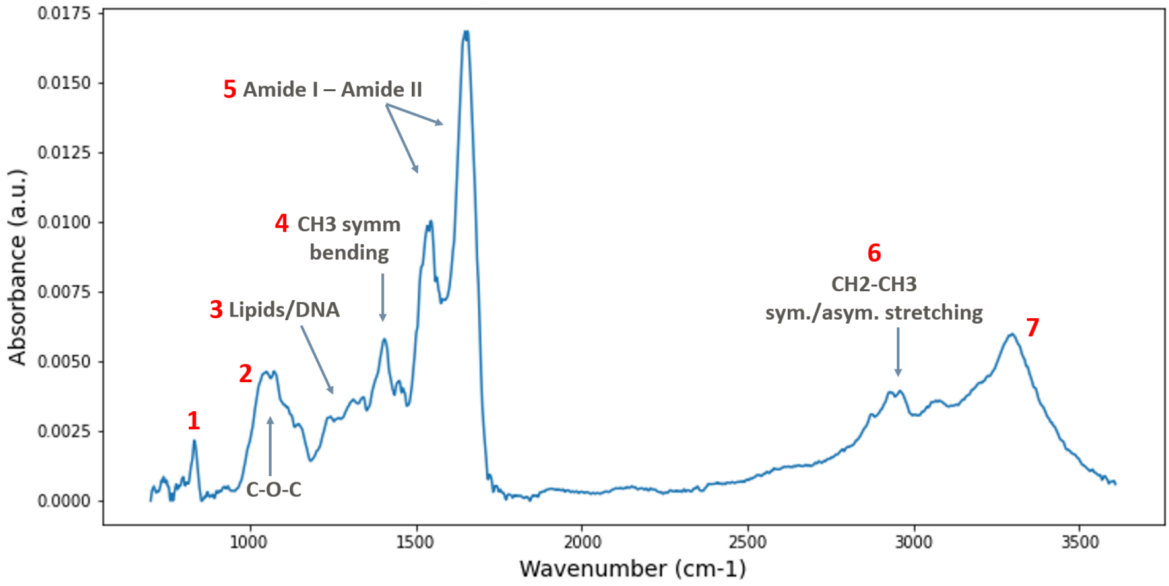

Figure A.2: Absorbance spectrum from the ATR-FTIR measurement of the UC-MSC-EVs. The numbered regions are assigned to the following bands peaks: (1) inorganic compounds of PBS at $850-950\ cm^{-1}$; (2) C-O-C and PO_2 (stretching) bands at $950-1300\ cm^{-1}$; (3,4) CH_2-CH_3 (bending) at around $1390-1470 cm^{-1}$, overlapping with the DNA and lipid contribution; (5) Amide I and Amide II at around $1550-1650\ cm^{-1}$ (6) CH_2 (stretching) bands at around $2850-2930\ cm^{-1}$; (7) Amide A band at around $3290\ cm^{-1}$.

The analysis reveals that the vibrational spectrum is dominated by two central peaks at $1650\ cm^{-1}$ and $1550\ cm^{-1}$, and one at $3290\ cm^{-1}$, which are characteristic of the Amide I and Amide II, commonly associated with the protein contribution. Area 1 has instead been assigned to the PBS buffer in which the sEVs are suspended, located

in the region of around $850 - 950\ cm^{-1}$. Area 2 has been assigned to the stretching vibrations of ethers (C-O-C), and diester phosphates (PO_2), at $950 - 1300\ cm^{-1}$. Lastly, the bending vibrations characteristic for the CH_2/CH_3 contributions, can be found in the spectral range of 1390 $cm-1$ and 1470 cm^{-1}.

To characterize the extracellular vesicles protein/lipid (P/N) ratio, two regions of interest have been investigated, the Amide I band for the protein contributions, and the stretching vibrations of CH_2/CH_3 for the lipid contributions, with a resulting P/L of 6.23. The choice of Amide I as a representative region for the protein contribution has to be attributed to its characteristic C=O (stretching) bond, which resides in the protein backbone. The Amide II and Amide A, representative of the N-H bending/stretching variations, have not been taken into account in the P/N calculation.
For the contribution of the lipid instead, the regions of 2850 and 2930 cm^{-1} have been considered as the most representative of the CH_2-groups and terminal CH_3-groups with which their acyl chains are enriched.

Appendix B

Complementary AFM images of SLB

B.1 Control experiment of PBS buffer effect on SLB

Figure B.1 reports a control experiment performed for the SLB composition of DOPC/SM (2:1) with 5 $mol\%$ in milliQ environment, where 30 μl of PBS have been added to the lipid bilayer to investigate possible lipid domains morphology changes related to the buffer in which the sEVs are suspended.

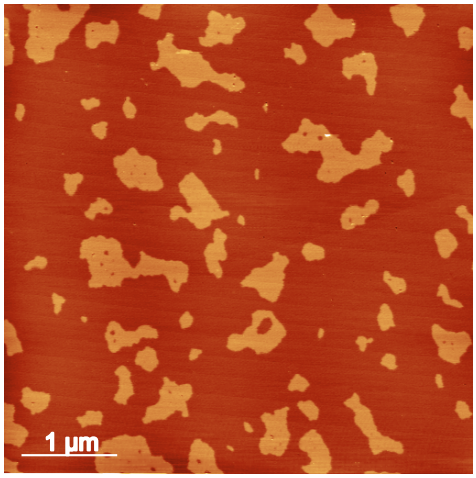

Figure B.1: AFM topographic image of DOPC/SM (2:1) with 5 $mol\%$ chol SLB after addition of 30 μl of PBS, acquired at room temperature, in AC-mode in liquid.

The AFM topographic image confirms that no evident effects can be noted, ensuring

that the SLB morphological changes upon sEVs addition, are only related to sEVs-SLB interaction, and not to the buffer contribution.

B.2 AFM phase channel of SLB after sEVs-MDA-MB-231 interaction

The AFM phase channel provides information about the coexistence of diverse materials in the SLB, as observed by the color contrast be the areas of the SLB. Even though only a small degree shift can be observed, the L_o-sEVs protrusions described in Figure 6.8 domains are characterized by the coexistence of sEVs-related compounds (in orange/red color) and lipid-related compounds in green, close to the surrounding L_d phase.

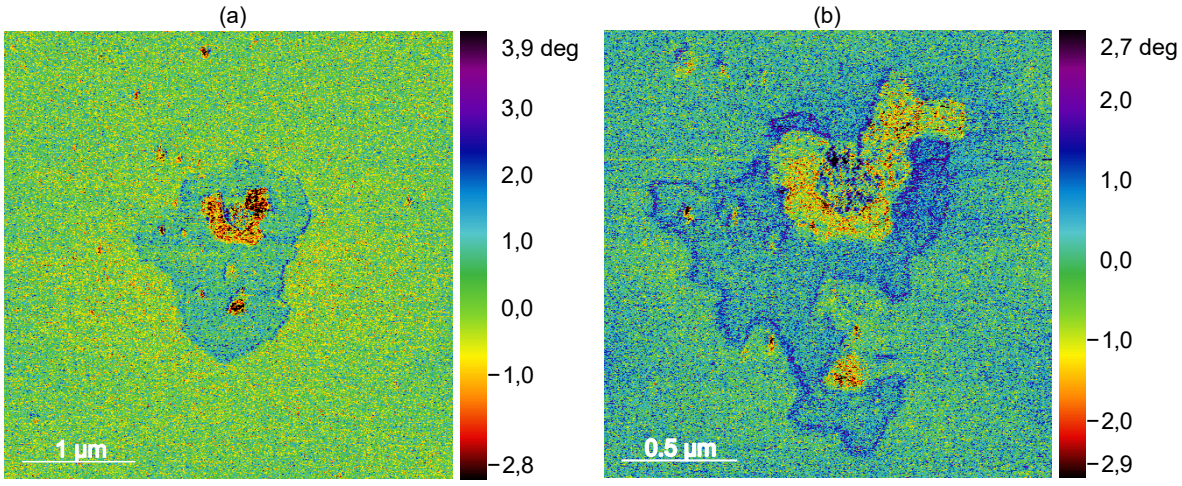

Figure B.2: Time-resolved AFM phase channel of DOPC/SM (2:1) with 17 $mol\%$ chol SLB after addition of sEVs-MDA-MB-231, acquired at $27°C$ in AC-mode in liquid, with a time-lapse of 5 min.

Bibliography

[1] Siewert J Marrink et al. "Computational modeling of realistic cell membranes". In: *Chemical reviews* 119.9 (2019), pp. 6184–6226.

[2] Alf Honigmann and Arnd Pralle. "Compartmentalization of the cell membrane". In: *Journal of molecular biology* 428.24 (2016), pp. 4739–4748.

[3] Gerrit Van Meer, Dennis R Voelker, and Gerald W Feigenson. "Membrane lipids: where they are and how they behave". In: *Nature reviews Molecular cell biology* 9.2 (2008), pp. 112–124.

[4] Erdinc Sezgin and Petra Schwille. "Model membrane platforms to study protein-membrane interactions". In: *Molecular membrane biology* 29.5 (2012), pp. 144–154.

[5] Chiranjeevi Peetla, Andrew Stine, and Vinod Labhasetwar. "Biophysical interactions with model lipid membranes: applications in drug discovery and drug delivery". In: *Molecular pharmaceutics* 6.5 (2009), pp. 1264–1276.

[6] Lukas K Tamm and Harden M McConnell. "Supported phospholipid bilayers". In: *Biophysical journal* 47.1 (1985), pp. 105–113.

[7] Joshua A Jackman and Nam-Joon Cho. "Supported lipid bilayer formation: beyond vesicle fusion". In: *Langmuir* 36.6 (2020), pp. 1387–1400.

[8] Xiang Yu and Jie Zheng. "Cholesterol promotes the interaction of Alzheimer β-amyloid monomer with lipid bilayer". In: *Journal of molecular biology* 421.4-5 (2012), pp. 561–571.

[9] Fabio Perissinotto et al. "Iron-mediated interaction of alpha synuclein with lipid raft model membranes". In: *Nanoscale* 12.14 (2020), pp. 7631–7640.

[10] Paulina D Rakowska et al. "Nanoscale imaging reveals laterally expanding antimicrobial pores in lipid bilayers". In: *Proceedings of the National Academy of Sciences* 110.22 (2013), pp. 8918–8923.

[11] Katja Kastl et al. "Kinetics and thermodynamics of annexin A1 binding to solid-supported membranes: a QCM study". In: *Biochemistry* 41.31 (2002), pp. 10087–10094.

[12] Jannik B Larsen et al. “How membrane geometry regulates protein sorting independently of mean curvature”. In: *ACS Central Science* 6.7 (2020), pp. 1159–1168.

[13] Leonid Margolis and Yoel Sadovsky. “The biology of extracellular vesicles: The known unknowns”. In: *PLoS biology* 17.7 (2019), e3000363.

[14] Kinsley C French, Marc A Antonyak, and Richard A Cerione. “Extracellular vesicle docking at the cellular port: Extracellular vesicle binding and uptake”. In: *Seminars in cell & developmental biology*. Vol. 67. Elsevier. 2017, pp. 48–55.

[15] Federico Colombo, Erienne G Norton, and Emanuele Cocucci. “Microscopy approaches to study extracellular vesicles”. In: *Biochimica et Biophysica Acta (BBA)-General Subjects* 1865.4 (2021), p. 129752.

[16] Beatrice Senigagliesi et al. “Triple negative breast cancer-derived small extracellular vesicles as modulator of biomechanics in target cells”. In: *Nanomedicine: Nanotechnology, Biology and Medicine* 44 (2022), p. 102582.

[17] John S O’Brien. “Cell membranes—composition: structure: function”. In: *Journal of theoretical biology* 15.3 (1967), pp. 307–324.

[18] José C Dıaz and Jovan Kamcev. “Ionic conductivity of ion-exchange membranes: Measurement techniques and salt concentration dependence”. In: *Journal of Membrane Science* 618 (2021), p. 118718.

[19] S Jonathan Singer and Garth L Nicolson. “The Fluid Mosaic Model of the Structure of Cell Membranes: Cell membranes are viewed as two-dimensional solutions of oriented globular proteins and lipids.” In: *Science* 175.4023 (1972), pp. 720–731.

[20] G Vereb et al. “Dynamic, yet structured: the cell membrane three decades after the Singer–Nicolson model”. In: *Proceedings of the national academy of sciences* 100.14 (2003), pp. 8053–8058.

[21] Xiaobing Chen, Ziareena Al-Mualem, and Carlos Baiz. “Lipid Landscapes: Vibrational Spectroscopy for Decoding Membrane Complexity”. In: (2023).

[22] Timothée Rivel, Christophe Ramseyer, and Semen Yesylevskyy. “The asymmetry of plasma membranes and their cholesterol content influence the uptake of cisplatin”. In: *Scientific reports* 9.1 (2019), p. 5627.

[23] Michael Edidin. “The state of lipid rafts: from model membranes to cells”. In: *Annual review of biophysics and biomolecular structure* 32.1 (2003), pp. 257–283.

[24] Kai Simons and Winchil LC Vaz. “Model systems, lipid rafts, and cell membranes”. In: *Annu. Rev. Biophys. Biomol. Struct.* 33 (2004), pp. 269–295.

[25] Thomas Pomorski et al. “Lipid distribution and transport across cellular membranes”. In: *Seminars in cell & developmental biology*. Vol. 12. 2. Elsevier. 2001, pp. 139–148.

[26] Kai Simons and Julio L Sampaio. “Membrane organization and lipid rafts”. In: *Cold Spring Harbor perspectives in biology* 3.10 (2011), a004697.

[27] Erick J Dufourc. “Sterols and membrane dynamics”. In: *Journal of chemical biology* 1.1-4 (2008), pp. 63–77.

[28] Kai Simons. “Cell membranes: A subjective perspective”. In: *Biochimica et Biophysica Acta (BBA)-Biomembranes* 1858.10 (2016), pp. 2569–2572.

[29] Nigel Chaffey. *Alberts, B., Johnson, A., Lewis, J., Raff, M., Roberts, K. and Walter, P. Molecular biology of the cell. 4th edn.* 2003.

[30] Helen Watson. “Biological membranes”. In: *Essays in biochemistry* 59 (2015), pp. 43–69.

[31] Ünal Coskun and Kai Simons. “Cell membranes: the lipid perspective”. In: *Structure* 19.11 (2011), pp. 1543–1548.

[32] Jelske N van der Veen et al. “The critical role of phosphatidylcholine and phosphatidylethanolamine metabolism in health and disease”. In: *Biochimica et Biophysica Acta (BBA)-Biomembranes* 1859.9 (2017), pp. 1558–1572.

[33] Dick Hoekstra et al. “Membrane dynamics and cell polarity: the role of sphingolipids”. In: *Journal of lipid research* 44.5 (2003), pp. 869–877.

[34] Massimo Masserini and Daniela Ravasi. “Role of sphingolipids in the biogenesis of membrane domains”. In: *Biochimica et Biophysica Acta (BBA)-Molecular and Cell Biology of Lipids* 1532.3 (2001), pp. 149–161.

[35] Gauri A Patwardhan and Yong-Yu Liu. “Sphingolipids and expression regulation of genes in cancer”. In: *Progress in lipid research* 50.1 (2011), pp. 104–114.

[36] Giovanni D’Angelo et al. “Glycosphingolipids: synthesis and functions”. In: *The FEBS journal* 280.24 (2013), pp. 6338–6353.

[37] Drew Marquardt et al. “Cholesterol’s location in lipid bilayers”. In: *Chemistry and Physics of Lipids* 199 (2016), pp. 17–25.

[38] Henna Ohvo-Rekilä et al. “Cholesterol interactions with phospholipids in membranes”. In: *Progress in lipid research* 41.1 (2002), pp. 66–97.

[39] Oskar Engberg et al. “The affinity of cholesterol for different phospholipids affects lateral segregation in bilayers”. In: *Biophysical journal* 111.3 (2016), pp. 546–556.

[40] Harden M McConnell and Arun Radhakrishnan. “Condensed complexes of cholesterol and phospholipids”. In: *Biochimica et Biophysica Acta (BBA)-Biomembranes* 1610.2 (2003), pp. 159–173.

[41] Sandra Tan, Hwee Tong Tan, and Maxey CM Chung. "Membrane proteins and membrane proteomics". In: *Proteomics* 8.19 (2008), pp. 3924–3932.

[42] Robert Ian Nicholson, Julia Margaret Wendy Gee, and Maureen Elaine Harper. "EGFR and cancer prognosis". In: *European journal of cancer* 37 (2001), pp. 9–15.

[43] Sara Sigismund, Daniele Avanzato, and Letizia Lanzetti. "Emerging functions of the EGFR in cancer". In: *Molecular oncology* 12.1 (2018), pp. 3–20.

[44] Sylviane Lambert et al. "Ligand-independent activation of the EGFR by lipid raft disruption". In: *Journal of Investigative Dermatology* 126.5 (2006), pp. 954–962.

[45] Patrıcia MR Pereira et al. "Caveolin-1 mediates cellular distribution of HER2 and affects trastuzumab binding and therapeutic efficacy". In: *Nature communications* 9.1 (2018), p. 5137.

[46] Borui Li et al. "Lipid raft involvement in signal transduction in cancer cell survival, cell death and metastasis". In: *Cell proliferation* 55.1 (2022), e13167.

[47] Thomas Harder. "Formation of functional cell membrane domains: The interplay of lipid–and protein–mediated interactions". In: *Philosophical Transactions of the Royal Society of London. Series B: Biological Sciences* 358.1433 (2003), pp. 863–868.

[48] Kai Simons and Derek Toomre. "Lipid rafts and signal transduction". In: *Nature reviews Molecular cell biology* 1.1 (2000), pp. 31–39.

[49] Toshiyuki Murai et al. "The role of lipid rafts in cancer cell adhesion and migration". In: *International journal of cell biology* 2012 (2012).

[50] Faustino Mollinedo and Consuelo Gajate. "Lipid rafts as major platforms for signaling regulation in cancer". In: *Advances in biological regulation* 57 (2015), pp. 130–146.

[51] Claudia Grossmann et al. "Colocalization of mineralocorticoid and EGF receptor at the plasma membrane". In: *Biochimica et Biophysica Acta (BBA)-Molecular Cell Research* 1803.5 (2010), pp. 584–590.

[52] M Pickl and CH Ries. "Comparison of 3D and 2D tumor models reveals enhanced HER2 activation in 3D associated with an increased response to trastuzumab". In: *Oncogene* 28.3 (2009), pp. 461–468.

[53] Kimberly S George and Shiyong Wu. "Lipid raft: A floating island of death or survival". In: *Toxicology and applied pharmacology* 259.3 (2012), pp. 311–319.

[54] Anil Badana et al. "Lipid raft integrity is required for survival of triple negative breast cancer cells". In: *Journal of breast cancer* 19.4 (2016), pp. 372–384.

[55] J Bernd Helms and Chiara Zurzolo. "Lipids as targeting signals: lipid rafts and intracellular trafficking". In: *Traffic* 5.4 (2004), pp. 247–254.

[56] Alex J Laude and Ian A Prior. "Plasma membrane microdomains: organization, function and trafficking". In: *Molecular membrane biology* 21.3 (2004), pp. 193–205.

[57] Clotilde Théry et al. "Minimal information for studies of extracellular vesicles 2018 (MISEV2018): a position statement of the International Society for Extracellular Vesicles and update of the MISEV2014 guidelines". In: *Journal of extracellular vesicles* 7.1 (2018), p. 1535750.

[58] Sushmita Mukherjee and Frederick R Maxfield. "Role of membrane organization and membrane domains in endocytic lipid trafficking". In: *Traffic* 1.3 (2000), pp. 203–211.

[59] Erdinc Sezgin et al. "The mystery of membrane organization: composition, regulation and roles of lipid rafts". In: *Nature reviews Molecular cell biology* 18.6 (2017), pp. 361–374.

[60] Laura Ann Mulcahy, Ryan Charles Pink, and David Raul Francisco Carter. "Routes and mechanisms of extracellular vesicle uptake". In: *Journal of extracellular vesicles* 3.1 (2014), p. 24641.

[61] Erik R Abels and Xandra O Breakefield. "Introduction to extracellular vesicles: biogenesis, RNA cargo selection, content, release, and uptake". In: *Cellular and molecular neurobiology* 36 (2016), pp. 301–312.

[62] Rosa Vona, Elisabetta Iessi, and Paola Matarrese. "Role of cholesterol and lipid rafts in cancer signaling: a promising therapeutic opportunity?" In: *Frontiers in cell and developmental biology* 9 (2021), p. 622908.

[63] Thomas KM Nyholm et al. "The affinity of sterols for different phospholipid classes and its impact on lateral segregation". In: *Biophysical Journal* 116.2 (2019), pp. 296–307.

[64] Michihiro Sugahara et al. "The structural role of cholesterol in biological membranes". In: *Journal of the American Chemical Society* 123.32 (2001), pp. 7939–7940.

[65] Zhenlu Zhang et al. "Host lipids in positive-strand RNA virus genome replication". In: *Frontiers in microbiology* 10 (2019), p. 286.

[66] Yicong Ma et al. "Cholesterol partition and condensing effect in phase-separated ternary mixture lipid multilayers". In: *Biophysical journal* 110.6 (2016), pp. 1355–1366.

[67] Martin R Krause and Steven L Regen. "The structural role of cholesterol in cell membranes: from condensed bilayers to lipid rafts". In: *Accounts of chemical research* 47.12 (2014), pp. 3512–3521.

[68] Marc Eeman and Magali Deleu. "From biological membranes to biomimetic model membranes". In: *Biotechnologie, Agronomie, Société et Environnement* 14.4 (2010).

[69] John R Silvius. "Role of cholesterol in lipid raft formation: lessons from lipid model systems". In: *Biochimica et Biophysica Acta (BBA)-Biomembranes* 1610.2 (2003), pp. 174–183.

[70] Frederick R Maxfield and Ira Tabas. "Role of cholesterol and lipid organization in disease". In: *Nature* 438.7068 (2005), pp. 612–621.

[71] Irena Levitan, Dev K Singh, and Avia Rosenhouse-Dantsker. "Cholesterol binding to ion channels". In: *Frontiers in physiology* 5 (2014), p. 65.

[72] Julie Grouleff et al. "The influence of cholesterol on membrane protein structure, function, and dynamics studied by molecular dynamics simulations". In: *Biochimica et Biophysica Acta (BBA)-Biomembranes* 1848.9 (2015), pp. 1783–1795.

[73] Gunter P Eckert et al. "Cholesterol modulates amyloid beta-peptide's membrane interactions". In: *Pharmacopsychiatry* 36.S 2 (2003), pp. 136–143.

[74] Etienne Ho Kit Mok and Terence Kin Wah Lee. "The pivotal role of the dysregulation of cholesterol homeostasis in cancer: implications for therapeutic targets". In: *Cancers* 12.6 (2020), p. 1410.

[75] Pedro MR Cruz et al. "The role of cholesterol metabolism and cholesterol transport in carcinogenesis: a review of scientific findings, relevant to future cancer therapeutics". In: *Frontiers in pharmacology* 4 (2013), p. 119.

[76] Yee-Hung M Chan and Steven G Boxer. "Model membrane systems and their applications". In: *Current opinion in chemical biology* 11.6 (2007), pp. 581–587.

[77] Abolfazl Akbarzadeh et al. "Liposome: classification, preparation, and applications". In: *Nanoscale research letters* 8 (2013), pp. 1–9.

[78] Hamdi Nsairat et al. "Liposomes: Structure, composition, types, and clinical applications". In: *Heliyon* (2022).

[79] Edward T Castellana and Paul S Cremer. "Solid supported lipid bilayers: From biophysical studies to sensor design". In: *Surface Science Reports* 61.10 (2006), pp. 429–444.

[80] Gregory J Hardy, Rahul Nayak, and Stefan Zauscher. "Model cell membranes: Techniques to form complex biomimetic supported lipid bilayers via vesicle fusion". In: *Current opinion in colloid & interface science* 18.5 (2013), pp. 448–458.

[81] Kalani J Seu et al. “Effect of surface treatment on diffusion and domain formation in supported lipid bilayers”. In: *Biophysical journal* 92.7 (2007), pp. 2445–2450.

[82] Christian Hennesthal and Claudia Steinem. “Pore-spanning lipid bilayers visualized by scanning force microscopy”. In: *Journal of the American Chemical Society* 122.33 (2000), pp. 8085–8086.

[83] Andreas Janshoff and Claudia Steinem. “Transport across artificial membranes–an analytical perspective”. In: *Analytical and bioanalytical chemistry* 385 (2006), pp. 433–451.

[84] Peter Walde et al. “Giant vesicles: preparations and applications”. In: *ChemBioChem* 11.7 (2010), pp. 848–865.

[85] Qingchuan Li et al. “Electroformation of giant unilamellar vesicles in saline solution”. In: *Colloids and Surfaces B: Biointerfaces* 147 (2016), pp. 368–375.

[86] Yiting Zhang, Haruto Obuchi, and Taro Toyota. “A Practical Guide to Preparation and Applications of Giant Unilamellar Vesicles Formed via Centrifugation of Water-in-Oil Emulsion Droplets”. In: *Membranes* 13.4 (2023), p. 440.

[87] Emel I Goksu et al. “AFM for structure and dynamics of biomembranes”. In: *Biochimica et Biophysica Acta (BBA)-Biomembranes* 1788.1 (2009), pp. 254–266.

[88] Ralf P Richter and Alain R Brisson. “Following the formation of supported lipid bilayers on mica: a study combining AFM, QCM-D, and ellipsometry”. In: *Biophysical journal* 88.5 (2005), pp. 3422–3433.

[89] Valeria Rondelli et al. “Building a biomimetic membrane for neutron reflectivity investigation: Complexity, asymmetry and contrast”. In: *Biophysical Chemistry* 229 (2017), pp. 135–141.

[90] S Ladha et al. “Lateral diffusion in planar lipid bilayers: a fluorescence recovery after photobleaching investigation of its modulation by lipid composition, cholesterol, or alamethicin content and divalent cations”. In: *Biophysical journal* 71.3 (1996), pp. 1364–1373.

[91] Nam-Joon Cho et al. “Quartz crystal microbalance with dissipation monitoring of supported lipid bilayers on various substrates”. In: *Nature protocols* 5.6 (2010), pp. 1096–1106.

[92] Noel F Bonet, Daniel G Cava, and Marisela Vélez. “Quartz crystal microbalance and atomic force microscopy to characterize mimetic systems based on supported lipids bilayer”. In: *Frontiers in Molecular Biosciences* 9 (2022), p. 935376.

[93] Giovanna Fragneto. “Neutrons and model membranes”. In: *The European Physical Journal Special Topics* 213.1 (2012), pp. 327–342.

[94] Frédéric Pincet et al. “FRAP to characterize molecular diffusion and interaction in various membrane environments”. In: *PloS one* 11.7 (2016), e0158457.

[95] Lin Guo et al. “Molecular diffusion measurement in lipid bilayers over wide concentration ranges: a comparative study”. In: *ChemPhysChem* 9.5 (2008), pp. 721–728.

[96] Gerd Binnig, Calvin F Quate, and Ch Gerber. “Atomic force microscope”. In: *Physical review letters* 56.9 (1986), p. 930.

[97] Se-Hui Jung et al. “Molecular imaging of membrane proteins and microfilaments using atomic force microscopy”. In: *Experimental & Molecular Medicine* 42.9 (2010), pp. 597–605.

[98] Nabil A Amro et al. “High-resolution atomic force microscopy studies of the Escherichia coli outer membrane: structural basis for permeability”. In: *Langmuir* 16.6 (2000), pp. 2789–2796.

[99] Peter Fechner et al. “Structural information, resolution, and noise in high-resolution atomic force microscopy topographs”. In: *Biophysical Journal* 96.9 (2009), pp. 3822–3831.

[100] Toshio Ando, Takayuki Uchihashi, and Noriyuki Kodera. “High-speed AFM and applications to biomolecular systems”. In: *Annual review of biophysics* 42 (2013), pp. 393–414.

[101] Hans Gunstheimer et al. “Photothermally driven AFM of biological samples”. In: *Biophysical Journal* 122.3 (2023), 548a.

[102] Yves F Dufrêne et al. “Imaging modes of atomic force microscopy for application in molecular and cell biology”. In: *Nature nanotechnology* 12.4 (2017), pp. 295–307.

[103] Ignacio Casuso, Felix Rico, and Simon Scheuring. “Biological AFM: where we come from–where we are–where we may go”. In: *Journal of Molecular Recognition* 24.3 (2011), pp. 406–413.

[104] A Raudino, MG Sarpietro, and M Pannuzzo. “Differential scanning calorimetry (DSC): theoretical fundamentals”. In: *Drug-Biomembrane Interaction Studies*. Elsevier, 2013, pp. 127–168.

[105] César Leyva-Porras et al. “Application of differential scanning calorimetry (DSC) and modulated differential scanning calorimetry (MDSC) in food and drug industries”. In: *Polymers* 12.1 (2019), p. 5.

[106] Patrick Garidel, Christof Johann, and Alfred Blume. “Thermodynamics of lipid organization and domain formation in phospholipid bilayers”. In: *Journal of liposome research* 10.2-3 (2000), pp. 131–158.

[107] Ruthven NAH Lewis, David A Mannock, and Ronald N McElhaney. "Differential scanning calorimetry in the study of lipid phase transitions in model and biological membranes: practical considerations". In: *Methods in Membrane Lipids* (2007), pp. 171–195.

[108] Julian M Sturtevant. "The effect of sodium chloride and calcium chloride on the main phase transition of dimyristoylphosphatidylcholine". In: *Chemistry and physics of lipids* 95.2 (1998), pp. 163–168.

[109] Costas Demetzos. "Differential scanning calorimetry (DSC): a tool to study the thermal behavior of lipid bilayers and liposomal stability". In: *Journal of liposome research* 18.3 (2008), pp. 159–173.

[110] M Grava et al. "Small extracellular vesicles impact on target membrane structure and dynamics". In: *Il nuovo cimento C* 45.6 (2022), pp. 1–4.

[111] Miriam Grava et al. "Calorimetry of extracellular vesicles fusion to single phospholipid membrane". In: *Biomolecular Concepts* 13.1 (2022), pp. 148–155.

[112] Erwin Chargaff, Randolph West, et al. "The biological significance of the thromboplastic protein of Wood." In: *Journal of Biological Chemistry* 166 (1946), pp. 189–197.

[113] Peter Wolf. "The nature and significance of platelet products in human plasma". In: *British journal of haematology* 13.3 (1967), pp. 269–288.

[114] Erica Bazzan et al. "Critical review of the evolution of extracellular vesicles' knowledge: From 1946 to today". In: *International Journal of Molecular Sciences* 22.12 (2021), p. 6417.

[115] Isabel Huang-Doran, Chen-Yu Zhang, and Antonio Vidal-Puig. "Extracellular vesicles: novel mediators of cell communication in metabolic disease". In: *Trends in Endocrinology & Metabolism* 28.1 (2017), pp. 3–18.

[116] James Jabalee, Rebecca Towle, and Cathie Garnis. "The role of extracellular vesicles in cancer: cargo, function, and therapeutic implications". In: *Cells* 7.8 (2018), p. 93.

[117] Edit I Buzas. "Opportunities and challenges in studying the extracellular vesicle corona". In: *Nature cell biology* 24.9 (2022), pp. 1322–1325.

[118] Stefano Gelibter et al. "The impact of storage on extracellular vesicles: A systematic study". In: *Journal of Extracellular Vesicles* 11.2 (2022), e12162.

[119] Fumin Yuan, Ya-Min Li, and Zhuhui Wang. "Preserving extracellular vesicles for biomedical applications: Consideration of storage stability before and after isolation". In: *Drug Delivery* 28.1 (2021), pp. 1501–1509.

[120] Thanaporn Liangsupree, Evgen Multia, and Marja-Liisa Riekkola. "Modern isolation and separation techniques for extracellular vesicles". In: *Journal of Chromatography A* 1636 (2021), p. 461773.

[121] Brett G Zani and Elazer R Edelman. "Cellular bridges: Routes for intercellular communication and cell migration". In: *Communicative & integrative biology* 3.3 (2010), pp. 215–220.

[122] Ciro Tetta et al. "Extracellular vesicles as an emerging mechanism of cell-to-cell communication". In: *Endocrine* 44 (2013), pp. 11–19.

[123] Rong Xu et al. "Extracellular vesicles in cancer—implications for future improvements in cancer care". In: *Nature reviews Clinical oncology* 15.10 (2018), pp. 617–638.

[124] Abhimanyu Thakur, Zhubo Wei, and Huanhuan Joyce Chen. "Extracellular vesicles and cell-cell communication in normal cellular processes and cancer". In: *Frontiers in Molecular Biosciences* 10 (2023), p. 1172797.

[125] Xu Zhang et al. "Engineered extracellular vesicles for cancer therapy". In: *Advanced Materials* 33.14 (2021), p. 2005709.

[126] Xinyi Zhang et al. "The biology and function of extracellular vesicles in cancer development". In: *Frontiers in Cell and Developmental Biology* 9 (2021), p. 777441.

[127] Janine Stam et al. "Isolation of extracellular vesicles with combined enrichment methods". In: *Journal of Chromatography B* 1169 (2021), p. 122604.

[128] Gisela Ströhle, Jingxuan Gan, and Huiyan Li. "Affinity-based isolation of extracellular vesicles and the effects on downstream molecular analysis". In: *Analytical and bioanalytical chemistry* 414.24 (2022), pp. 7051–7067.

[129] Thomas A Hartjes et al. "Extracellular vesicle quantification and characterization: common methods and emerging approaches". In: *Bioengineering* 6.1 (2019), p. 7.

[130] Valeria Rondelli et al. "Integrated strategies for a holistic view of extracellular vesicles". In: *ACS omega* 7.23 (2022), pp. 19058–19069.

[131] Zamila Khatun et al. "Elucidating diversity of exosomes: biophysical and molecular characterization methods". In: *Nanomedicine* 11.17 (2016), pp. 2359–2377.

[132] Chun-yi Chiang and Chihchen Chen. "Toward characterizing extracellular vesicles at a single-particle level". In: *Journal of biomedical science* 26.1 (2019), pp. 1–10.

[133] Déborah LM Rupert et al. "Methods for the physical characterization and quantification of extracellular vesicles in biological samples". In: *Biochimica et Biophysica Acta (BBA)-General Subjects* 1861.1 (2017), pp. 3164–3179.

[134] Frank AW Coumans, Elmar L Gool, and Rienk Nieuwland. "Bulk immunoassays for analysis of extracellular vesicles". In: *Platelets* 28.3 (2017), pp. 242–248.

[135] Shailender Singh Kanwar et al. "Microfluidic device (ExoChip) for on-chip isolation, quantification and characterization of circulating exosomes". In: *Lab on a Chip* 14.11 (2014), pp. 1891–1900.

[136] Gary J Doherty and Harvey T McMahon. "Mechanisms of endocytosis". In: *Annual review of biochemistry* 78 (2009), pp. 857–902.

[137] Ilaria Prada and Jacopo Meldolesi. "Binding and fusion of extracellular vesicles to the plasma membrane of their cell targets". In: *International journal of molecular sciences* 17.8 (2016), p. 1296.

[138] Kareemah Ni et al. "The evolving role of caveolin-1: a critical regulator of extracellular vesicles". In: *Medical Sciences* 8.4 (2020), p. 46.

[139] Frank Pfrieger and Nicolas Vitale. "Cholesterol and the journey of extracellular vesicles". In: *Journal of lipid research* 59.12 (2018), pp. 2255–2261.

[140] Wojciech Szlasa et al. "Lipid composition of the cancer cell membrane". In: *Journal of bioenergetics and biomembranes* 52 (2020), pp. 321–342.

[141] Sarah L Veatch and Sarah L Keller. "Separation of liquid phases in giant vesicles of ternary mixtures of phospholipids and cholesterol". In: *Biophysical journal* 85.5 (2003), pp. 3074–3083.

[142] William Trewby, Duncan Livesey, and Kislon Voıtchovsky. "Buffering agents modify the hydration landscape at charged interfaces". In: *Soft Matter* 12.9 (2016), pp. 2642–2651.

[143] Bianca Y van Duyl et al. "Sphingomyelin is much more effective than saturated phosphatidylcholine in excluding unsaturated phosphatidylcholine from domains formed with cholesterol". In: *Febs Letters* 547.1-3 (2003), pp. 101–106.

[144] Fabio Perissinotto et al. "Structural insights into fusion mechanisms of small extracellular vesicles with model plasma membranes". In: *Nanoscale* 13.10 (2021), pp. 5224–5233.

[145] Ruby May A Sullan et al. "Cholesterol-dependent nanomechanical stability of phase-segregated multicomponent lipid bilayers". In: *Biophysical journal* 99.2 (2010), pp. 507–516.

[146] Lin Chen, Zhiwu Yu, and Peter J Quinn. "The partition of cholesterol between ordered and fluid bilayers of phosphatidylcholine: a synchrotron X-ray diffraction study". In: *Biochimica et Biophysica Acta (BBA)-Biomembranes* 1768.11 (2007), pp. 2873–2881.

[147] David Regan et al. “Lipid bilayer thickness measured by quantitative DIC reveals phase transitions and effects of substrate hydrophilicity”. In: *Langmuir* 35.43 (2019), pp. 13805–13814.

[148] Jacqueline Burré, Manu Sharma, and Thomas C Südhof. “α-Synuclein assembles into higher-order multimers upon membrane binding to promote SNARE complex formation”. In: *Proceedings of the National Academy of Sciences* 111.40 (2014), E4274–E4283.

[149] Jared C Lawrence et al. “Real-time analysis of the effects of cholesterol on lipid raft behavior using atomic force microscopy”. In: *Biophysical journal* 84.3 (2003), pp. 1827–1832.

[150] Craig D Blanchette et al. “Using nucleation rates to determine the interfacial line tension of symmetric and asymmetric lipid bilayer domains”. In: *Langmuir* 23.11 (2007), pp. 5875–5877.

[151] Craig D Blanchette et al. “Quantifying growth of symmetric and asymmetric lipid bilayer domains”. In: *Langmuir* 24.4 (2008), pp. 1219–1224.

[152] S Boudard et al. “Controlling the pathway of formation of supported lipid bilayers of DMPC by varying the sodium chloride concentration”. In: *Thin Solid Films* 495.1-2 (2006), pp. 246–251.

[153] Teresa Peiró-Salvador et al. “Buffers may adversely affect model lipid membranes: a cautionary tale”. In: *Biochemistry* 48.47 (2009), pp. 11149–11151.

[154] William Foster et al. “Self-assembly of small molecules at hydrophobic interfaces using group effect”. In: *Nanoscale* 12.9 (2020), pp. 5452–5463.

[155] Kenneth Jacobson and Demetrios Papahadjopoulos. “Phase transitions and phase separations in phospholipid membranes induced by changes in temperature, pH, and concentration of bivalent cations”. In: *Biochemistry* 14.1 (1975), pp. 152–161.

[156] Vıctor Toribio et al. “Development of a quantitative method to measure EV uptake”. In: *Scientific Reports* 9.1 (2019), p. 10522.

[157] Rikhia Ghosh, Vahid Satarifard, and Reinhard Lipowsky. “Different pathways for engulfment and endocytosis of liquid droplets by nanovesicles”. In: *Nature Communications* 14.1 (2023), p. 615.

[158] Ana J Garcıa-Sáez et al. “Pore formation by a Bax-derived peptide: effect on the line tension of the membrane probed by AFM”. In: *Biophysical journal* 93.1 (2007), pp. 103–112.

[159] Reid C Van Lehn et al. “Lipid tail protrusions mediate the insertion of nanoparticles into model cell membranes”. In: *Nature communications* 5.1 (2014), p. 4482.

[160] Katharine Hammond, Maxim G Ryadnov, and Bart W Hoogenboom. "Atomic force microscopy to elucidate how peptides disrupt membranes". In: *Biochimica et Biophysica Acta (BBA)-Biomembranes* 1863.1 (2021), p. 183447.

[161] George A Pantelopulos and John E Straub. "Regimes of complex lipid bilayer phases induced by cholesterol concentration in MD simulation". In: *Biophysical journal* 115.11 (2018), pp. 2167–2178.

[162] Sarah L Veatch and Sarah L Keller. "Miscibility phase diagrams of giant vesicles containing sphingomyelin". In: *Physical review letters* 94.14 (2005), p. 148101.

[163] DJ Müller and Andreas Engel. "The height of biomolecules measured with the atomic force microscope depends on electrostatic interactions". In: *Biophysical journal* 73.3 (1997), pp. 1633–1644.

[164] Frédérick de Meyer and Berend Smit. "Effect of cholesterol on the structure of a phospholipid bilayer". In: *Proceedings of the National Academy of Sciences* 106.10 (2009), pp. 3654–3658.

[165] HM Seeger et al. "Effect of physical parameters on the main phase transition of supported lipid bilayers". In: *Biophysical journal* 97.4 (2009), pp. 1067–1076.

[166] Qianqian Bao et al. "Tumor-derived extracellular vesicles regulate cancer progression in the tumor microenvironment". In: *Frontiers in Molecular Biosciences* 8 (2022), p. 796385.

[167] Carolina Paba et al. "Lipid bilayer fluidity and degree of order regulates small EVs adsorption on model cell membrane". In: *Journal of Colloid and Interface Science* 652 (2023), pp. 1937–1943.

[168] Beatrice Senigagliesi et al. "Subcellular elements responsive to the biomechanical activity of triple-negative breast cancer-derived small extracellular vesicles". In: *Biomolecular Concepts* 13.1 (2022), pp. 322–333.

[169] Sabina M Maté et al. "Boundary region between coexisting lipid phases as initial binding sites for Escherichia coli alpha-hemolysin: A real-time study". In: *Biochimica et Biophysica Acta (BBA)-Biomembranes* 1838.7 (2014), pp. 1832–1841.

[170] Peter I Kuzmin et al. "Line tension and interaction energies of membrane rafts calculated from lipid splay and tilt". In: *Biophysical journal* 88.2 (2005), pp. 1120–1133.

[171] Jian Zhong et al. "Effects of lipid composition and phase on the membrane interaction of the prion peptide 106–126 amide". In: *Biophysical journal* 96.11 (2009), pp. 4610–4621.

[172] Ethan J Miller, Kislon Voıtchovsky, and Margarita Staykova. "Substrate-led cholesterol extraction from supported lipid membranes". In: *Nanoscale* 10.34 (2018), pp. 16332–16342.

[173] Michael H Chiu and Elmar J Prenner. "Differential scanning calorimetry: An invaluable tool for a detailed thermodynamic characterization of macromolecules and their interactions". In: *Journal of Pharmacy and Bioallied Sciences* 3.1 (2011), p. 39.

[174] Hilde A Rinia et al. "Visualizing detergent resistant domains in model membranes with atomic force microscopy". In: *Febs Letters* 501.1 (2001), pp. 92–96.

[175] Marie-Cécile Giocondi et al. "Phase topology and growth of single domains in lipid bilayers". In: *Langmuir* 17.5 (2001), pp. 1653–1659.

[176] Tian-Xiang Xiang and Bradley D Anderson. "Liposomal drug transport: a molecular perspective from molecular dynamics simulations in lipid bilayers". In: *Advanced drug delivery reviews* 58.12-13 (2006), pp. 1357–1378.

[177] Heng-Liang Wu et al. "Phase transition behaviors of the supported DPPC bilayer investigated by sum frequency generation (SFG) vibrational spectroscopy and atomic force microscopy (AFM)". In: *Physical chemistry chemical physics* 18.3 (2016), pp. 1411–1421.

[178] Simon J Attwood, Youngjik Choi, and Zoya Leonenko. "Preparation of DOPC and DPPC supported planar lipid bilayers for atomic force microscopy and atomic force spectroscopy". In: *International journal of molecular sciences* 14.2 (2013), pp. 3514–3539.

[179] Roberta Verta et al. "Generation of Spike-Extracellular Vesicles (S-EVs) as a Tool to Mimic SARS-CoV-2 Interaction with Host Cells". In: *Cells* 11.1 (2022), p. 146.

[180] Mahmoud Gheblawi et al. "Angiotensin-converting enzyme 2: SARS-CoV-2 receptor and regulator of the renin-angiotensin system: celebrating the 20th anniversary of the discovery of ACE2". In: *Circulation research* 126.10 (2020), pp. 1456–1474.

[181] Yosef Yarden. "Biology of HER2 and its importance in breast cancer". In: *Oncology* 61.Suppl. 2 (2001), pp. 1–13.

[182] Irina S Babina et al. "Lipid rafts as master regulators of breast cancer cell function". In: *Breast cancer-carcinogenesis, cell growth and signalling pathways* 401 (2011), p. 428.

[183] Miriam Stoeber et al. "Model for the architecture of caveolae based on a flexible, net-like assembly of Cavin1 and Caveolin discs". In: *Proceedings of the National Academy of Sciences* 113.50 (2016), E8069–E8078.

[184] Nikolas K Teiwes et al. "Pore-Spanning Plasma Membranes Derived from Giant Plasma Membrane Vesicles". In: *ACS Applied Materials & Interfaces* 13.22 (2021), pp. 25805–25812.

[185] Yanli Zhang et al. “Reconstitution of Caveolin-1 into artificial lipid membrane: Characterization by transmission electron microscopy and solid-state nuclear magnetic resonance”. In: *Molecules* 26.20 (2021), p. 6201.

[186] Fabio Perissinotto et al. “Multi-technique analysis of extracellular vesicles: not only size matters”. In: *Advances in Biomembranes and Lipid Self-Assembly*. Vol. 32. Elsevier, 2020, pp. 157–177.

[187] Andrea Ridolfi et al. “AFM-based high-throughput nanomechanical screening of single extracellular vesicles”. In: *Analytical chemistry* 92.15 (2020), pp. 10274–10282.